



• La Silla
• La Serena
• Santiago

EL MENSAJERO

MAIN LIBRARY

No. 48 – June 1987

A TIME FOR CHANGE

At its December meeting last year, I informed Council of my wish to terminate my appointment as Director General of ESO following the approval of the VLT proposal, expected later this year. Already at the time of my reappointment three years ago, Council was aware that I did not intend to serve out a full third five-year term, because of the desire to have more time for other activities. Now that the preparatory phase of the VLT has been completed with the formal presentation of the project to Council on 31 March and with approval likely before the end of the year, 1 January 1988 seems to be the optimal time for a change in the management of ESO.*

* On 4 June, Council unanimously appointed Prof. H. van der Laan to be Director General for a five-year period from 1 January 1988.

During the coming decade, the VLT project will profoundly affect all of ESO's activities as well as its interaction with the scientific community in the member countries. Not only is the VLT a large project in financial terms, but most ESO staff members will have to give it a large part of their time. The same is the case for many scientists and engineers in the member countries, since it is foreseen that much of the VLT instrumentation will be developed in the European laboratories.

While ESO will have to devote many of its resources to the VLT, at the same time other essential needs will present themselves: SEST is just beginning to function, the NTT is almost completed and needs to be fully instrumented, and hopefully the ECF will have the Space Telescope to worry about. All of this

opens up an era of great opportunity for European astronomers, but it will require a major effort to utilize the new instruments in an effective way while the construction of the VLT proceeds.

A particularly important aspect of this relates to the functioning of La Silla, which, of course, will have to remain a top priority. It is here, more than anywhere else, that the European astronomical community finds the fruits of the large investments that have been made.

Several years ago, we decided to see if sites could be found for the VLT with a quality still higher than that of La Silla, even though La Silla ranks among the best sites in the world. Subsequent studies have shown that Paranal has a substantially lower frequency of clouds and a very much lower humidity. Seeing



The road to Paranal (February 1987; photo: C. Madsen).

measurements are under way, and the first results, though as yet inconclusive, look promising. It therefore was decided that the VLT proposal should present Paranal as the more likely option, even though a definitive choice need not be made before three years from now.

Paranal is a remote place in one of the world's driest deserts. While a good gravel road passes close by, there is no village or anything within many kilometers. So the complete infrastructure will have to be built there by ESO. A development of Paranal along the lines of La Silla would be costly and time-consuming, but fortunately also not necessary.

Remote control is being used at La Silla on an experimental basis. For the VLT it will be the principal mode of use. Remote diagnostics and trouble shooting will undoubtedly follow. With such technologies, it would seem that the Paranal site may be run with a comparatively small number of highly qualified staff. Another factor which reinforces this conclusion is that the VLT – like the NTT – will be operated with very few instrument exchanges.

Suppose the VLT were placed at Paranal, what about the other ESO telescopes? With its 16-m equivalent diameter, the VLT would represent nearly 85% of the total photon collecting area of the ESO telescopes. It would seem hard to imagine that ESO would



Professor H. van der Laan, who will become Director General from January 1, 1988.

continue to operate another site at high cost for the remaining 15%. In the long run, there appears to be only one solution: if the VLT were to be placed at Paranal, all of ESO's telescopes would have to be operated there. This might involve the moving of some of the La Silla telescopes. Moving the 2.2 m, CAT, 1.5 m DK and SEST would not present major problems; the 3.6 m is too cumbersome to move, except perhaps as a "zenith telescope" for cosmological studies. What really would be useful to move more than a decade from now remains to be seen at that time.

The NTT poses a particular problem. Within a year, it will be ready for installation in Chile. If Paranal were ultimately to be chosen as the VLT site, would it not be more rational to place it there? While

the advantages of learning to operate a modern telescope on Paranal before the arrival of the VLT would be important, there are serious problems with regard to the time scale; these are currently being analyzed. Should it appear that the Paranal location would cause undue delays, the NTT would still be placed at La Silla.

Astronomers have been accustomed to look at telescopes as instruments of almost eternal use. This was perhaps reasonable at a time in which maintenance needs were small and instrumentation relatively simple. At present, however, the annual costs of operating and instrumenting a modern telescope at a remote site and processing the resulting data far exceed the capital investment prorated over one or two decades. It follows that the acquisition of new telescopes must automatically be accompanied by the closing of existing ones.

The VLT represents ESO's long range future. Without it the Organization could not survive very long. However, for more than a decade, La Silla will continue to provide the data essential for the scientific work of a large community. It is clear, therefore, that even if Paranal were to be developed, everything will have to be done to guarantee the continuation of the functioning of La Silla at its present high level of quality.

L. WOLTJER
Director General

The Swedish-ESO Submillimetre Telescope

R. S. BOOTH, Onsala Space Observatory, Chalmers Tekniska Högskola, Göteborg, Sweden

M. J. DE JONGE, Institut de Radioastronomie Millimétrique, Grenoble, France

P. A. SHAVER, European Southern Observatory

Introduction

Dramatic changes have taken place during the past two years at the southern end of the telescope ridge on La Silla and now, where once stood a meteorological station, stands a 15-m submillimetre telescope. The telescope, designed by IRAM engineers, has been built on behalf of the Swedish Natural Science Research Council (NFR) and ESO. It will be operated jointly by ESO and NFR (through the Onsala Space Observatory).

The Swedish-ESO Submillimetre Telescope, acronym SEST, while not actually breaking new ground at ESO, since some groups have already used the 3.6-m and other telescopes at submillimetre wavelengths, represents a

significant breakthrough as a dedicated sensitive millimetre-submillimetre instrument. It is the only telescope of its kind in the southern hemisphere and among the first such instruments in the world.

SEST will extend the observational part of the radio spectrum towards the infrared and will enable European astronomers to probe the molecular clouds of the southern Milky Way and other nearby galaxies, providing information on stellar evolution and galactic dynamics. It will enable them to investigate the radio continuum properties of the stars, HII regions and interstellar dust in this new wavelength region, and provide valuable new data on quasars and radio galaxies in the submillimetre wavelength regime. SEST may also be-

come an extension of the existing VLBI arrays for the study of the submilliarc-second properties of low declination radio sources.

Background

The idea of building an IRAM design telescope on La Silla was first conceived by the astronomers of IRAM and Onsala Space Observatory, and enthusiastically supported by ESO. The outcome of the subsequent negotiations between the parties and their funding agencies was an agreement between the Swedish Natural Sciences Research Council and ESO to install and operate the 15-m telescope on La Silla and share the expense and the observing time over a 15-year period. IRAM agreed to build the

telescope under contract with ESO. As part of the agreement, Onsala Space Observatory has the technical responsibility for the first receivers and the overall project.

The formal agreements were signed at a small ceremony at Onsala Space Observatory on June 26, 1984. Under a separate Nordic agreement related to the Nordic Optical Telescope (NOT), Finnish astronomers will benefit from 10% of the Swedish observing time.

The Importance of La Silla

La Silla is an important site for SEST on two counts. The first is its southern location, making the telescope unique as the only major telescope in the southern hemisphere to operate below 3 mm wavelength. The second is the low atmospheric attenuation above this dry mountain site. Figure 2 shows the relative transmission of the atmosphere as a function of frequency for 1 and 4 mm of precipitable water. The atmospheric water vapour content above La Silla is below 4 mm for nearly one hundred per cent of the time during the winter months, with some days below 1 mm. These are very good observing conditions, and early experience with the telescope shows the enormous improvement over a typical sea-level site.

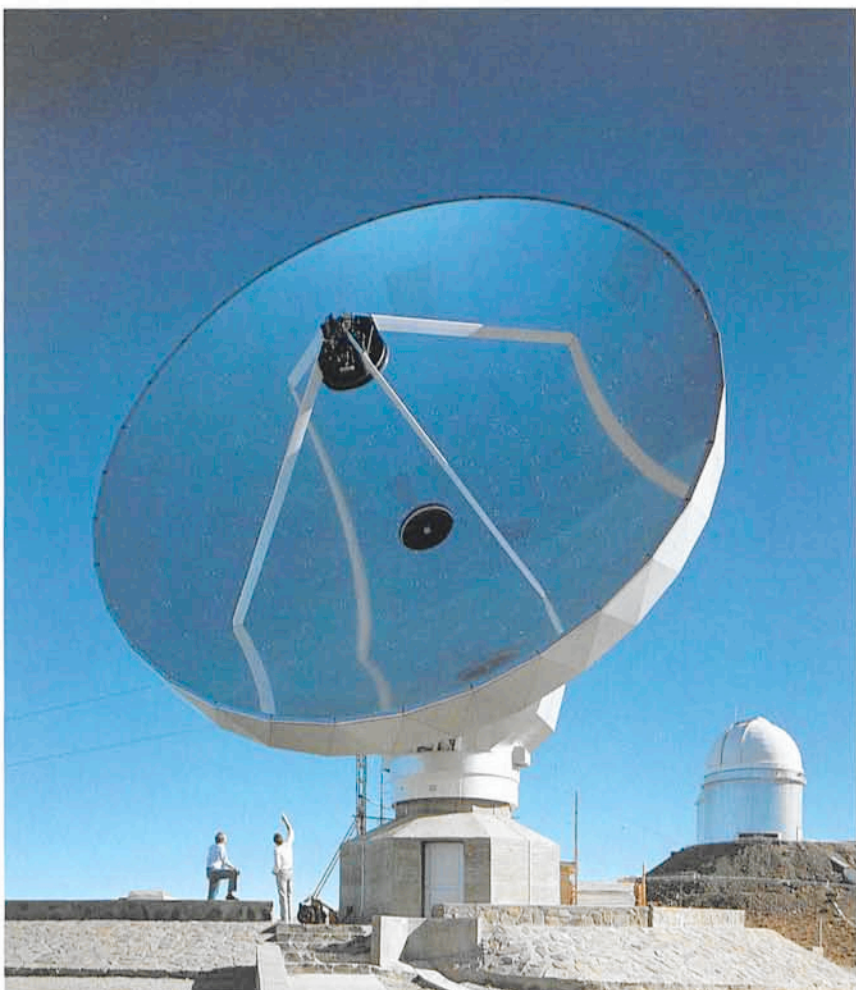


Figure 1: The 15-m Swedish-ESO Submillimetre Telescope.

The Telescope

The general specifications for SEST are given in Table 1. The telescope is designed to achieve a reflector profile accuracy of 50 microns r.m.s., giving good (coherent) performance down to wavelengths ≤ 0.8 mm (375 GHz). (The Ruze criterion on performance of radio telescopes gives 50% efficiency at a wavelength of $16 \times$ r.m.s. error).

The antenna (described by Jean DeLannoy at the Aspenäs ESO-IRAM-Onsala Workshop on (sub)millimetre astronomy) is identical to three others being built by IRAM on the Plateau de Bure, France, as movable elements of an interferometer. From the outset, therefore, an essential design requirement was the capability to operate without a radome or other enclosure normally associated with telescopes of this precision. This is only achieved through new technology. The new concept behind these antennae is the extensive use of carbon fibre, in both the backing structure and the reflector. The material is light-weight and therefore gravitational distortion is small, and it has a low temperature coefficient, thereby minimizing the effects of temperature gradients on the surface profile. Finally, the telescope is designed using von

Hoerner's homology principle, which means that it is not an extremely stiff structure and is allowed to distort as a function of elevation angle. The flexure is, however, constrained such that the reflector always retains a parabolic form and, by the simple expedient of moving the subreflector an appropriate predetermined amount, the focus is maintained and with it the efficiency of the paraboloid. The telescope can operate within the specifications in winds up to 14 ms^{-1} and under temperature gradients of up to 10°C across the surface.

The SEST reflector consists of 176 panels, each mounted at 5 points, all of which have servo-controlled motors for adjustment. The telescope has been surveyed by A. Greve of IRAM using a direct (theodolite and measuring tape) method in the zenith pointing position. By successive adjustment of the panels a parabolic profile has been achieved with an r.m.s. accuracy of 80 microns. Further such adjustment, it is hoped, will result in an r.m.s. of better than 70 microns. Final trimming of the surface will be attempted either using the technique of holography on a satellite transmission

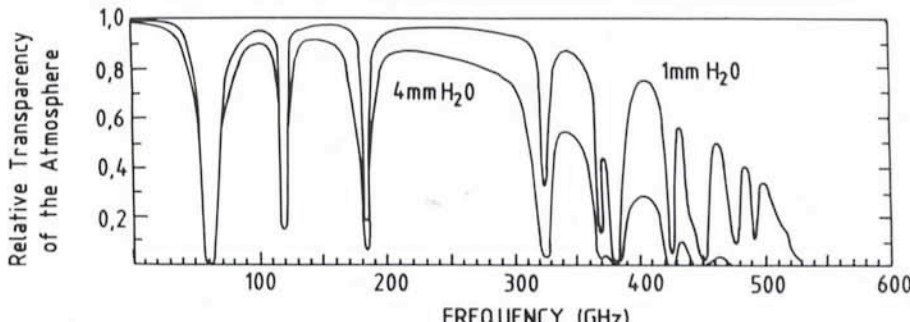


Figure 2: Transmission through the atmosphere with 1 and 4 mm of atmospheric water vapour.

TABLE 1. SEST Specification

Main reflector	Axisymmetric paraboloid
Diameter	15 m
f/D	0.325
Tolerance	50 microns r.m.s.
Focus for receivers	Cassegrain
Subreflector diameter	1.5 m
Magnification	15.7
Half power beam width (12 db edge tapes)	50" at λ 3 mm 17" at λ 1 mm
Pointing accuracy	2 arcseconds
Environmental constraints	
Max. wind for operation	14 m s ⁻¹
Max. wind for survival	56 m s ⁻¹
Icing load	10 cm
(De-icing heaters are provided)	

or by optical methods. The latter technique may be possible because individual panels have a highly reflective surface with a precision of ~ 16 microns on average. The optical performance of the SEST reflector was inadvertently tested during construction when, due to an oversight, the reflector pointed within 10 degrees of the sun; the consequent concentration of power at the edge of the sub-reflector caused some damage to the sub-reflector and several panels, which has since been repaired. Because of the good optical performance of the panels it is hoped that SEST may be used as a "light bucket" at frequencies considerably in excess of 375 GHz.

Receivers

Under the NFR-ESO agreement, Onsala Space Observatory (Department of Radio and Space Science of Chalmers University of Technology) is responsible for the first receivers. All are dual polarization systems based on Schottky-diode mixer front-ends cooled to 15 K in closed cycle refrigerators. They are designed to be controlled and monitored by computer. A chopper wheel system is available for calibration and beam-switching. The front-ends feed cooled FET intermediate frequency amplifiers, centre frequency 4 GHz, although a 1.5 GHz I.F. is also available. A con-

tinuum back-end and two Acousto-Optic spectrometers (AOS), built by the University of Cologne, will be provided. The first AOS (bandwidth 100 MHz, resolution 50 kHz) is already in use, and a second (bandwidth 500 MHz, resolution 50 kHz) is being built.

The first receiver in operation on SEST tunes over the band 85–117 GHz and has an instantaneous bandwidth of 500 MHz. Its noise temperature is 250 K, single side-band (SSB). This is being used for telescope tests, pointing, etc., and will be the first available for observation. The second receiver system is still under construction. It is designed to cover the range 220–280 GHz (B/W 500 MHz) and the expected noise temperature is ~ 600 K (SSB). The SEST submillimetre receiver will also be built at Onsala, and will cover a band near 345 GHz. Finally, we are discussing the possibility of providing a submillimetre broad-band bolometer system for continuum observations and a VLBI back-end is also under consideration.

Control and Data Analysis

SEST and its associated instrumentation is controlled by two networked mini-computers: an HP A900 and an HP A600. The A900, the main computer, has 1.5 megabytes of primary memory and 120 megabytes of disk space. The

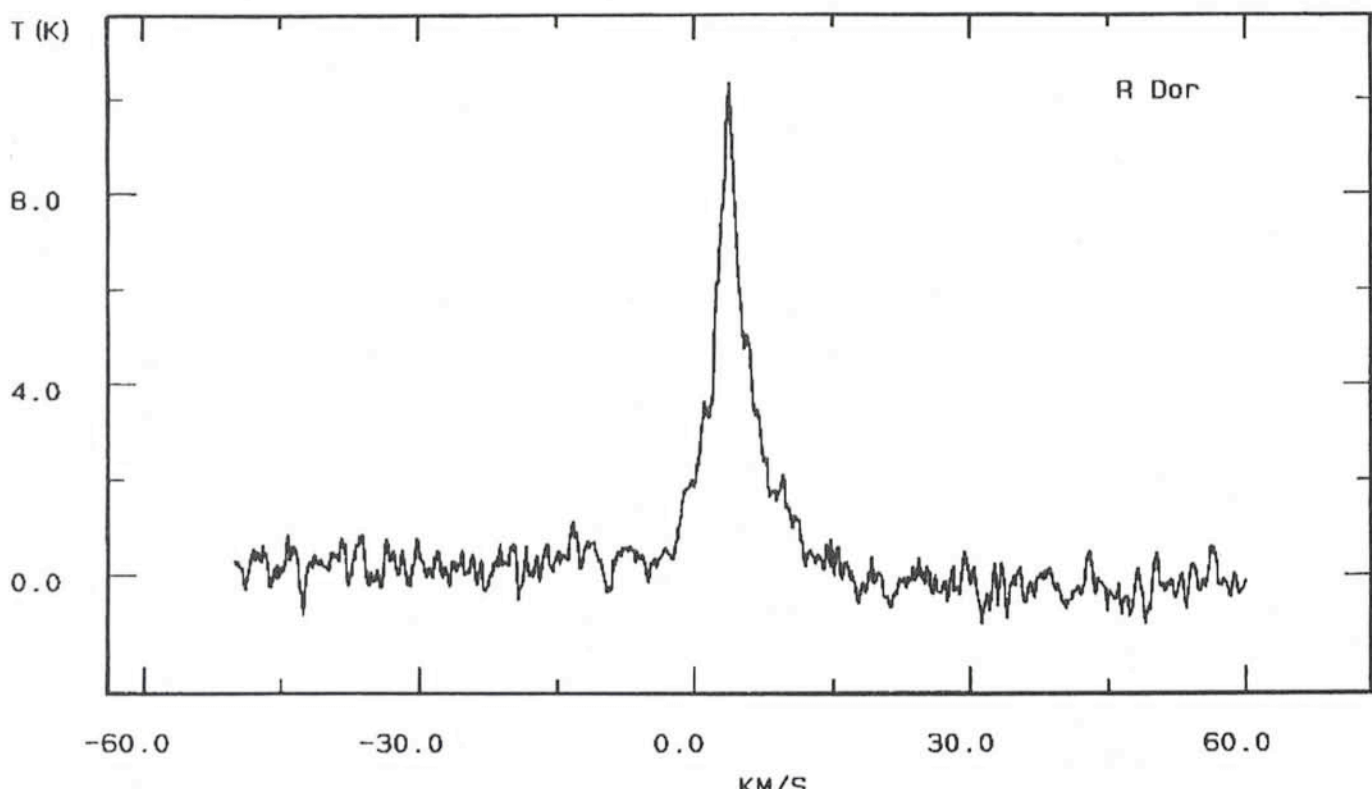


Figure 3: Spectrum of the new 86 GHz SiO maser discovered in the Mira variable R Doradus.

A600 is at present dedicated to the control of the AOS spectrometers. Instruments and sensors are interfaced to the computers via the industry standard bus systems GPIB and CAMAC.

Two popular on-line data reduction packages designed for radio astronomy are supported. These are POPS (People Oriented Parsing Service), a system developed in the USA, and Toolbox, a system developed in Germany. Users may also write their data to tape using the well-known FITS format for reduction by other popular off-line systems.

Proposals for SEST Observations

Routine observations using SEST will be allocated on a six-month basis, in accordance with the standard ESO observing schedule. They are expected to commence with period 41, starting 1 April 1988, for which the proposal deadline is 15 October 1987.

In the meantime, there will be opportunities for limited observations using the first receiver (85–117 GHz) and AOS (50 kHz resolution) starting in August or September, during the testing and calibration phase. These opportunities are necessarily restricted to astronomers with considerable experience in millimetre wave observations, who are willing to work with an evolving system and contribute to its development. Proposals for this period should be submitted as soon as possible to the Visiting Astronomers Office in Garching.

Operations

The operation of SEST on La Silla is in the hands of a team comprising:

Scientist in Charge:

Lars E.B. Johansson

Microwave Engineers:

Magne Hagstrom, Nick Whyborn;

Software Scientists:

David Murphy, Michael Olberg

This dedicated group has been heavily involved with receiver and software development for more than a year. Two further persons will soon be added to this team.

Following its completion under the supervision of Dietmar Plathner, the new telescope was handed over to the team at La Silla on March 13, 1987 and "first light" was obtained on March 24. Commissioning is now under way, and series of tests designed to determine the pointing and homology characteristics and the receiver performance, and to streamline the control system, are in progress. When these are complete, experienced millimetre astronomers will be invited to try out the system. SEST should become generally available in early 1988 after the 230 GHz receiver has been commissioned. Proposals will be accepted for the ESO October deadline. Sweden and ESO will handle their respective proposals through separate programme committees and time will be allocated to the two parties on a 50–50 basis.

Scientific Programme

The scientific programme for SEST depends, of course, on the interests of the user community. A full discussion of the potential programmes for the telescope took place during the Aspenäs workshop (ESO Conference and Workshop Proceedings No. 22, 1985). While the millimetre and submillimetre spectral region is usually considered the province of molecular line astronomy and cosmochemistry, we saw a great deal of interest in continuum studies both of interstellar dust, active galactic nuclei

and quasars, and the cosmic background radiation since the Sunyaev-Zeldovich decrement changes sign between 2 mm and 800 microns wavelength.

In the field of molecular spectroscopy the southern sky has great potential because the southern Milky Way contains a plethora of important dark clouds and HII regions, many with unusual features. Probably one of the most important although poorly understood discoveries of molecular line astronomy is the fact that so many protostars in the Galaxy go through the stage of bipolar outflow. The southern sky is rich in optical signposts of bipolar flows, such as Herbig-Haro objects, and this points to a feast of new observational data. Their observations in the new wavelength range and with the higher resolution provided by SEST should help us understand this unexpected phenomenon.

At the other end of the evolutionary scale, the study of mass loss from evolved stars, Mira variables and red giants is an exciting prospect, particularly in view of the host of IRAS objects now waiting to be observed at millimetre wavelengths. One of the first observations with SEST provided the detection of a new 86 GHz SiO maser in a Mira variable, R Doradus (Figure 3).

In the past few years we have seen much interesting work on the carbon monoxide distribution and molecular cloud dynamics in nearby galaxies. Again IRAS has been an inspiration and we now find that extragalactic CO is detectable in galaxies with recessional velocities greater than $8,000 \text{ km s}^{-1}$. The southern sky is rich in active galaxies and their observation will enhance the statistical data base needed to relate star formation rates to molecular emission, IR and continuum radio fluxes.

Finally, solar system objects will not be neglected with SEST. In fact, it may be possible to observe comet Wilson already next month. Observations of

planetary atmospheres and the continuum emission from planets and asteroids at submillimetre wavelengths will be of great interest.

We look forward to these exciting discoveries, which have been made possible by the dedicated efforts of the many people involved.

List of ESO Preprints

491. B. Barbanis: Irregular Periodic Orbits. *Celestial Mechanics*. March 1987.
492. L. Milano, M. Rigutti, G. Russo and A. Vittone: Some Observed Peculiarities of the Triple System V 701 Cen. *Astronomy and Astrophysics*. April 1987.
493. S. Cristiani: Observation of the HII Galaxy Giving Origin to the $Z = 0.3930$ Absorption System of the QSO 1209+107. *Astronomy and Astrophysics Letters*. March 1987.
494. L. Koch-Miramond and M. Aurière: X-Ray and UV Observations of Omega Centauri with EXOSAT. *Astronomy and Astrophysics*. March 1987.
495. S. Cristiani et al.: Radial Velocities of Galaxies in the Cluster Klemola 22 from Observations with Optopus, the ESO Multiple Object Spectroscopic Facility. *Astronomy and Astrophysics*. April 1987.
496. E. Giraud: Malmquist Bias in the Determination of the Distance to the Hercules Supercluster. *Astronomy and Astrophysics*. April 1987.
497. G. Garay: The Orion Radio Zoo: Pigs, Deers and Foxes. Invited talk given at the V. IAU. Regional Latin-American Meeting, Merido, Mexico (October 6–10, 1986). April 1987.
498. B. Binggeli, G.A. Tammann and A. Sandage: Studies of the Virgo Cluster. VI. Morphological and Kinematical Structure of the Virgo Cluster. *Astronomical Journal*. April 1987.
499. T. Le Bertre: Optical and Infrared Observations of Two Type-II OH/IR Sources. *Astronomy and Astrophysics*. April 1987.
500. Supernova 1987 A in the LMC. Astrometry (R.M. West et al.), Photometry (S. Cristiani et al.), Polarimetry (H.E.

- Schwarz and R. Mundt), Infrared Observations (P. Bouchet et al.), Medium and High-resolution Spectroscopy (I.J. Danziger et al.; A. Vidal-Madjar et al.) *Astronomy and Astrophysics, Letters*. March 1987.
501. H. Dekker and B. Delabre: Simple, Wide-Band Atmospheric Dispersion Corrector. *Applied Optics*. May 1987.
502. L. Milano, G. Russo and A. Terzan: FS Lup: A Contact Binary in Poor Thermal Contact. *Astronomy and Astrophysics*. May 1987.
503. L. Binette, A. Robinson and T.J.-L. Courvoisier: The Ionizing Continua of Active Galactic Nuclei: Are Power Laws Really Necessary? *Astronomy and Astrophysics*. May 1987.
504. L. Binette, T.J.-L. Courvoisier and A. Robinson: Constraints on the Soft X-Ray Continuum of AGN Derived from Photoionization Models. *Astronomy and Astrophysics*. May 1987.
505. T.J.-L. Courvoisier and M. Camenzind: Magnetic Field and Synchronization in Mildly Relativistic Shocks. *Astronomy and Astrophysics*. May 1987.

High Speed Multicolour Photometry of the X-ray Burster MXB 1636-53

R. SCHOEMBS, M. PFEIFFER, R. HAEFNER, Universitäts-Sternwarte München
H. PEDERSEN, ESO

1. Introduction

X-ray burst sources are thought to be low-mass binary systems in which a mass-losing late-type main-sequence star transfers matter via an accretion disk onto a neutron star. The high potential energy of the material is converted to high kinetic energy, which subsequently thermalizes and escapes as X-rays. Depending on the temperature, the strength of the magnetic field and the accretion rate of the neutron star, a thermonuclear flash can occur on its surface from time to time. Within seconds a total energy of about 10^{39} erg is released. The resulting radiation is predominantly in the X-ray band. Burst intervals are mostly irregular and range from hours to days. There is no clear relation between the shape of the burst, the intervals and the continuously emitted X-ray level. Black-body fits to the energy distribution of the bursts yield temperatures up to 10^7 K and a radius of the emitting area of approximately 10 km thus supporting the neutron star model.

Optical bursts correlated with X-ray bursts have been observed for several sources. The shape of an optical burst is similar to that recorded in the X-ray range, whereas its energy content is a fraction of 10^{-4} only. Nevertheless, this is more than expected from an extrapolation of the X-ray spectrum. Usually the optical burst is delayed by a few seconds. This can be understood as a consequence of the longer light path from the X-ray source via the place of reprocessing to the observer, compared to the path on the direct way.

MXB 1636-53 (optical counterpart: V 801 Ara) is one of the best studied examples in both the X-ray domain and the optical region. Several coincident X-ray/optical bursts were recorded and

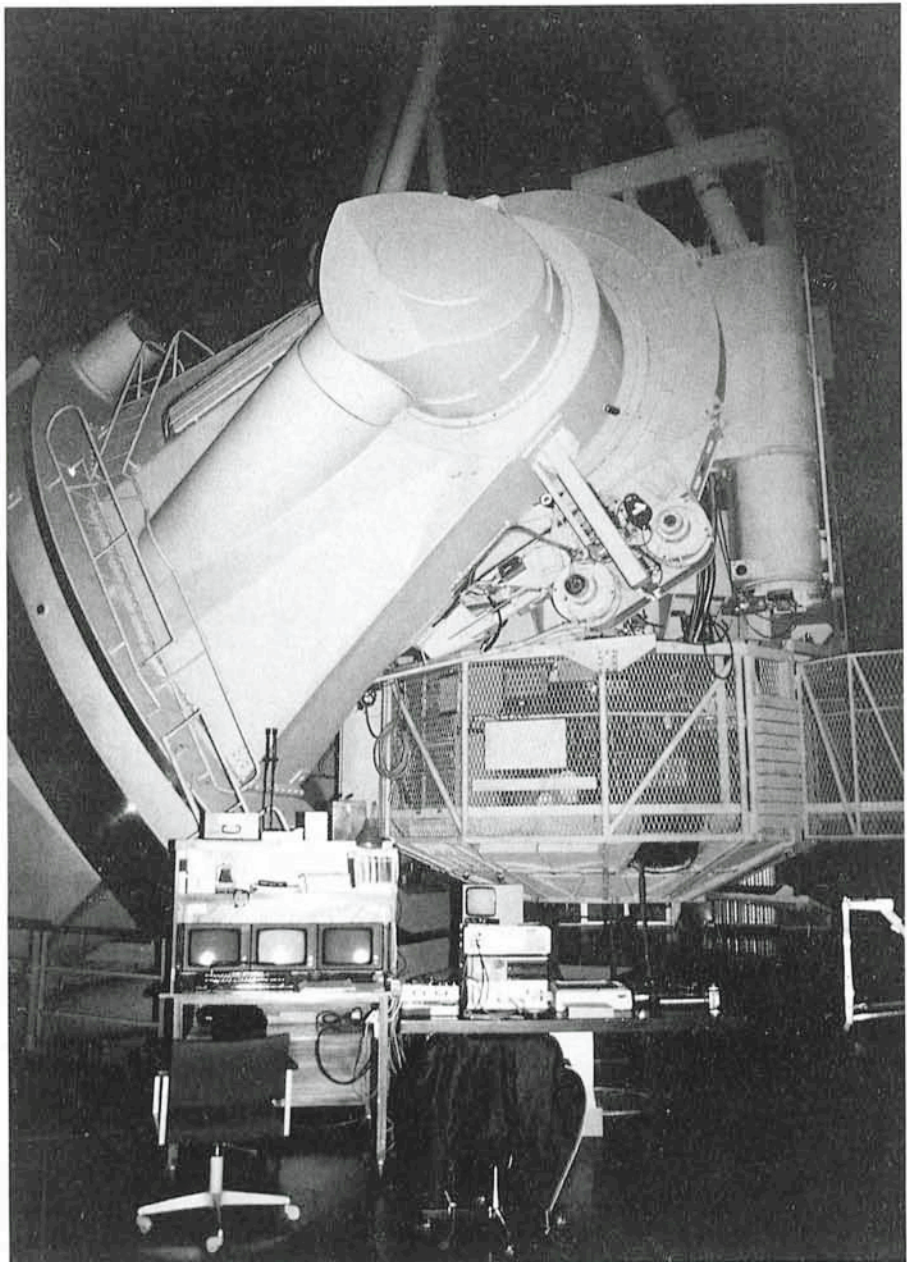


Figure 1: The data-acquisition system of the photometer placed inside the dome of the 3.6-m telescope during observations.

the data concerning this system contributed appreciably to our knowledge on bursters. Initially optical data were obtained in unfiltered light and could merely give crude estimates of the properties of the disk. The delay from X-ray burst to optical burst was found to be about 2.5 seconds (Pedersen et al., 1982; Matsuoka et al., 1984). Black-body fits to the energy distribution yielded a temperature of about 50,000 K for the disk during burst, twice as large as during quiescence. UBV burst light curves obtained later on showed that the single-temperature black body reprocessing model is only approximatively correct. Slow modulations in the persistent optical flux of about 4 hours were interpreted as due to binary motion (Lawrence et al., 1983).

The aim of our observing campaign was twofold: (i) More data concerning the spectral development during optical burst should be collected to further investigate the physical state of the accretion disk and the processes converting X-rays into optical light. (ii) Long data sequences should be recorded to improve the period of the suspected orbital variation and to obtain information about variations of the system in UBVRI which might even allow to derive more system parameters.

The original plans for coordinated simultaneous X-ray observations had to be abandoned since unfortunately EXOSAT got out of control shortly before our observation and the Japanese TENMA X-ray observatory was not operating at the time in question. In the following we report on the optical observations and on the provisional results.

2. Preparation and Observations

Four nights (May 12–15, 1986) at the 3.6-m telescope were granted to the project. We used the three-channel UBVRI photometer developed at the Universitäts-Sternwarte München (Barwig et al., 1987). The instrument provides for simultaneous multicolour recording of object, comparison star and sky, thus it allows photometric work even under otherwise unfavourable meteorological conditions.

Photometry of MXB 1636-53 demanded measurements at high time resolution simultaneously in 15 data channels. To do this, a new programme package had to be written. The final version allows to reach 10 msec time resolution without deadtime with an economic output of roughly 1 Mbyte within 20 minutes corresponding to one 8" floppy disk. The disks can be loaded alternately into one of the two drives while the other one is recording. The

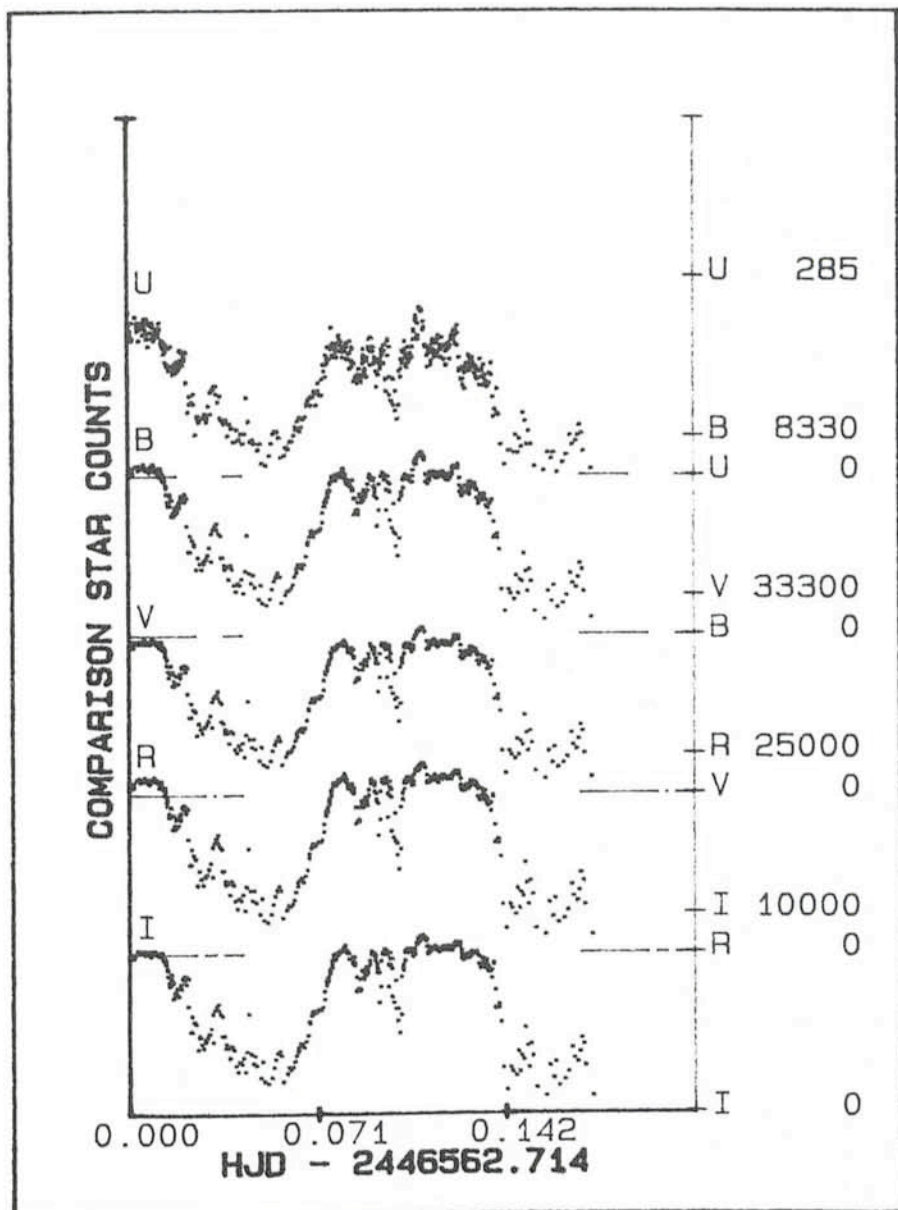


Figure 2: Atmospheric transparency variations during the first night (4 h) represented by the comparison star counts.

programme provides for real time graphics and statistical information.

Before starting the observations we were not sure whether our TV acquisition system would be sufficiently sensitive and the built-in autoguider would co-operate with the 3.6-m telescope. But from the very beginning the instrumentation worked without problems. Since the cables were not sufficiently long for the control room, the computer system and displays had to be placed in the dome and thus also the observers. We were afraid to extend the cables since this would make the system more vulnerable to electrical pick-up noise. Straylight from displays, etc. and other sources of interference were carefully checked before we started our observations and their influences were

kept below detection. Figure 1 shows the instrumental setup in the dome.

Regrettably, the observations were impeded by excessive wind and by clouds. Useful observations could be performed only during parts of the first, second and fourth night, while the third night was lost completely. As an example, Figure 2 shows the count-rates obtained for the comparison star during the first night. Only at the very beginning a short time interval of fairly stable transparency was encountered. The second part of the second night and the end of the last night were very cloudy.

Due to the special observing technique and the properties of the star field around MXB 1636-53 it was necessary to use a hitherto unknown star as comparison. After some time we suspected

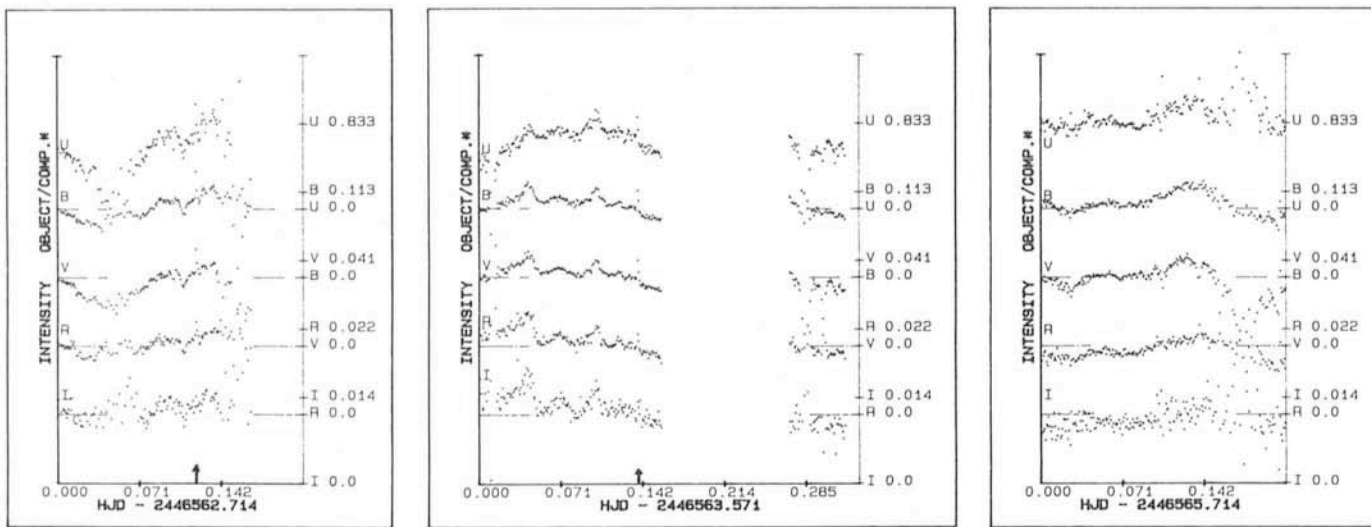


Figure 3a, b, c: Condensed light curves (rel. intensity) of MXB 1636-53 which show the whole observing period, covering the nights of May 11/12, 12/13, 14/15 respectively. Arrows indicate the position of the identified bursts.

that it might be variable, and thus the photometer was prepared for a different comparison star. Their calibration, performed at a later date, yielded results constant within 0.1 magnitude.

Integrations of 40 msec for the object and 200 msec for sky and comparison star were used. The aperture of the diaphragms throughout the observing period was 7". Table 1 shows typical photon fluxes as measured in UBVRI under good transparency conditions.

According to atmospheric refraction the count-rates in U and I are attenuated at larger zenith distances. This effect is at least partly compensated by the reference channel.

3. Reduction and Results

The reduction procedure makes use of separately measured dark counts and of transformation coefficients which, for each colour, relate the sensitivity of the three channels. A file is produced which contains HJD-time and the five object intensities relative to the comparison star. Using magnitudes or fluxes of the comparison star they can be converted into absolute values. The reduction programme offers options by which the effective integration time (which equals the time resolution) can be increased to a fixed value or to a variable amount depending on sky transparency. The latter mode was used because of the variable transparency in order to yield data of fairly comparable rms.

For the determination of the transformation coefficients photometric conditions are required. Good conditions were never encountered during the whole observing period. Thus the quality of the transformation coefficients is lim-

ited, causing incomplete compensation of the atmospheric variations during very cloudy skies. This was the case at the beginning and end of the first night and at the end of the second and third night. Figures 3a, b, c show the full extent of the light curve, binned to 80 sec/dot. Significant, slow variations were present during all three nights. The time constant of these variations is variable, being shorter during the second night, while the amplitude is larger dur-

ing the first and the last night. Correlated colour variations occur at some of the peaks.

A periodogram analysis of the new data revealed a possible period of 3.76 h. This is consistent with the 3.78 h period determined by Pedersen et al., (1981). However, the significance of our period is not high, because of the large gaps and superposed irregular variations. Figure 4 shows a phase diagram of data in V, calculated for the period P

TABLE 1: Average fluxes (counts/sec)

Channel	U	B	V	R	I
MXB 1636-53	50	200	175	100	25
Comparison star 1 (-22°, +94°)	65	2285	6875	4950	2335
Comparison star 2 (+151°, -19°)	250	2915	4855	2140	745
Sky (7" diaphragm)	60	180	400	235	115

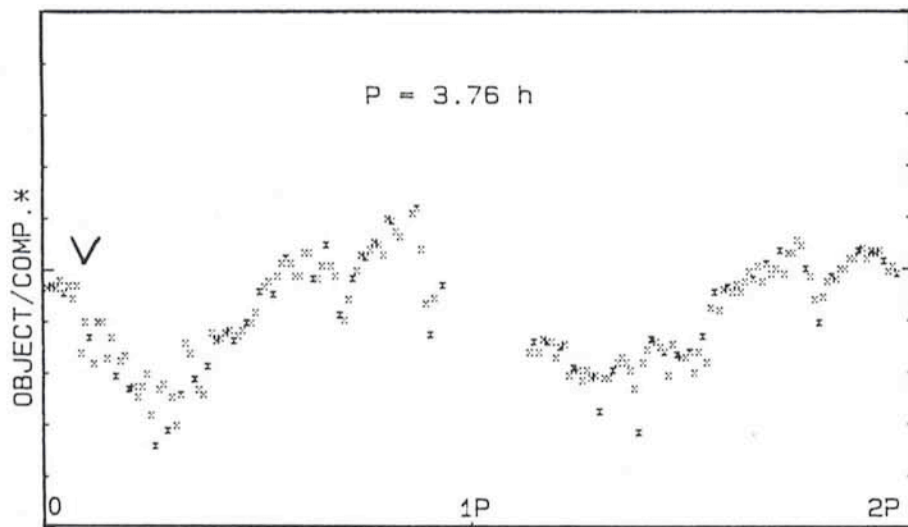


Figure 4: Phase diagram of the condensed light curve of MXB 1636-53 with twice the period of 3.76 hours.

= 2.3.76 h. The two representations of the light curve are thus based on statistically independent data. Their shape and the occurrence of some repeating features is striking. Especially the dip near maximum, not explicitly mentioned by Pedersen et al., is well represented in their phase diagram.

Apart from these slow variations two bursts were detected. In Figure 3a and b their position is indicated by arrows. The burst light curves with high time resolution are superposed for comparison in Figure 5. The scales are the same in both cases, but the zeropoints were shifted to separate UBVR. The data were smoothed by a recursive low-pass filter. Burst 1, observed during the first night, is less intense and has a slower onset than burst 2, which has a rise time of less than two seconds. This limits the extension of the visible emitting area to about $6 \cdot 10^{10}$ cm. In colour B (highest count-rates) a double-peak structure is shown for burst 2 with a separation of about 3 seconds. Similar features were found by Sztajno et al. 1985 in the X-ray band. The colours of the optical bursts are consistent with a very hot source. Cooling effects during descent are indi-

Two New Slide Sets From ESO

ESO announces the publication of two new slide sets, available from July 1, 1987:

- Objects in the Southern Sky
- Supernova 1987 A in the Large Magellanic Cloud

Both sets include 20 high-quality 5 × 5 cm slides, accompanied by a comprehensive, explanatory text and presented in a folder with a beautiful cover. The first set contains spectacular colour views of selected objects in the southern sky, as photographed with ESO telescopes during the recent years. The second set in which some slides are in colour and others in black-and-white, summarizes the most important observations of the brightest supernova since 383 years. Apart from images of the LMC field before and after the explosion, it also includes selected spectra and other observational results from La Silla

The sets, which are also useful for educational purposes, may be obtained by sending 35,- DM, which is the equivalent of the cost price, incl. postage, to:

ESO Information and Photographic Service
Karl-Schwarzschild-Straße 2
D-8046 Garching bei München
Federal Republic of Germany

Do not forget to indicate your name and accurate address. Please note that the delivery time may be a few weeks.

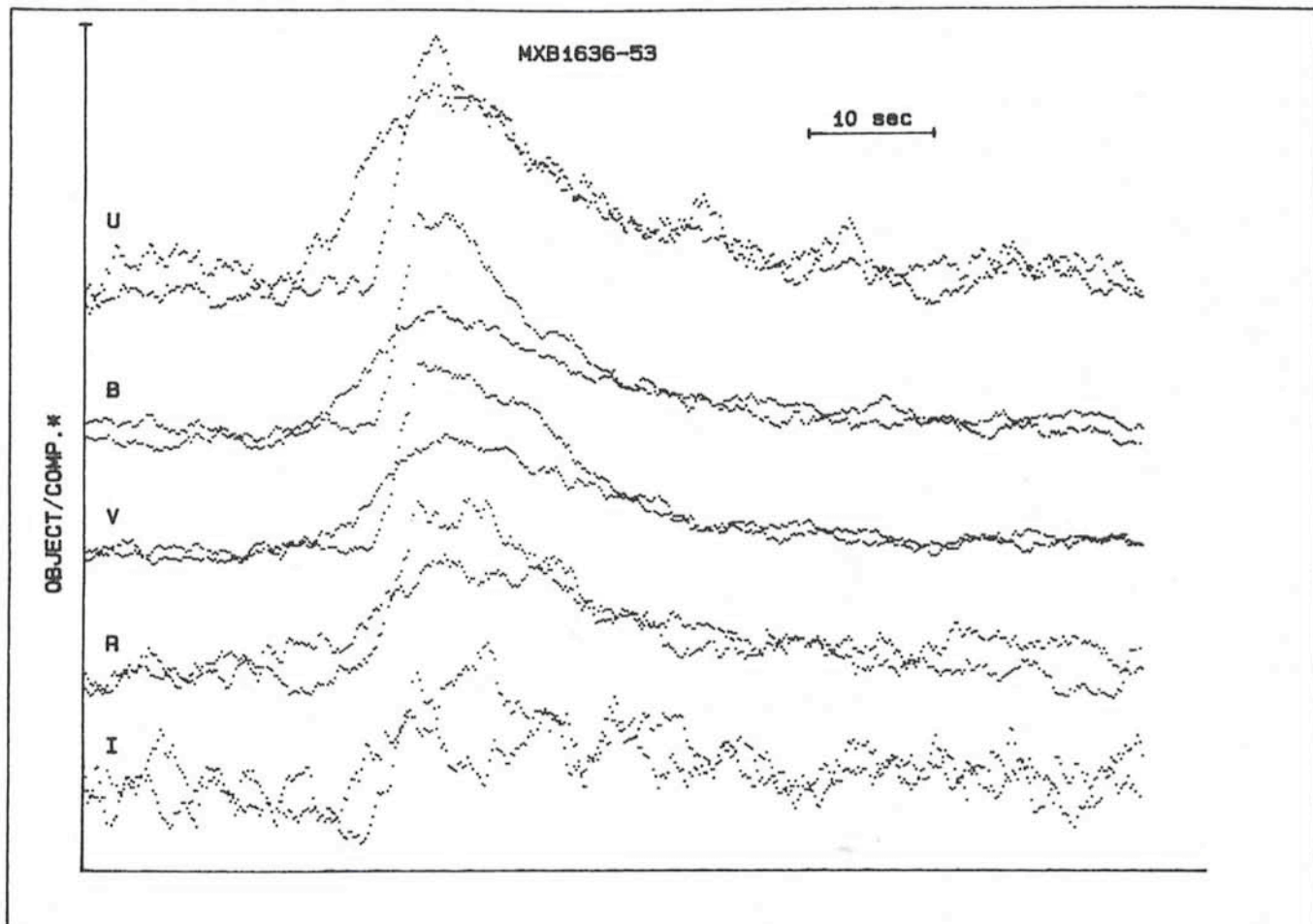


Figure 5: The two observed bursts superposed to demonstrate similarities and differences (1 point \triangleq 320 msec). Burst 1, observed during the first night is less intense and has a slower onset than burst 2. The curves were smoothed (FWHM = 50 points) in order to reduce the noise.

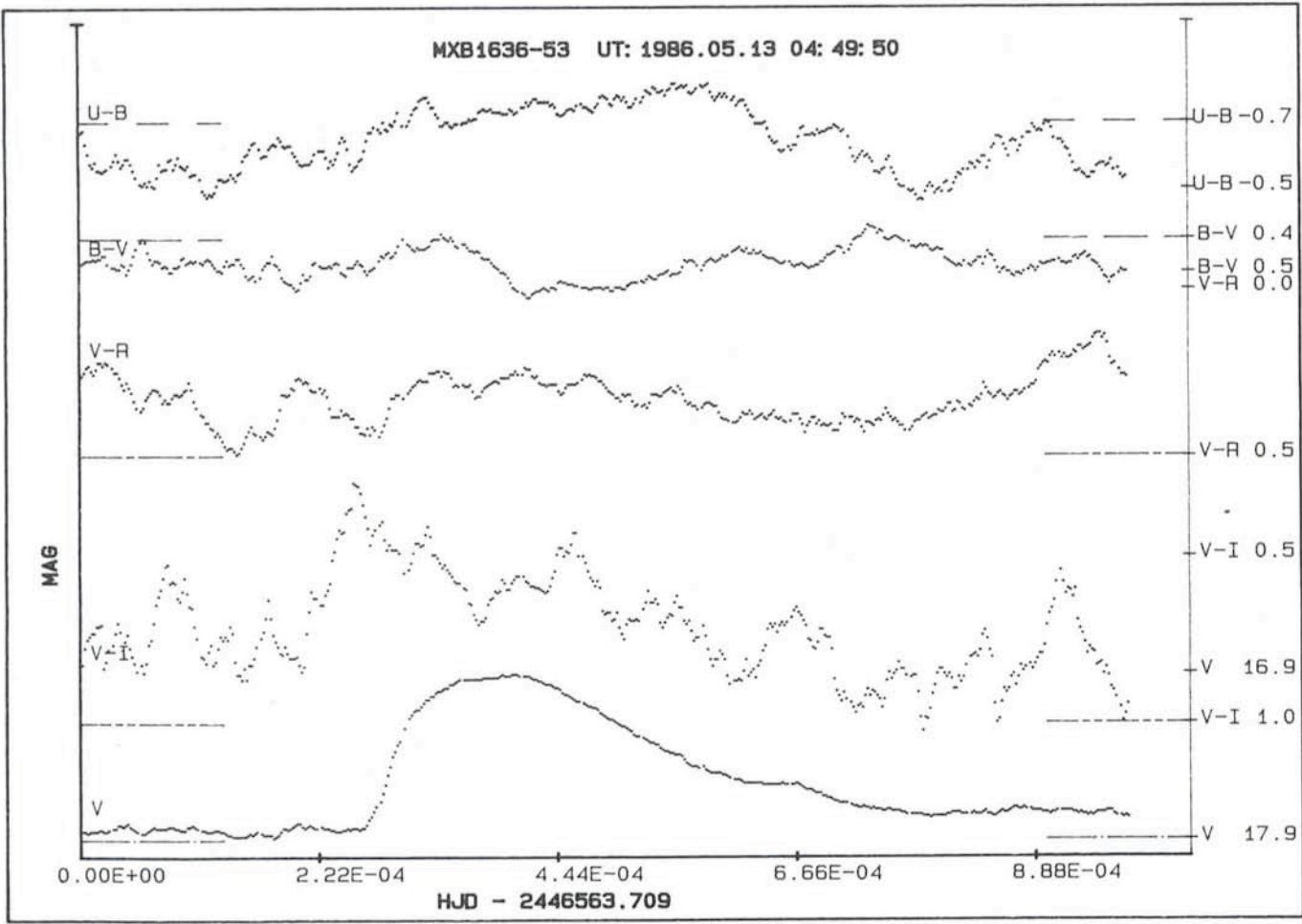


Figure 6: Burst 2 and its colour variations. The curves were smoothed (FWHM = 50 points) in order to reduce the noise in the colours (1 point \approx 320 msec).

cated (see Fig. 6). A detailed analysis, however, requires more than two samples in order to enable the separation of individual characteristics from the general behaviour and to improve the signal-to-noise ratio. These considerations led to a successful application for further observations in July 1987, possibly in collaboration with ASTRO-C, the new Japanese X-ray observatory.

References

- Barwig, H., Schoembs, R., Buckenmayer, C.: 1987 *Astron. Astrophys.*, **175**, 327.
- Lawrence et al.: 1983, *The Astrophysical Journal*, **271**, 793.
- Matsuoka, M. et al.: 1984, *The Astrophysical Journal*, **283**, 774.
- Pedersen et al.: 1982, *The Astrophysical Journal*, **263**, 325.
- Pedersen, H., van Paradijs, J., Lewin, W.: 1981, *Nature*, **294**, 725.
- Sztajno, M., van Paradijs, J., Lewin, W.H.G., Trümper, J., Stollman, G., Pietsch, W., van der Klis, M.: 1985, *The Astrophysical Journal*, **299**, 487.

Line and Continuum Imaging

S. di Serego Alighieri*, ST-ECF

The study of line emitting objects often requires to image separately the line emission from the continuum one, in order to discriminate the different physical components. This is generally not possible with the broad bands of the standard photometric systems, like UVRI. Rather one should use narrower bands selected according to the wavelengths of the emission lines. I discuss here the techniques to obtain pure and calibrated line and continuum images. "Pure" means that the line image is free from the contribution of the continuum and vice versa. Since narrow-band imaging is not a new technique, I will restrict myself to the considerable improvements recently offered by the availability of linear and calibratable detectors, of interference filter sets and of

powerful and versatile image reduction systems. Although I will concentrate here on images of active galaxies obtained with the ESO telescopes and CCD cameras at La Silla and reduced using MIDAS, the following discussion can be applied with small modifications to any class of line emitting objects and to other sites, detectors and reduction systems. I will first give some hints on how to conduct the observations and then discuss the reduction procedure. A technical note containing more detailed information is available from the author for those interested in actually using these techniques.

Observing Hints

It is necessary to obtain exposures both with a filter centred on the emission line and with a filter on the nearby continuum. The latter is used to derive the

* Affiliated to the Astrophysics Division, Space Science Department, European Space Agency.

morphology of the component of the object, which emits continuum radiation, and to subtract the continuum contamination in the line exposure. The final quality of the images depends considerably on the filter selection. The line filter should be very narrow, compatible with the radial velocity range of the line emitting material, in order to minimize the continuum (and sky) contamination and to allow a proper correction of the wavelength-dependent nonuniformities (interference fringes) by flat-fielding. The transmission curve of the filter should be examined to check that the line falls where the transmission is high and that there are no other emission lines within the filter bandpass. Regions of rapidly varying transmission (filter wings) should be avoided, since a small filter tilt or even the converging beam of the telescope can change the transmission considerably. In practice 20–50 Å wide filters can be used. Image quality interference filters exist in the ESO filter set for common emission lines. For the [OIII] λ 5007 and H α lines such filters are available to cover a range of redshifts for extragalactic objects. The continuum filter can be broader (100–200 Å) to increase the S/N ratio, but must be free of lines over its entire range. A (nuclear) spectrum of the source is a useful help in the filter selection.

It is advisable to take – at least – two exposures of the object in each filter to eliminate cosmic ray signatures and to check on the detection of faint features. Some observers offset the telescope slightly – a few arcseconds – between the first and second exposure. This allows to eliminate permanent CCD defects like bad columns, but requires rebinning of one image before it can be compared with the other one, thereby decreasing its resolution and therefore making the comparison of the two images more problematic. I prefer to take the two images in the same conditions as far as possible. Exposure times in the continuum filter can be shorter, e.g. inversely proportional to the filter width. Telescope focus should be checked frequently, since it changes during the night and with the filter thickness.

As usual, dark exposures should be taken and subtracted from the object exposures. The dark signal is so linear with the exposure time that it is sufficient to take darks at a few exposure times and interpolate between them. An exception to this linearity are the so-called "bias" exposures (i.e. 1 sec. darks), which have higher signal than expected from the extrapolation of longer dark exposures. This might be due to the heating of the CCD produced by its frequent reading while taking a series of very short exposures. Even the

technique of measuring the "bias" level from the "overscan" area of a CCD frame (i.e. the few columns following the physical pixels) must be used very carefully, since this area is contaminated by the signal in the rest of the CCD, because of charge transfer inefficiencies. There is in fact no need to measure and subtract the "bias" separately: the dark subtraction removes sufficiently well all *additive* components, before flat-fielding deals with the *multiplicative* ones. Small residuals would anyway be removed by the sky subtraction process. I have noticed that the dark signal increases considerably and shows an horizontal line in the middle of the field (for the RCAs) if the CCD has been exposed to high ambient illumination (e.g. while mounting it). This persistence effect can last for days. Simple precautions can be taken to avoid it.

Flat-field exposures should obviously be obtained for every filter. Good results can be reached with dome flats using day light. The illumination from internal lamps is usually not sufficiently uniform. Experience has shown that flat-fields and darks are good for a whole run, provided that no modifications are made to the CCD camera or to the filters on the filter wheels. Hopefully in the near future this will become true on longer time scales, so that the observer could take the calibration exposures from an archive.

A good spectrophotometric standard star (e.g. from Oke, 1974, *Ap.J. Suppl.* 27, 21) must be observed each night through all the filters used during that night. The star should be well exposed, but below saturation, and exposure times longer than 10 seconds should be used, so that the inaccuracy due to the uncertainty of the exact exposure time is negligible. If these two latter requirements are incompatible, it is acceptable to defocus the telescope.

Reduction Procedure

After the usual dark subtraction and flat-fielding, a major problem in the reduction of long exposure CCD frames is the elimination of cosmic ray signatures. These are not only a cosmetic problem,

but can affect considerably the flux measurement and are difficult to distinguish from stars in poorly sampled images (e.g. EFOSC). Cosmic rays can be removed by median filtering, but better results are obtained with the MIDAS command AVERAGE/WINDOW (FCOMPARE in IHAP). This command computes a special average of two or more aligned exposures: for each pixel the average is computed using only the pixel contents in the original frames, which do not deviate from the median of the contents of that pixel by more than an allowed uncertainty, related to the expected noise level. The other pixel contents are presumed to be contaminated and discarded from the average. Differences in exposure time and background level in the original images are accounted for by special frame descriptors. The allowed uncertainty is computed separately for each pixel and is made up of two parts: a constant one, which is related to the read-out noise and depends only on the input parameter BGERR, and a second one, which is related to the photon noise and depends on the pixel content through the input parameter SNOISE.

Table 1 lists the recommended values of these parameters for some of the CCDs commonly used at La Silla. These values have been derived empirically from the width of the main peak in the histogram of the difference between two short exposure darks (for BGERR) and of the difference of two well-exposed flat-fields (for SNOISE). They provide rejection of the cosmic ray signatures larger than four times the r.m.s. read-out noise or six times the r.m.s. photon noise. These rather high rejection thresholds ensure that the original images are modified only where it is strictly necessary. They can be lowered for some applications, like the cleaning of dark exposures. The higher threshold recommended for the photon noise allows for the differences in the original images which often occur in regions of large gradients (e.g. the wings of the stellar profiles) because of seeing variations or residual misalignments. It is useful to check the result of the AVERAGE/WINDOW command by comparing it with a normal average of the original

TABLE 1

CCD	Gain*	Read-out noise* e ⁻	Gain factor* e ⁻ ADU ⁻¹	BGERR	SNOISE
# 3	G50	40	10.5	10.4	1.40
# 5	G30	49	13.5	10.2	1.16
# 7	G100	18	6.0	5.6	1.65

* From "CCD detectors available at La Silla", ESO Techn. Rep. by P. Sinclair, June 1986.

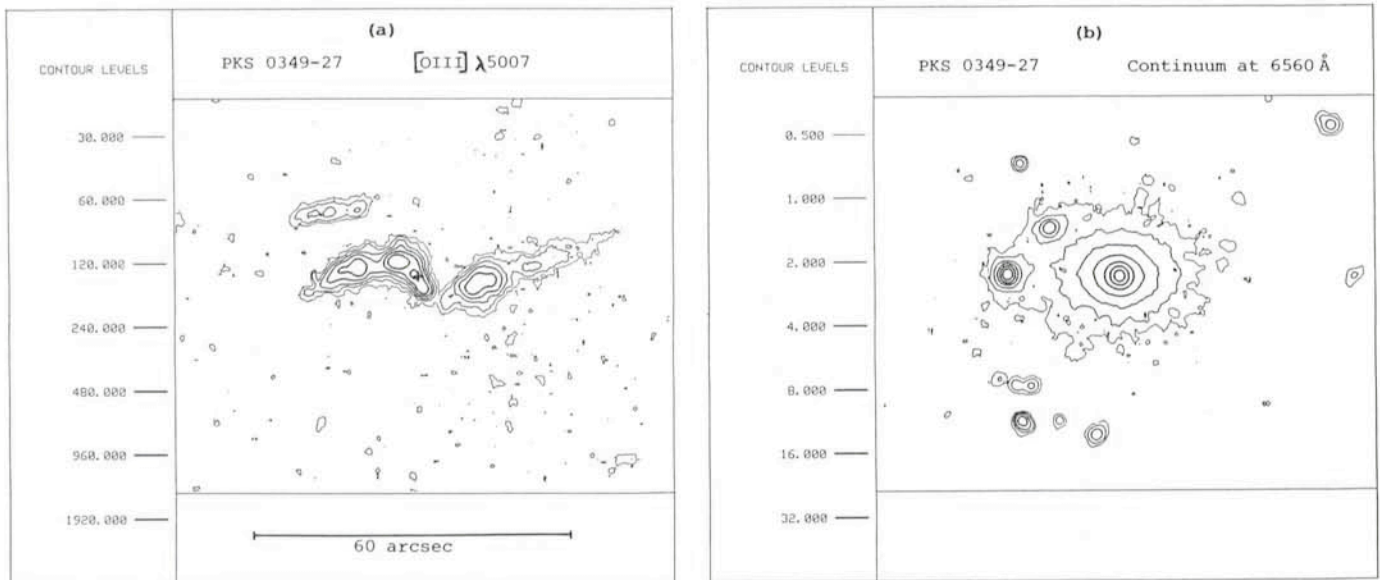


Figure 1: contour plots of $[OIII]\lambda 5007$ (a) and continuum (b) images of the radio galaxy PKS 0349-27 derived from CCD exposures obtained with the 2.2-m telescope at La Silla. The cross marks the position of the galaxy nucleus. Contour levels are listed on the left and are in units of 10^{-18} $\text{ergcm}^{-2} \text{s}^{-1} \text{arcsec}^{-2}$ for the line image and of $10^{-18} \text{ ergcm}^{-2} \text{s}^{-1} \text{\AA}^{-1} \text{arcsec}^{-2}$ for the continuum one.

CCD frames: the difference should be positive restricted to the pixels affected by cosmic rays. The input parameters to the AVERAGE/WINDOW command can alternatively be derived from the CCD characteristics:

$$BGERR = 2.75 \frac{N}{F}; \quad SNOISE = 4.25 \sqrt{\frac{1}{F}}$$

where N is the CCD read-out noise (in e^- , r.m.s) and F is the gain factor (in $e^- \text{ADU}^{-1}$).

As mentioned earlier, the "pure" line image is obtained – after sky subtraction – from the exposure in the line filter by subtracting a properly scaled copy of the continuum exposure. The determination of this scaling factor is a critical one, since the final line fluxes will depend strongly on it in the regions where the continuum is bright. Different methods can be used to derive the scaling factor, depending on the application. One is to ensure that stellar images are well subtracted, at least on average, in the final line – continuum image. Unfortunately it is usually not justified to assume that the spectrum of the continuum component of the object under study has the same shape than the average spectrum of the stars in the field. Moreover for extragalactic objects even a small redshift can change considerably the relative amount of continuum radiation falling in the two filters. A way to solve these difficulties for extragalactic objects is to use, instead of stars, other galaxies in the field at the same redshift as the object under study, but without emission lines. Clearly this method can be used only very rarely. The scaling factor can also be evaluated

by "trials and errors", that is by increasing it until one starts to have negative values in the line-continuum image. Good results are produced in this case only for objects which have regions of bright continuum but no line emission. A more general method, which I have finally adopted for the imaging of active galaxies, is to evaluate the scaling factor directly from the observations of the standard star and from the relative exposure times. The best results with this method are obtained if some assumption can be made on the shape of the continuum spectrum to be subtracted, so that differences in its average value in the two filters can be compensated for. For example in the case of radio galaxies, the spectrum of the "standard" elliptical galaxy given by Yee and Oke, 1978 (*Ap. J.* **226**, 753) has been used successfully.

Last but not least the images are flux calibrated using the observations of the standard star and the assumption that the latter were taken in the same conditions as the object exposures except for the airmass. First from the measured count rate C_s (in $e^- s^{-1}$) of the standard star and from its flux f_{is} tabulated in the literature we compute the equivalent area S :

$$S = \frac{h \cdot c \cdot C_s}{\int f_{is}(\lambda) \cdot A(\lambda, a_s) \cdot E(\lambda) \cdot \varphi \cdot d\lambda}$$

where A is atmospheric transmission for the airmass a of the observation ($A = 10^{-0.4aK(\lambda)}$, $K(\lambda)$ being the atmospheric extinction in magnitude per airmass) and E is the efficiency of the telescope + filter + detector combination, derived by multiplying the measured efficiencies of

the single components. Then the images of the object can be flux calibrated if an assumption can be made on the shape of its spectrum (within the filter band). Two cases are examined here:

1. In the line-continuum image the radiation from the object is concentrated at the wavelength λ_e of the emission line; then the flux F_{io} at λ_e can be computed from the measured count rate C_o :

$$F_{io} = \frac{h \cdot c \cdot C_o}{S \cdot A(\lambda_e, a_o) \cdot E(\lambda_e) \cdot \lambda_e}$$

2. For the continuum image the average flux density within the filter band is:

$$f_{io} = \frac{h \cdot c \cdot C_o}{S \cdot \int A(\lambda, a_o) \cdot E(\lambda) \cdot \lambda \cdot d\lambda}$$

For a good calibration it is important that the wavelength dependence of E is evaluated correctly. On the contrary, the absolute value of E is not critical. If an error of, say, a factor of two is made in the evaluation of the detector quantum efficiency, this factor is taken into account by the equivalent area S computed from the standard star observation and will not affect the flux calibration. If, on the other hand, even the absolute value of E is evaluated correctly (and the night is photometric), then S is equal to the collecting area of the telescope. For most of the standard star observations, which I have obtained with the CCDs at La Silla, S is equal to the collecting area of the telescope within 20 %. The value of S provides then a useful check on the instrument performance and on the observing conditions. For calibration of narrow-band images I have prepared a database of MIDAS tables containing filter

transmission curves, detector efficiencies, mirror reflectivities, etc. This database is useful also in the preparation of the observations for estimating

the exposure times.

Figure 1 shows the results of the application of these techniques to the imaging of a radio galaxy, showing how

well the ionized gas can be separated from the stellar component in a case where the two have a clearly different structure.

Velocity and Velocity Dispersion Fields of NGC 6684: An SB0 Galaxy with a Ring

D. BETTONI, Astronomical Observatory of Padua, Italy

G. GALLETTA, Astronomy Department, University of Padua, Italy

1. Observations

NGC 6684 is a southern S0 galaxy of magnitude $B = 11.35$ showing a bright bar aligned about 20° from the minor axis of the disk and encircled by an elongated luminous ring ($b/a = 0.77$). This galaxy has been observed within a programme of study of stellar motions in barred galaxies, a subject which in the recent years has been analysed by many theoretical works but that has been studied observationally only by few authors. Among the galaxies for which the whole stellar velocity field is known, the velocity dispersion field has been studied only for NGC 936 (Kormendy, 1984).

NGC 6684 was observed in May 1983 and March 1984 at the 3.6-m telescope of the European Southern Observatory at La Silla, Chile. The spectra were taken using the Cassegrain Boller and Chivens spectrograph plus a 3-stage EMI image tube and setting the slit at four different position angles corresponding to the apparent major and minor axes of the disk, the bar major axis and to a P.A. at 45° from the major axis. The spectra of some early K-type giant stars were recorded each night, for use in the reductions as template stars of zero velocity dispersion. The exposure times were ranging from 30 to 55 minutes. The slit was set to a width of 1.5 arcseconds on the sky and to a length of 1.9 arcminutes. The plate scale along the slit image was $38.5 \text{ arcsec mm}^{-1}$, and the dispersion was 39 \AA/mm .

The spectroscopic observations of the galaxy were associated to a morphological study based on two 15-minute V frames taken with the 320×512 RCA CCD of the 1.5-m Danish telescope on the night of May 6/7, 1986 and on the analysis of the galaxy images on ESO (B) and ESO/SRC (J) charts. In the following we describe some of the more interesting results arising from our observations.

Data Reduction and Analysis

All the spectra have been digitized with the ESO PDS microdensitometer using a $12.5 \times 50 \mu$ slit and considering a wavelength interval of $3800\text{--}4500 \text{ \AA}$. No emission lines were detected in the spectra, but Ca II H and K absorption and G-band are well defined. All the PDS images were calibrated in intensity and wavelength and sky subtracted using the ESO-IHAP procedure at the Padova HP computer centre. The result-

ing images were continuum flattened and analysed with the Fourier Quotient Technique described in Bertola et al. (1984), giving simultaneously the radial velocity, the velocity dispersion and the line-strength parameter for each scan line of each spectrum. The curvature of the spectral lines has been measured from a full slit comparison spectrum by measuring with the Grant 2 coordinate machine of ESO the position of 12 spectral lines. It has been found quite negligible, producing a shift lower than

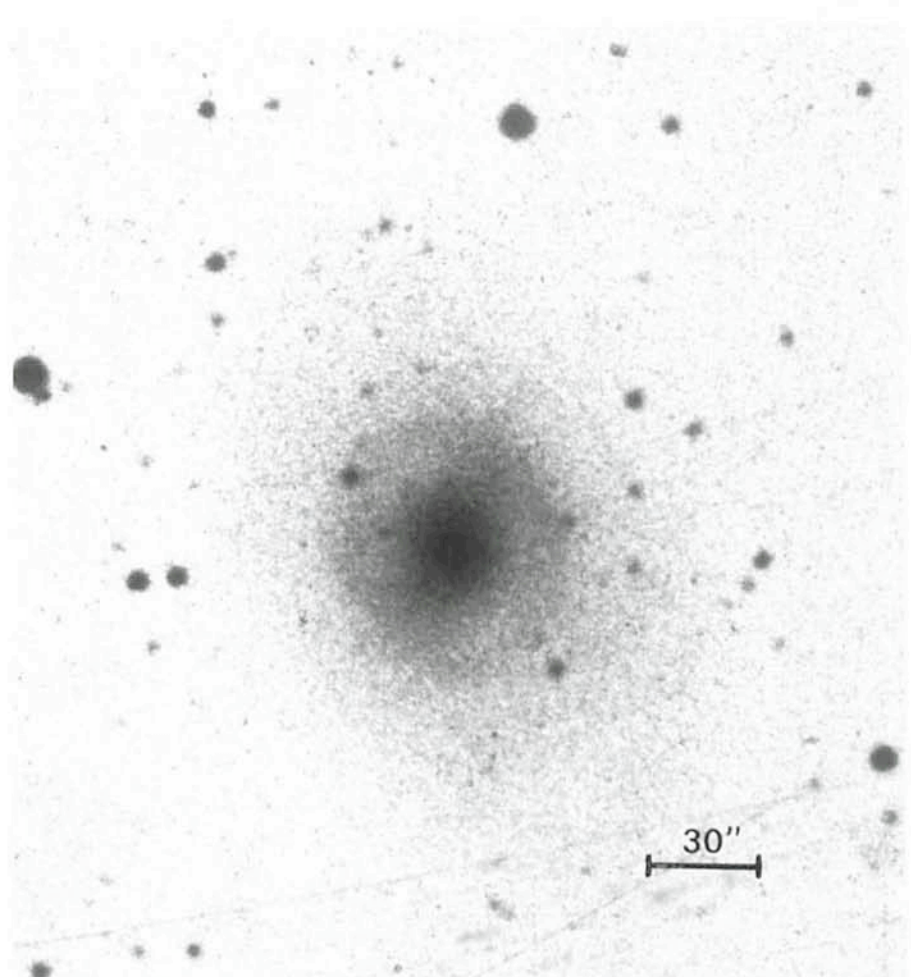


Figure 1: Image of NGC 6684 from ESO (B) chart.

TABLE 1: Intrinsic shape of the single component of NGC 6684, as deduced from the isophote flattening and orientation. The lines of the nodes have been assumed at $\Phi = 42^\circ$, P.A. of the disk, and the inclination of the galactic plane is $i = 48^\circ.4$.

component	OBSERVED PARAMETERS			INTRINSIC PARAMETERS				PROJECTED VALUES	
	q_o	$(\Phi - \Phi_n)_o$	r	δ	q	p	R	q_c	$(\Phi - \Phi_n)_c$
disk	0.69 ± 0.03	$0^\circ \pm 5^\circ$	—	0°	0.250	1.000*	—	—	—
bar	0.60 0.04	$108^\circ 2^\circ$	$30''$	102°	0.443	0.454	$44''$	0.600	108.0
ring	0.77 0.01	$174^\circ 2^\circ$	$37''$	102°	0.000*	0.847	$54''$	0.766	172.7
bulge	0.83 0.03	$166^\circ 8^\circ$	$10''$	159°	0.817	0.824	$11''$	0.830	166.0

* values assumed.

10 km/s for points having $r \leq 30''$ from the nucleus. All the velocities have been corrected to the Sun. The mean velocity and velocity dispersion of the nucleus are found to be $V_o = 866 \pm 22$ km/s and $\sigma_o = 93 \pm 12$ km/s respectively. The mean nuclear velocity is slightly higher than previous determinations for the redshift of NGC 6684: 812 ± 30 km/s (Corwin and Emerson 1982) and 823 km/s (de Vaucouleurs et al. 1976, RC 2).

The above data allow us to produce maps of the velocity dispersion and velocity fields. These are reproduced on the same scale in Figures 2 and 3 respectively. To analyse the large-scale kinematical features of the galaxy, all the data have been smoothed with a gaussian weighting function ($\text{FWHM} = 4''$) and rebinned at $3''$ interval before being plotted in the maps. The velocities are scaled to the systemic velocity and lines of equal velocity and velocity dispersion have been drawn interpolating by eye from the observed values. In the case of the velocity field, the curvature of the outer lines has been assumed from the estimate of the P.A. corresponding to the maximum velocity gradient made in the next paragraph. For the velocity dispersion we tried to show the elongation of the equivelocity lines due to the presence of the bar with respect to the more symmetric structure of the bulge + disk component.

The shape and the orientation of the four galaxy components (disk, ring, bar and bulge) has been measured on the CCD frames and on the ESO/SRC (J) and ESO (B) charts (Fig. 1), producing the mean values listed in the three first columns of the Table 1. They are, for each component: the observed axial ratio q_o , the position angle φ of the major axis (referred to that of the disk) and its extension r. Analysing the light distribution, we observed the presence of a progressive shift of the bar isophote to the NW, indicating a displacement of the bar centre with respect to the galaxy nucleus. The amount of this displacement has been evaluated as $2''$ to the NW. The

mean values listed in Table 1 were analysed in order to deduce the intrinsic shape of the light distribution. Since each one of the isophotes could be considered as the projection of an ellipsoidal shell with intrinsic axial ratios $q = c/a$, $p = b/a$ ($a > b > c$), it is possible

in principle to deduce the values of q and p by deprojecting the observed ellipticities and position angles. This is a simple geometrical problem which allows only one solution, providing that the orientation angles of each ellipsoid with respect to the line of sight are de-

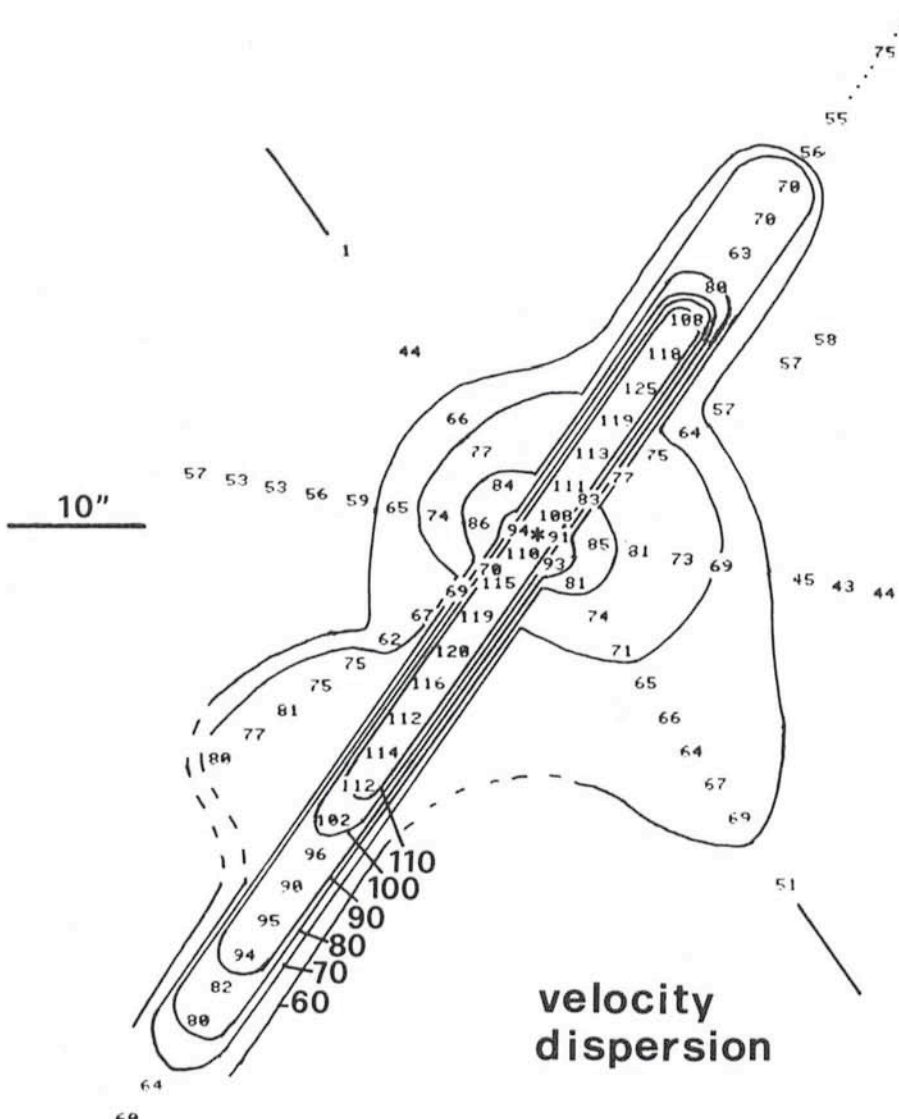


Figure 2: Map of the measured velocity dispersion. The original values have been smoothed with a gaussian weighing function ($\text{FWHM} = 4$ arcsec) and rebinned each 3 arcsec before being plotted in the maps. Lines of equal velocity dispersion have been drawn interpolating by eye from the observed values and taking into account the geometry of the system (bar+disk). An asterisk represents the position of the nucleus. The direction of the disk's major axis (full line), that of the bar (dotted line) and the scale of the image are shown.

fined (see Williams 1981, and Galletta 1983). The only exception to the uniqueness of the solution is the indeterminate case where the observed P.A. coincides with the line of the nodes. The analysis is composed by three main steps: First, from the apparent flattening of the disk, assuming an intrinsic axial ratio of 0.25 (Sandage et al. 1970), we deduce its inclination with respect to the plane of the sky and the P.A. φ_n of the line of the nodes. This produces the values $i = 48.4^\circ$ and $\varphi_n = 42^\circ$ respectively. Second, by means of these values we deproject on the plane of the galaxy all the distances r and the P.A. φ observed on the sky and we define, as a first approximation, the true extention R of each component of NGC 6684 and the angle δ formed by its major axis with the line of the nodes. Finally, synthetic isophotes are produced with different values of q and p and the resulting flattenings and P.A. are compared with the observed values of Table 1, until a satisfying agreement within the measuring errors is found. The values so obtained are indicated in Table 1, columns from 5 to 7, and the ranges of acceptable solutions are shown in Figure 4.

Discussion

The velocity dispersion field (Fig. 2) shows that σ is always decreasing outward, with the exception of the bar, where a narrow substructure of constant velocity dispersion (about 104 km/s) is seen. Since the bar is close to the zero velocity line, we can expect that the observed amplitude of the velocity dispersion is due to the sum of the stellar streamings along the bar. Contrary to the velocity map, the inner velocity dispersion field appears more symmetric around the nucleus instead of around the symmetry point of the velocities. If this effect is real, it indicates a quite complex velocity field.

The map of the velocity field shows two interesting features: First, the mean rotation at P.A. = 35° (near the major axis) and P.A. = 80° shows almost equal velocity values, an indication of elliptic orbits. An interpolation of the velocities observed outside the bar with a kinematical model of coplanar and elliptic orbits produces lines of equivelocity with a maximum velocity gradient at P.A. = 59° , 17° away from the direction of the disk major axis (see Fig. 3). Since at the maximum extent of the map ($\sim 40''$ from the nucleus) the light of the bulge dominates, we must suppose that the bulge of NGC 6684 possesses elliptic orbits. Second, the line of zero velocity, aligned with the bar, follows a pattern symmetric with respect to a

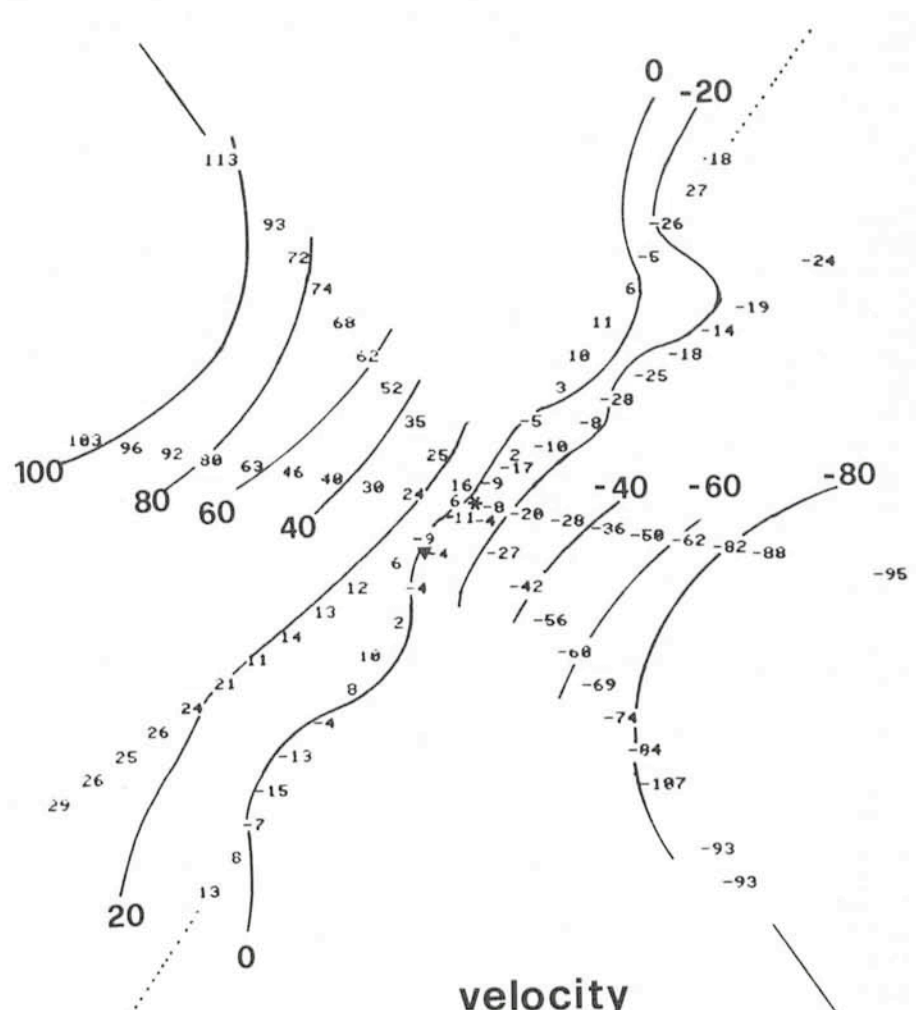


Figure 3: The same as in Figure 1, but for the rotation curves. All the velocity values are scaled to the systemic velocity. A small triangle represents the approximate position of the symmetry point of the rotation curves.

point not coincident with the galaxy nucleus. The position of this symmetry point, at about $4.5''$ SE from the nucleus, is indicated in Figure 3 with a small triangle. Obviously this asymmetry is not due to oscillations of the velocity values because of the measuring errors. As said in the previous paragraph, a similar displacement from the nucleus has been observed also in the light distribution of the bar, but at NW, at the other side with respect to the symmetry point of the kinematics. This type of displacement between the bar, the optical nucleus and the centre of symmetry of the rotation curves is typical of Magellanic-type and late-type barred spirals, where it is connected with the presence of one or two points of equilibrium in the gravitational field. In barred S0s, kinematical asymmetries like that of NGC 6684 have been reported for NGC 936 (Kormendy 1983), but in a system where the bar isophotes do not show any asymmetry with respect to the nucleus of the galaxy. We can then suppose that the symmetry point observed in NGC 6684

could represent, with respect to the system bar + bulge, something like a Lagrangian point in the three-body problems of celestial mechanics. The shape

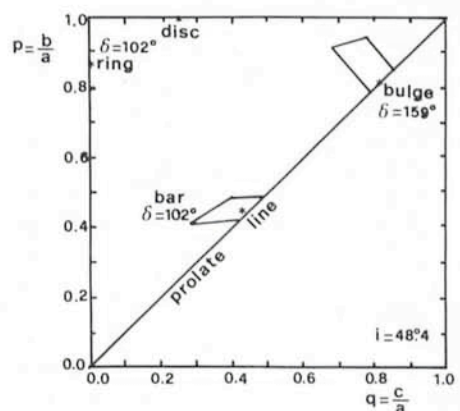


Figure 4: Areas of possible solutions, in the plane $c/a - b/a$, for the intrinsic flattenings of each component of NGC 6684, as coming from our analysis of the geometry of the system. The asterisks indicate the exact solutions found or adopted. The angle on the plane of the galaxy is also indicated.

of the isovelocity lines with $|v| \leq 20$ km/s is similar to that expected for the family of long axial orbits moving within the bars.

A geometrical model which can reproduce the shape of the isophotes has also been attempted, as described in the previous paragraph, by interpolation of the galaxy isophotes. From it results that (see Fig. 4 and Table 1): (1) The disk is probably oblate in shape. Despite the lack of kinematical information, its P.A. remains constant even if the flattening changes slightly, a feature typical of axisymmetric systems. (2) The bar is almost prolate, having similar axial ratios ($q = 0.44$, $p = 0.45$). (3) The ring cannot be circular, since it appears rounder

than the disk and slightly misaligned. Its flattening and orientation are consistent with an elliptic structure aligned with the bar axis and with axial ratio 0.847. (4) According to the kinematics, the bulge could be triaxial. From the analysis of the possible solutions, excluding shapes as flat as the disk, we found a possible axial ratio of $q = 0.817$, $p = 0.824$, almost prolate, and elongated on the plane of the disk at 57° from the bar axis. But the roundness of its isophotes makes this last result quite uncertain.

A more complete analysis of the data is now in progress and will be compared with the data for the other SB0 systems included in the programme.

References

- Bertola, F., Bettoni, D., Rusconi, L., Sedmak, G., 1984, *Astron. J.*, **89**, 356.
- Corwin, H.G.Jr., Emerson, D., 1982, *Mon. Not. R. Astron. Soc.*, **200**, 621.
- de Vaucouleurs, G., de Vaucouleurs, A., Corwin, H.G.Jr., 1976 (RC 2), *Second Reference Catalogue of Bright Galaxies* (Austin, University of Texas Press).
- Galletta, G., 1983, *Astrophys. Space Sc.*, **92**, 335.
- Kormendy, J., 1983, *Astrophys. J.*, **275**, 529.
- Kormendy, J., 1984, *Astrophys. J.*, **286**, 132.
- Sandage, A., Freeman, K.C., Stokes, N.R., 1970, *Astrophys. J.*, **160**, 831.
- Williams, T.B., 1981, *Astrophys. J.*, **244**, 458.

IDS Spectroscopy of Planetary Nebulae

A. ACKER, *Observatoire de Strasbourg, Centre de Données Stellaires, France*

B. STENHOLM, *Lund Observatory, Sweden*

I. Introduction

From 1982 to 1984, Lundström and Stenholm conducted low-resolution spectroscopy of faint emission-line objects in the southern Milky Way (see Lundström, Stenholm, 1984). Their experience showed that the IDS is very efficient for spectroscopy of faint emission-line objects. They established that a mean exposure time of 10 minutes permits a clear classification of the observed objects, and a study of their most intense lines. Based on this study, we have undertaken, since 1984, a spectroscopic survey of the planetary nebulae. This study has been conducted with a double aim:

- realization of an atlas of calibrated spectra, within the framework of the forthcoming *Strasbourg-ESO Catalogue of Galactic Planetary Nebulae*;
- a statistical study of properties of the nebulae, in relation with problems of stellar evolution.

That means that most of the 1,500 objects known (1,100 in the southern sky) should be observed, essentially at La Silla, and at the Observatoire de Haute-Provence for the northern objects.

Status reports showing the earlier situation were given by Stenholm (1986), and Stenholm, Acker (1987).

The apertures used are very small; most objects are, however, stellar-like, and this majority of objects is also the less observed part of the whole group. On the other hand, extended objects, particularly those of low surface brightness, are difficult to observe in this manner (10 minutes per object, in order to execute the programme during a reasonable period of time).

Table 2 presents the number of objects observed within each allocated observing run.

Here, we will report only about the observations done at La Silla. The status of the project is shown in the diagram in Figure 1. The reductions are carried out with the IHAP programme, working on the HP 1000 computer at La Silla, in Garching, at the Observatoire de Haute-Provence, and at the Institut de Physique du Globe de Strasbourg. Up to now, we have reduced all 723 spectra obtained at La Silla and measured line intensities for 220 of them.

Table 1: *Instrument Configurations*

	European Southern Observatory (ESO)	Observatoire Haute-Provence (OHP)
Telescope	1.52 m	1.93 m
Spectrograph	Boller & Chivens	CARELEC
Detector	IDS	CCD
Number of useful pixels	2053	511
Aperture	$4 \times 4''$	$2.5 \times 4''$
Approximate wavelength range	400–740 nm	385–740 nm
Dispersion	17 nm/mm	26 nm/mm
Approximate resolution	1 : nm	1 : nm
Normal exposure time	10 min	10 min

II. The Observations and Reductions

In Table 1, some instrumental and observational parameters are summarized.

Table 2:

LA SILLA		Observatoire de HAUTE-PROVENCE	
Telescope time	Number of observed objects	Telescope time	Number of observed objects
1983 (05) and 1984 (04) (9 nights)	127	1986-07-28 – 1986-08-5 (8 nights)	74 (12 southern)
1985-07-15 – 1985-07-21 (6 nights)	112	1986-12-19 – 1986-12-24 (5 nights)	61
1985-07-27 – 1985-08-05 (8.5 nights)	100	1987-03-06 – 1987-03-12 (6 nights)	5 (very bad weather)
1986-01-18 – 1986-01-25 (7 nights)	146		
1986-07-08 – 1986-07-14 (6 nights)	167		
1986-12-10 – 1986-12-16 (6 nights)	71		
Time given for period 39: 1987-07-12 – 1987-07-16 1987-07-20 – 1987-07-25 (9 nights)	723		140

lines with H α , the sulfur doublet around 672 nm, and the green [O III] doublet. As the instrumental profile is not gaussian, the total area A of the observed lines is larger than the sum S of the calculated gaussian components. We have found the following mean value of the ratio A/S = 1.038 \pm 0.05.

We have corrected the calculated blended area for this effect.

3. The Nonlinearity of the IDS System

M. Rosa (1985) and E.J. Wampler (1985) pointed out that the response of the IDS system shows a dependence with the value of the input-intensity.

Our measurements (Table 3) show that the observed and theoretical line ratios are equal for the [N II] lines, but differ for the [O III] doublet, in an identical way as that given by Rosa. However, this author proposed that the theoretical ratio is likely to be around 3.03. On the other hand, for a few very bright nebulae (NGC 5315, 6210, 6891, IC 4997), the very intense lines of [O III] flux $> 2.10^{-13}$ W/m²/nm) show a ratio equal to 2.9 \pm 0.2.

We have also compared our results with those of Gutierrez-Moreno et al. (1985). The ratio of our intensities to those of Gutierrez-Moreno has the following values:

NGC 5873 (16 lines): 0.91 \pm 0.21

NGC 5882 (17 lines): 1.21 \pm 0.32

IC 1297 (14 lines): 1.03 \pm 0.24

In conclusion, we calculate the line intensities relative to I(H β) = 100, without correction in a first step. Later we will refine this study with a larger number of reduced spectra.

all, to separate "true" planetary nebulae from misclassified ones. In two recent papers (Stenholm and Acker, 1987; Acker, Chopinet, Pottasch, Stenholm, 1987) we have shown, through our survey and IRAS data, and following com-

ments in the literature, that 196 are surely misclassified planetary nebulae, and 60 others are possibly not planetary nebulae. About one fourth of the misclassified planetary nebulae are in fact symbiotic or possible symbiotic stars;

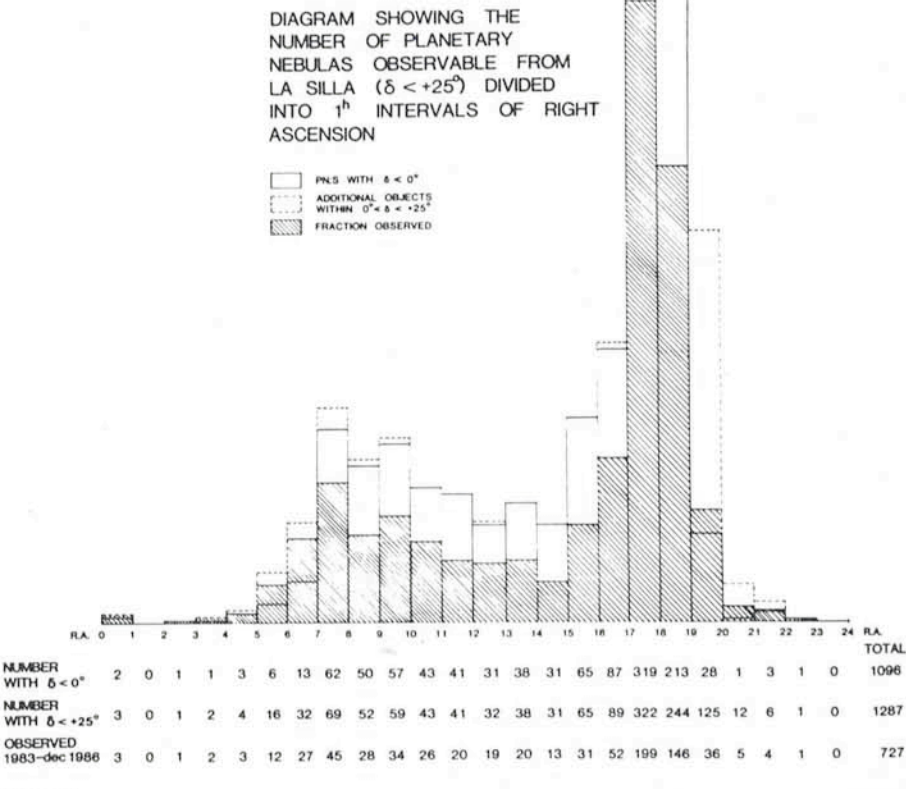


Figure 1.

IV. First Astronomical Results

1. Misclassified Planetary Nebulae

The qualitative analysis of the now 850 observed spectra permits, first of

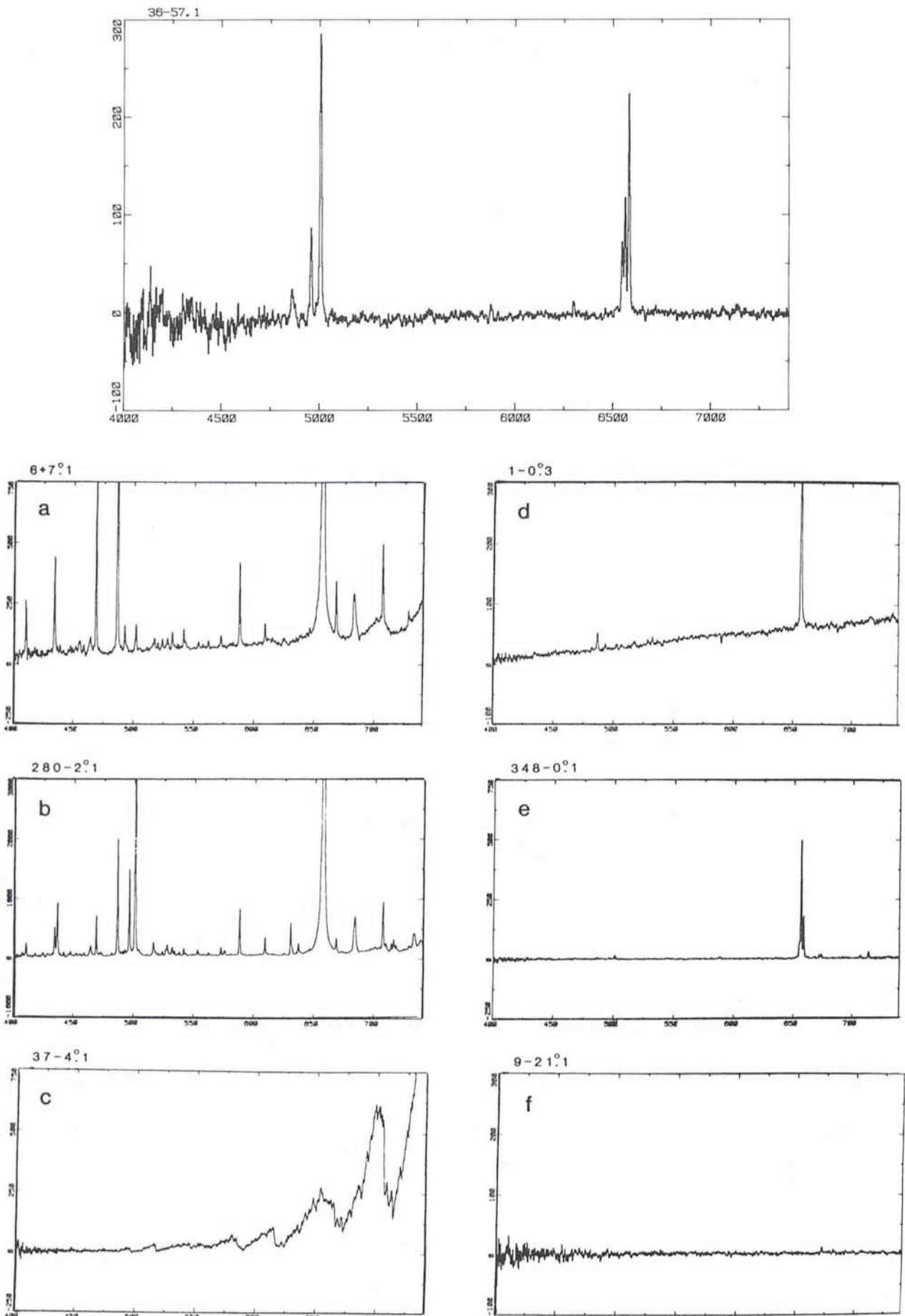


Figure 2: As examples only we present here some objects, previously catalogued as planetary nebulae, but dismissed as such in this paper. (a) and (b) show symbiotic stars, the latter with [OIII] lines (as in planetary nebulae) but otherwise characteristic of a symbiotic star; (c) is a late-type star showing broad molecular absorption bands; (d) is a H α emission star; (e) is a HII region; and (f) is a galaxy, only a faint, red-shifted H α line seen. Compare with the spectrum of a typical planetary nebula at the top.

results concerning nine of these stars are given in Acker, Lundstrom, Stenholm (1987). Other objects are galaxies (19), HII regions (22), plate faults (10), reflexion nebulae, late-type stars, emission-line stars, etc.

The misclassified objects are found mainly in the following discovery lists: Kohoutek (43 objects), Henize (He -2: 31 objects), ESO (30 objects), Wray (23), Haro (H2: 15 objects).

Figure 2 presents some objects compared to a classical planetary nebula.

2. Determination of Physical Properties of the Planetary Nebulae (in collaboration with J. Köppen and G. Jasniewicz)

Some of the measured line ratios allow, after reddening correction, the determination of the electronic temperature and density ([OIII] 4363/5007, [NII] 6583/5755, [SII] 6716/6731). In addition, if a sufficient number of lines are available, it is possible to estimate ionic abundances, computed through a theoretical model. J. Köppen has written a programme called "HOPPLA", used on the IBM 3081 K computer at the

Table 3:

Lines	Theoretical line ratio	Observed line ratio
[OIII] 5007 4959	2.88	3.04 ± 0.27 (185 PN)
[NII] 6583 6548	2.94	2.9 ± 0.5 (146 PN)

"Centre de Calcul de Strasbourg, CNRS".

From the first sample of about 200 spectra, it seems that for 27 objects the abundances are well determined; for 46, the data could be better, and for the other spectra, the parameters are poorly determined. Say one third of all observed objects can be used for further work.

This very homogeneous and reliable material will be treated statistically, with the collaboration of G. Jasniewicz, regarding galactic gradients and problems of stellar evolution. The first results of this kind will be presented at IAU Symposium 131, devoted to planetary nebulae, and held in Mexico in October 1987.

References

- Acker, A., Lundström, I., Stenholm, B.: 1987, *Astron. Astrophys.*, submitted.
- Acker, A., Chopinet, M., Pottasch, S.R., Stenholm, B.: 1987, *Astron. Astrophys.*, submitted.
- Gutierrez-Moreno, A., Moreno, H., Cortes, G.: 1985, *P.A.S.P.* **97**, 397.
- Lundström, I., Stenholm, B.: 1984, *The Messenger*, **37**, 35.
- Rosa, M.: 1985, *The Messenger*, **39**, 15.
- Stenholm, B.: 1986, Report VIII, Journée de Strasbourg "Les nébuleuses planétaires", Publ. Observatoire de Strasbourg p. 25.
- Stenholm, B., Acker, A.: 1987, *Astron. Astrophys. Suppl. Ser.* **68**, 51.
- Stenholm, B., Acker, A.: 1987, Proc. of the workshop on planetary nebulae in Frascati, Sept. 1986 (in press).
- Wampler, E.J.: 1985, *The Messenger*, **41**, 11.

ESO Exhibition in Brussels Visited by King Baudouin

An exhibition about the European Southern Observatory was organized in a collaboration between ESO, the Brussels Planetarium and the Belgian National ESO Committee. It was shown on television and was visited by a large public. The exhibition was originally scheduled to last from June 6 to 15, 1987, but due to the large interest (more than 1,500 visitors in two days!), it was prolonged until June 26.

It was a particular honour to receive a visit on June 9 by the Belgian Head of State, King Baudouin I, and by the Belgian Ministers of Education, Messrs. D. Coens and A. Duquesne. They were shown around by Prof. C. de Loore, President of the Belgian National ESO Committee. The King, who since long takes an active interest in astronomy, was informed about ESO and its future projects, especially about the Very Large Telescope, and expressed appreciation of the pictures and models on display. The King was presented with some large colour pictures of spectacular objects in the southern sky which had been specially prepared by ESO for this occasion. The King's visit was given wide coverage in the media.

The exhibition was opened by two delegates of the Belgium Ministry of

Education on Friday, June 5, in the presence of the members of the ESO Coun-



Dr. J.-P. Swings and Prof. C. de Loore explain the ESO VLT model to King Baudouin and the Belgian Ministers of Education, Messrs. D. Coens and A. Duquesne.

cil, who had met in Brugge the day before. The brief ceremony, with presentations by the delegates, by the Director-General of ESO, Prof. L. Woltjer, and by Prof. C. de Loore, was followed by a well-attended Press Conference.

More than 100 large colour photos (including many beautiful exposures of nebulae, galaxies, etc.) illustrated the scientific and technical activities of ESO and were accompanied by comprehensive texts. Recent results were shown, including Comet Halley and, not the least, the bright supernova in the Large Magellanic Cloud. The exhibition also featured large-scale models of ESO's NTT and VLT projects.

This year marks the 25th anniversary of the European Southern Observatory, which was founded in 1962 to foster cooperation in astronomy and to provide European scientists with a major modern observatory.



OPTOPUS Observations of Quasar Candidates

S. CRISTIANI, ESO, and Istituto di Astronomia della Università di Padova

1. Introduction

OPTOPUS is a fiber-optic instrument for multiple-object spectroscopy with the Boller & Chivens spectrograph and a

CCD detector at the 3.6-m telescope. The system has been described in detail by the Optical Instrumentation Group (1985, *The Messenger* 41, 25). Its application for observing Halley's comet has

been reported by Lund and Surdej (1986, *The Messenger* 43, 1). Here another "classical" use of multiple-object spectroscopy is presented: follow-up observations of quasar candidates.

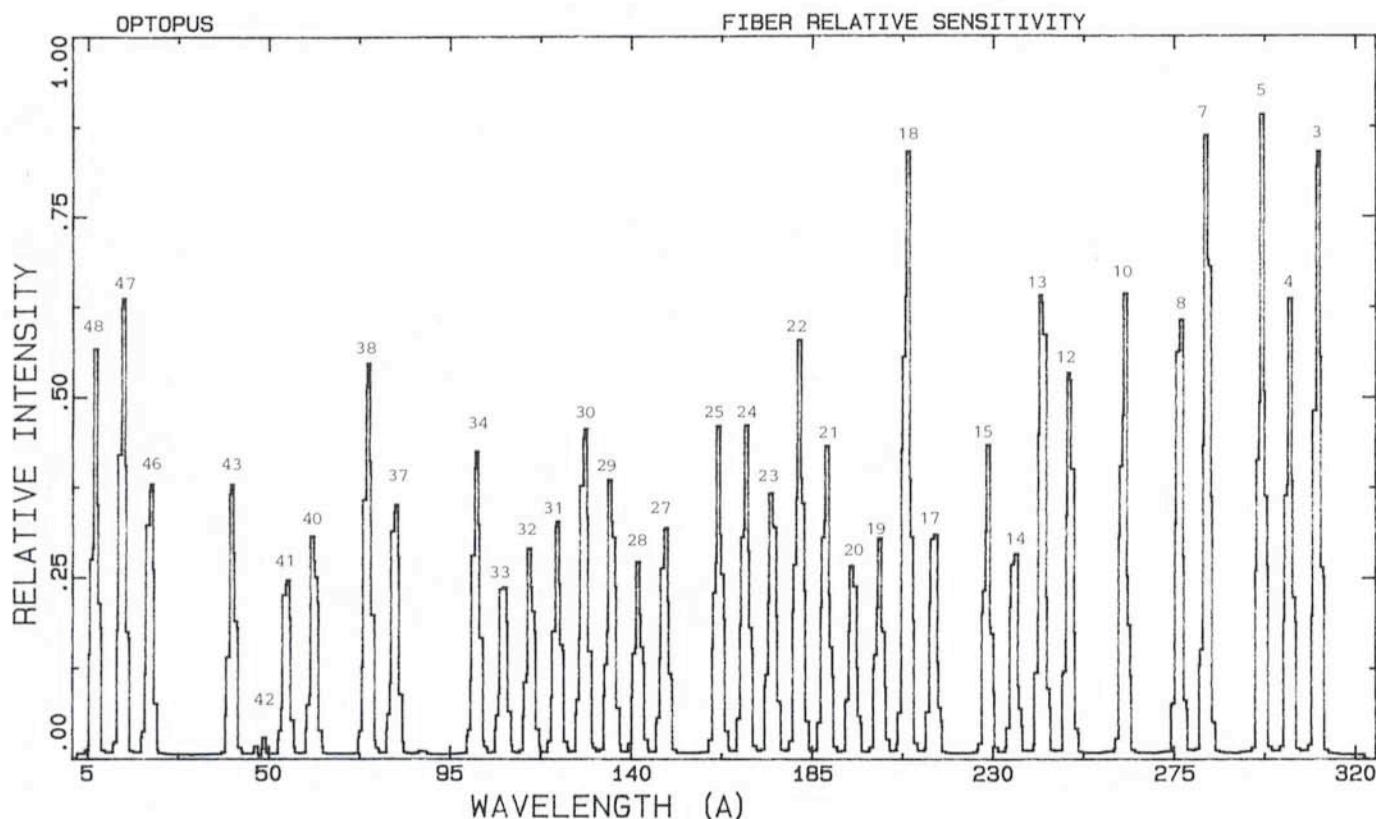


Figure 1: A plot of the relative sensitivity of the fibers, as derived from flat field exposures. Fiber 41 corresponds to a "bad" column on CCD 3.

2. Searching for Quasars

Colour anomalies (especially ultraviolet excess), variability and presence of strong emission lines in the spectrum are the optical criteria mostly used to distinguish quasar candidates from stars. Automated techniques, developed in the last years and applied to photographic plates or CCD transit surveys, yield a considerable number of quasar candidates, potentially providing the basic information to solve many questions about the universe. Slit spectroscopy, however, is required to confirm those candidates and obtain reliable measurements of their redshifts. This is the true bottle-neck of the process: the great discrepancy between the two hours at a Schmidt telescope needed to expose a good objective-prism plate, which will provide some hundreds of quasar candidates, and the about 100 hours required with a 4-m-class telescope, in order to check them spectroscopically one by one.

3. Observing with OPTOPUS

The possibility of taking spectra of many objects at the same time may mitigate the problem. As a matter of fact, the advantage of using a multi-object spectrograph depends on the combination of two factors: efficiency (limiting magnitude) and size of the ob-

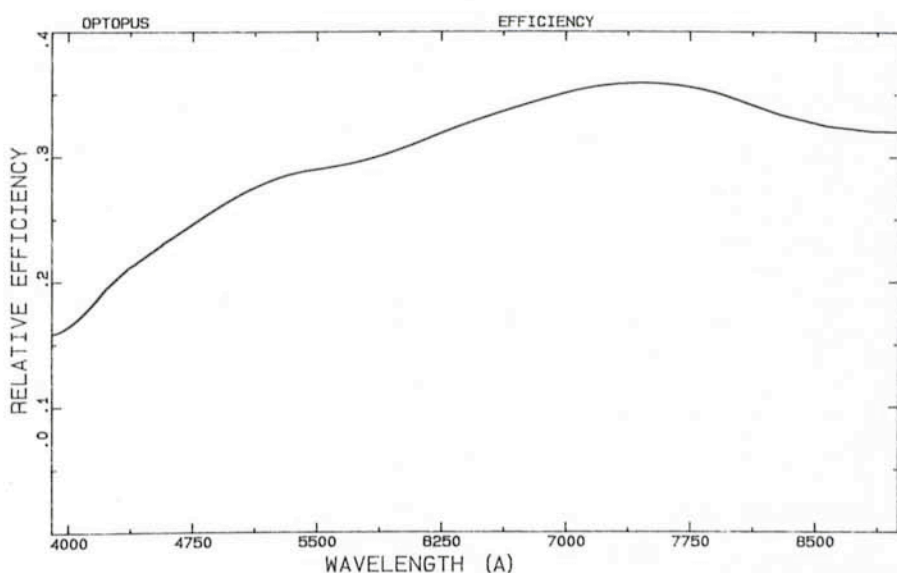


Figure 2: The absolute efficiency of OPTOPUS. It takes into account losses due to fiber/object misalignment and material absorption in the fibers.

servable field. In other words, one needs a decent number of interesting objects in the observable field, in order to justify both the observing time spent in changing templates and plugging fibers and a careful preparation of the observations (measuring accurate positions of the targets, finding the guide stars, having ready the observing plan well in advance).

In the case of OPTOPUS the observable field is a circle of 33 arcmin diameter,

in which a maximum number of 47 fibers can be plugged for spectroscopy with some topological restriction. The limiting magnitude is a function of the dispersion and will be discussed below.

Around Christmas 1986 OPTOPUS was used to observe some quasar candidates in the SA 94 field (see Barbieri and Christiani, 1986, *Astron. Astrophys. Suppl. Ser.* **63**, 1; and Barbieri, Cristiani, Iovino, Nota, 1987, *Astron. Astrophys. Suppl. Ser.* **67**, 551). In order to max-

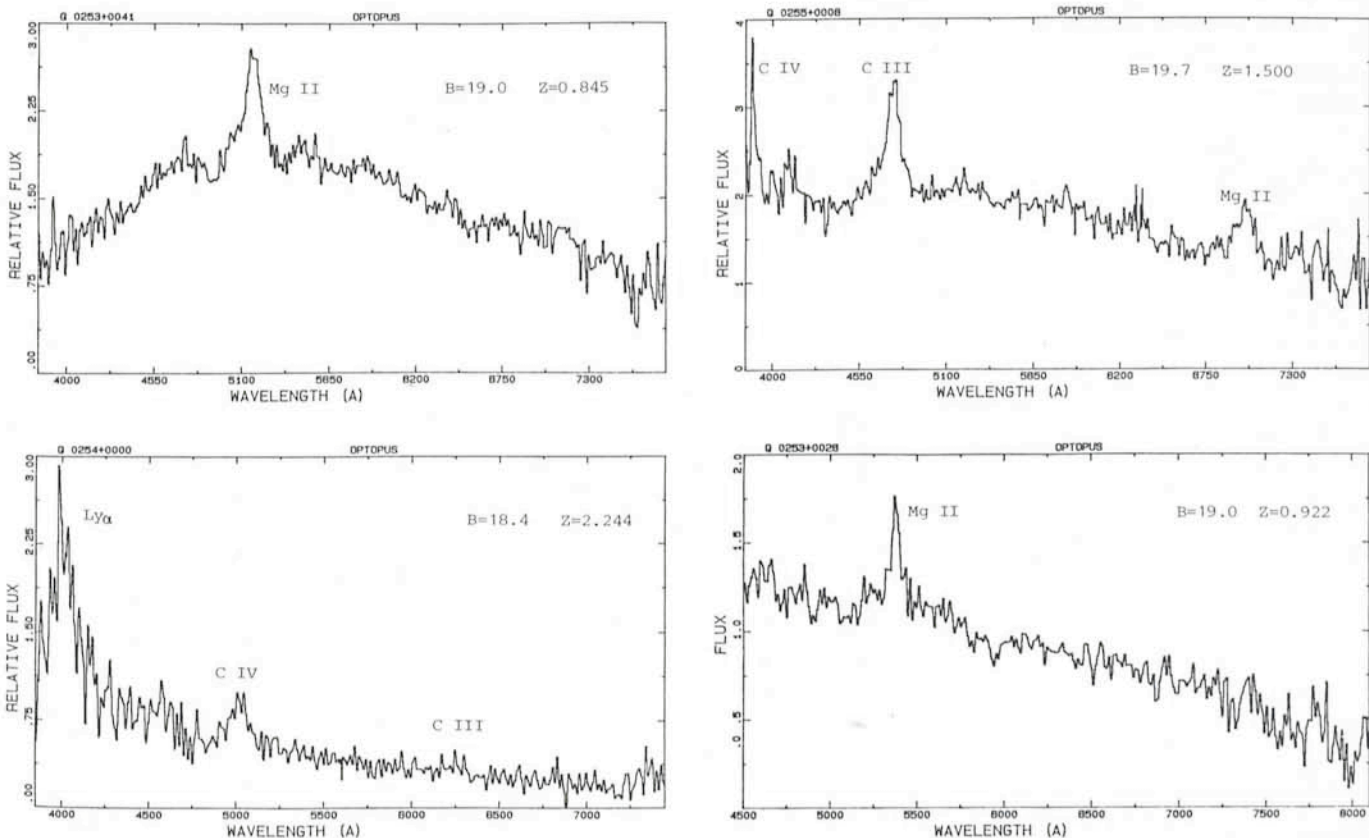


Figure 3: Spectra of four quasars obtained with OPTOPUS.

imize the efficiency of the system, a dispersion of 450 Å/mm was chosen. Not all the fibers have the same sensitivity, as shown in Figure 1, therefore fainter objects were assigned better fibers.

As a by-product of the observations, the absolute efficiency of OPTOPUS was derived. From the spectro-photometric calibration of some objects in the observed SA 94 fields it was possible to obtain the system response curve, which, compared with the one previously derived for the Boller & Chivens spectrograph in the normal slit configuration with the same grating and detector, provides the result of Figure 2.

4. Data Reduction

The reduction of OPTOPUS data is carried out very much in the same way used for slit spectra. Only the sky subtraction requires some additional care, especially at magnitudes fainter than $B = 18$.

An evaluation of the sky background corresponding to each fiber can be

accomplished by offsetting the telescope about one arcmin away from the actual field (at high galactic latitudes the probability of getting another object in the aperture corresponding to the fiber is negligible) and exposing for a convenient time. However, it is well known that the sky emission is neither constant during the night, nor uniform all over the sky. A better estimate can then be obtained by combining different sky exposures taken during the night, say one at the middle and one at the end of the night, and using a few fibers to monitor the sky during the "object-exposure".

5. Results and Final Considerations

Sixty objects, down to $B = 19.7$ were observed in two fields during the December 1986 run. Seven of them turned out to be quasars; four are shown in Figure 3. The result is not at all disappointing, since the experiment mainly aimed at checking that no low-redshift

quasars are missed by the usual UV excess criteria.

The performances of the instrument turned out to be better than expected: from these observations it appears possible to reach $B = 20$ with a spectral resolution of 25 Å and a $S/N > 5$, by taking two exposures of one hour for each field (in order to filter out cosmic rays) and properly subtracting the sky background as described above. At this limit, about ten quasars per template are expected. Using an efficient slit spectrograph like EFOSC, assuming a success rate of 50 per cent (required for an honest completeness) and 15 minutes exposure time per candidate, it would require about 5 hours of frantic work to do what can be accomplished in 3 hours of more relaxed OPTOPUS observations. Of course EFOSC allows much greater flexibility and OPTOPUS observations have to be carefully planned with large advance, nevertheless, the fiber-optics spectrograph offers a valuable possibility which should not be neglected by the observers.

An efficient aid in preparing observing proposals and runs, as well as the papers which follow:

SIMBAD, the CDS Database

A. HECK and D. EGRET, C.D.S., Observatoire Astronomique, Strasbourg, France

Preparing an Observing Proposal . . .

. . . has become an increasingly challenging exercise. With an ever higher pressure on space experiments and on large ground-based telescopes (and in particular those of ESO), it has become imperative to present extremely well-prepared documents to selection committees to get the observing time sought for.

In fact, scientists are now complaining that writing a good observing proposal requires as much time, care and energy as a paper for a refereed journal. The rationale has not only to be scientifically justified, but often a description of previous related work and of the methodology that shall be used for reducing and exploiting the data, have to be included. Reasons for additional and/or repeated observations have also to be explained. More and more frequently, combined or simultaneous (ground/space or multi-wavelength) observations are solicited and must be appropriately requested and subsequently organized.

These tasks are made much easier by a tool such as SIMBAD, a database providing all basic astronomical data available on the proposed targets, as well as the corresponding bibliography. More and more proposal writers are using it, as well as an increasing number of selection committee members.

The usefulness of SIMBAD does not stop at the writing of the proposals for observing time. The preparation of the observing runs themselves can also be greatly facilitated. Once these are completed, the reduction of the observations, their comparison with already published results and eventually the writing of new papers is significantly helped by getting the fundamental astronomical data and the relevant bibliography from SIMBAD. Never again should referees reject manuscripts for the reason of overlooked published papers!

Astronomical Quiz

It is no secret for the readers of this journal that practically every astronomical catalogue uses a different notation

to designate the objects it gathers. In the past, this has already led a few times to the situation where two astronomers studied the same object under different identifiers without ever noticing it!

Most of us also remember the great difficulty of searching for various data spread over different catalogues for a sample of stars or even for a single star. The only common point between these catalogues was generally the appearance of the coordinates, often imprecise and relative to different epochs. Subsequently, how was an exhaustive survey of the papers relevant to the objects under study obtained? The available compilations were subject oriented, and when object designations were used as key words, generally no synonymy relations were provided.

The situation began to improve by the pioneering work undertaken in France at the beginning of the seventies by the astronomers of the Strasbourg Data Centre (CDS) and of a few collaborating institutions who started to establish, as modern Benedictines armed with computers, correspondences between the various catalogues. Since its founda-

tion, CDS has maintained its clear leadership in the field of astronomical data banks.

A Little SIMBAD History

In 1972, the French National Institute of Astronomy and Geophysics (INAG, now the National Institute of the Sciences of the Universe – INSU) decided to create a *Centre de Données Stellaires* with the following aims:

- to compile the most important stellar data available in machine-readable form (positions, proper motions, magnitudes, spectra, parallaxes, colours, etc.),
- to improve them through critical evaluation and comparison,
- to distribute the results to the astronomical community, and
- to carry out its own research.

This centre has been installed at Strasbourg Observatory and is headed by a Director (presently C. Jaschek) who is responsible to a Council composed of six French and six foreign astronomers.

Besides collecting astrometric, photometric, spectroscopic and other catalogues, the first important accomplishment of the CDS has been to construct an enormous dictionary of stellar synonyms called the *Catalogue of Stellar Identifications* (CSI). Some stars have more than thirty different designations.

This catalogue has been complemented by the *Bibliographical Star Index* (BSI) giving, for each star and from the major astronomical periodicals from 1950 onwards, the bibliographical references to the papers mentioning this star. On the average, a star is cited in five publications, but some stars are quoted in more than five hundred papers.

Taking advantage of the fact that, through the CSI, any identification can give access to all connected catalogues, and thus to their data, a user-friendly conversational software system has been built around it, leading to the present dynamic configuration of the SIMBAD (*Set of Identifications, Measurements and Bibliography for Astronomical Data*) base accessible from remote stations.

Subsequently, data on non-stellar galactic and extragalactic objects were included, together with their bibliographical references (from 1983 onwards). Taking account of this, and in order to retain well-known abbreviations like CDS, CSI and BSI, the word *stellar* appearing in them has been replaced by *Strasbourg*.

Some Basic Data on SIMBAD

(April 1987)

700,000 Objects
100,000 non-stellar objects
2,000,000 cross-correlated identifications
1,000,000 on-line measurements
600,000 bibliographical object-indexed references from
90 astronomical periodicals scanned

Present Status

Thus SIMBAD represents much more than a mere accumulation of catalogues. Presently, it is most likely the largest base of basic astronomical data in the world. It contains about 700,000 objects including about 100,000 non-stellar objects (mostly galaxies) for which more than 2,000,000 identifications have been recorded. More than 1,000,000 measurements are provided on-line. These figures will be quickly out of date with the planned inclusion of the Guide Star Catalogue of the Hubble Space Telescope (of the order of 20 million objects).

The table of synonyms and the connected catalogues can be accessed through any *object designation* (about 400 different types) or by *object coordi-*



The maps (as of April 1987) represent the locations of SIMBAD user stations (●) in Europe and in the rest of the world. Collaborating data centres (★) are also indicated. The STARLINK centre at Rutherford Appleton Laboratory acts as a distributing node for its own network.

nates, equatorial, ecliptic (at any equinox) or galactic. In the latter mode, one may request to get all objects within a rectangle or a circle of given dimensions around a given position. *Criteria* can also be specified on parameters such as magnitude, existence of various types of data, etc. With this information, *maps* can be produced, making SIMBAD a precious auxiliary for creating identifying fields and preparing ground or space observing runs or programmes.

The bibliographic index contains references to stars from 1950 to 1983, and to all objects outside the solar system from 1983 onwards. Presently there are more than 600,000 references taken from the 90 most important astronomical periodical publications.

SIMBAD is accessible through *data networks*, including the French TELETEL public service. The European Space Agency (ESA) IUE Ground Observatory in Madrid was actually the first foreign station connected to SIMBAD which was used operationally for checking target coordinates and as an open service to visiting astronomers. It has been followed by other space centres like the Space Telescope Science Institute in Baltimore and NASA Goddard Space Flight Center in Greenbelt. The Space Telescope European Coordinating Facility in Garching is also connected through its host, the European Southern Observatory. Other stations with access to SIMBAD include places like the STARLINK node at Rutherford Appleton Laboratory, Caltech at Pasadena (CA), the Center for Astrophysics at Cambridge (MA), the Very Large Array in Socorro (NM), the Canada-France-Hawaïi Telescope in Kamuela (HI), the Anglo-Australian Observatory in Epping, the South African Astronomical Observatory in Capetown, etc. (see maps).

To the present, there are more than a hundred centres in sixteen countries regularly interrogating SIMBAD. The figures are rapidly increasing. Apart from a simple terminal, the only requirement for accessing SIMBAD is obtaining an account number from CDS which will be used for invoicing. Astronomers without access to a data network can mail their requests to the Data Centre which will then return a printout with the corresponding data. In the same way, copies of individual catalogues (from a list of more than 500) can be obtained on magnetic tapes. Some of them (about 50) are also available on microfiche. Data transfer is also possible via the major computer networks.

SIMBAD is continuously growing and kept up-to-date, not only by the Strasbourg CDS staff, but also by many

cooperating persons in other institutions. All the catalogues available at CDS have been produced by specialists, so that their high quality is guaranteed. Some catalogues, prepared at CDS itself and available as *CDS Special Publications*, are made in fields where the Strasbourg personnel has specific qualifications. Thus the *Catalogue of Stellar Groups* lists some 30,000 stars according to their spectral peculiarities.

Collaboration with other institutes having specialization in specific fields is then a natural consequence. This is particularly the case for Bordeaux, Meudon and Paris (bibliography), Geneva and Lausanne (photometry), Heidelberg (astrometry) and Marseille (radial velocities).

To encourage exchanges with other countries, *formal agreements* have been signed, in particular with NASA (USA), the Astronomical Council of the USSR Academy of Sciences and the Potsdam Zentralinstitut für Astrophysik (German Democratic Republic). CDS is also collaborating with Japan (Kanazawa Institute of Technology) and the United Kingdom (STARLINK). The goal of these agreements is to allow all astronomers in the world to have access to all existing catalogues.

Other CDS Activities

On a much larger scale, CDS takes also an active part in space projects like HIPPARCOS and TYCHO which are heavily dependent on SIMBAD for the preparation of their respective input catalogues. The Space Telescope GSSS team is collaborating with the CDS for the inclusion of the stellar cross identifications from SIMBAD in the *ST Guide Star Catalogue*. CDS acts also as the European disseminator of the IRAS observational material and has been requested by ESA to homogenize the IUE log of observations.

CDS plays a role also in the various discussions which should lead in the near future to the setting up of a *European astronomical data network*. Ideally, SIMBAD could be connected through such a network with the observing logs of the main ground and space observatories. Specific colloquia have been organized by CDS on this matter.

Apart from smaller scale CDS scientific meetings taking place twice per year, Strasbourg Observatory has organized several important colloquia on data collection, dissemination and analysis, as well as on statistical methods in astronomy. All these meetings were great successes and revealed the importance that the astronomical community attaches to this type of work.

Interest in CDS work is also shown by the growing number of astronomers visiting it, either to get to know the CDS or to set up a collaborative project. CDS stays in touch with its users and other interested persons by a six-monthly *Bulletin* distributed free of charge. Apart from keeping readers updated on CDS services and the latest developments, it contains also general papers and news about other data centres' activities.

In its Special Publication series, CDS also publishes *directories* gathering all practical data available on, on the one hand, astronomical associations and societies (IDAAS) and, on the other hand, institutions employing professional astronomers or researchers in astronomy (IDPAI).

The research activities of the scientific staff (currently eight persons) are essentially centred on statistical methodology and its applications to astrophysics, on classification problems, on distance and luminosity determinations, as well as on studies of peculiar objects.

Finally

If you want to have access to SIMBAD or, more generally, if you are interested in the CDS services, you can get in touch directly with us at:

C.D.S.
Observatoire Astronomique
11, rue de l'Université
F-67000 Strasbourg
France

Telephone: +33-88.35.82.00
Telex: 890506 starobs f
EARN/BITNET address: U01117 at
FRCCSC21.

ESO Press Releases

The following Press Releases have been published since March 12, 1987, the date when *Messenger 47* was distributed.

PR 06/87: The Unusual Behavior of Supernova 1987 A in LMC (31 March); with colour photo of the supernova and the Tarantula Nebula.

PR 07/87: Important Events in the Southern Sky (14 May); with one B/W photo of Comet Wilson.

PR 08/87: ESO Exhibition at the Heysel Planetarium in Brussels (25 May).

PR 09/87: A New Edition of the ESO Publications and Picture Catalogue is now available from the ESO Information and Publication Service.

PR 09/87: Hunting the Black Hole (16 June), with one B/W photo.

PR 10/87: Is the Universe Younger than Previously Thought? (3 July)

A Study of the Neutral and Ionized Io Tori

R. PRANGE, Laboratoire de Physique Stellaire et Planétaire, France

A. VIDAL-MADJAR, Institut d'Astrophysique Paris, France

J.C. GÉRARD, Institut d'Astrophysique Liège, Belgium

1. Introduction

Historically, the discovery and the first observations of the neutral clouds, and then of the plasma tori near Io were made by ground-based spectroscopic observations about a decade ago (NaI: Brown, 1974; KI: Trafton, 1975; SII: Kupo et al., 1976). The neutral emission lines are due to resonant scattering of allowed transitions from the solar lines, while the optical emissions from the ionized tori are excited by collisions with electrons (the lines from 3000 Å to 10000 Å, including the visible, arise from forbidden transitions, while the far U.V. lines later observed from space-craft are due to electron-excited, allowed transitions). The lines studied in the Io tori emissions are listed in Table 1, together with their reported intensity.

Images of the emitting areas have been obtained significantly later (NaI: Matson et al., 1978; SI: Pilcher et al., 1985).

There are quite a number of questions concerning the thermodynamic equili-

brium of the sodium cloud (such as density and temperature, loss mechanisms in various cloud regions, lifetimes of the neutrals, mass loss rate, mass loading rate) for which we now begin to obtain the first answers through observations of the extent of the cloud, its east-west and north-south asymmetries, its longitudinal and temporal variations and its velocity fields, by means of imaging and high resolution spectroscopic methods. However, much remains unknown in a region close to the satellite itself, within a few arcseconds, where the observations are very difficult due to the high surface albedo of Io near the resonant lines of Na (5890–96 Å). We must recall that the first images were obtained with a ~17 arcsec and later with a ~10 arcsec coronographic mask. In this region, the presence of an unknown atomic sink is suspected (Brown, 1983).

There are presently two ways to get access to this region. The first one is spectroscopic in nature and is based on registration of the solar spectrum reflected by Jupiter or one of its satellites: provided the incident ray has crossed the Io Na cloud before reflection, we observe the absorption Na line in the reflected solar Fraunhofer line with contamination by the continuum from Io. This method had been proposed by some of us (R. Prange, R. Ferlet, A. Vidal-Madjar and C. Emerich) for the 39th ESO observing period, but time was not allocated. It has once been successfully applied on Europa during

the mutual phenomena, see Schneider et al., 1986. The second method employs mapping of the near surface environment of Io with a very narrow band filter and very good spatial resolution and stability, in order to improve the contrast between the diffused light from Io and the cloud line. This is one of the purposes of our present programme "Study of the ionized and neutral Io tori" at La Silla.

The potassium cloud is about 15 times fainter than the sodium cloud, and it obeys the same physical laws, except for the lifetime. Therefore, it has not been thoroughly studied. No imaging at all has been done of the oxygen cloud.

As for the ionized tori, only one systematical spatial/temporal survey has been achieved up to now (Pilcher et al., 1985) in the SII 6731 Å line. Few other images exist in SII and SIII, but they give rather contradictory results, especially what concerns longitude dependence of the emissions, and they seem to testify to temporal variations, not yet understandable due to the limited data.

2. Our Observing Programme at La Silla

Most of us are interested in the study of Jupiter's environment, and especially of the magnetosphere/atmosphere coupling. F. Paresce, J.C. Gérard and A. Vidal-Madjar have already been allocated observing time on the GTO programme of the Hubble Space Telescope

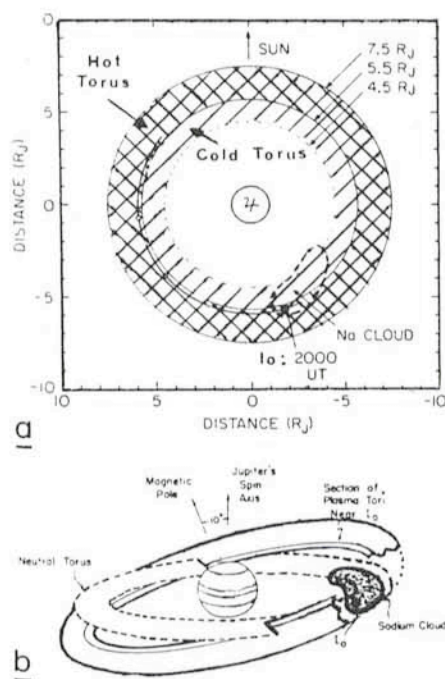


Figure 1: Schematic geometry of the plasma and neutral tori illustrating the neutral cloud shape and how the ionized particles can kick the neutral species out. (A) Projection onto the plane of the ecliptic (adapted from Bagenal and Sullivan, 1981). (B) Perspective edge-on view (adapted from Trafton, 1980).

TABLE 1: Neutral and ionized emissions of the Io tori.

GROUND-BASED			FROM SPACE from Durrance et al. (1983)		
Species	Wavelength	Intensity	Species	Wavelength	Intensity
NaI	5890 Å	up to	OI	1304 Å	3 R
	5896 Å	30 KR		1296 Å	1.3 R
KI	7665 Å	500 R	SI	1425 Å	2.5 R
	7699 Å			1256 Å	4 to 40 R
OI	5577 Å	200 R	SII	1199 Å	15 to 60 R
	4227 Å	≤5 KR		1729 Å	17 to 47 R
SII	6717 Å	400 R	OIII	1664 Å	3 to 12 R
	6731 Å				
	4069 Å	50 R			
OII	3726 Å	50 R	SIV	1406 Å	2 R
	3729 Å				
SIII	6312 Å	50 R			
	3722 Å				

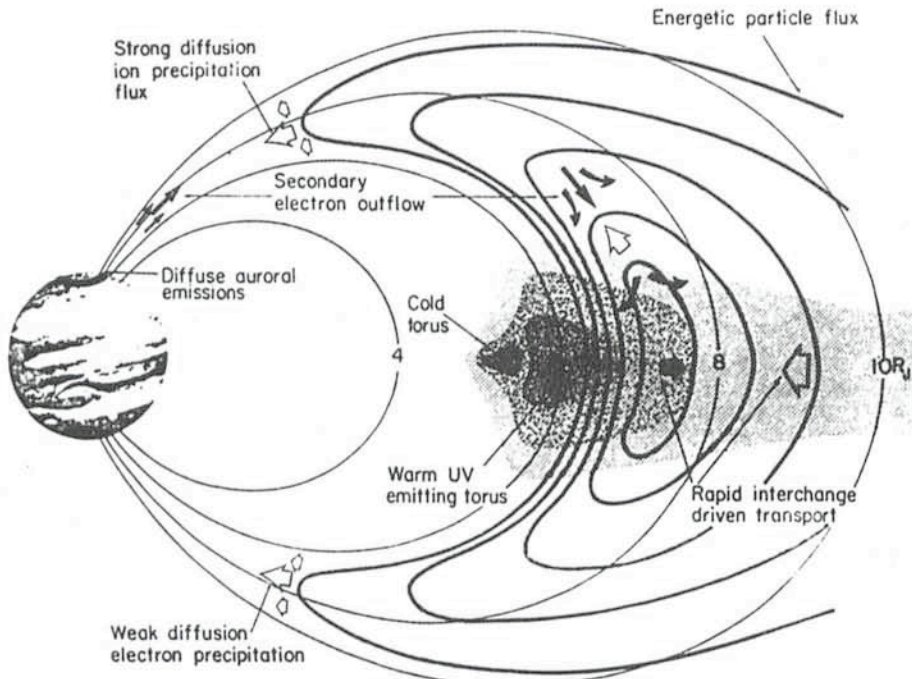


Figure 2: Schematic meridian section of the Jupiter/Io magnetospheric coupled systems, showing the cold and hot tori. Io is on the $\sim 6 R_J$ shell close to the peak of the hot torus (from Thorne 1981).

(HST). Included in this programme is a high spatial (latitude-longitude) resolution (and then temporal survey) study of the H Ly α and H₂ He-Ly U.V. emissions excited by the precipitation of magnetospheric particles along field lines. Since these precipitations are (totally or partially) monitored by the Io tori, we had long ago suggested that a correlated study of the Jovian aurorae and of the Io tori would give a clue to these questions (Vidal-Madjar et al., 1982). There is currently no spacecraft which is able to observe simultaneously the auroral zone of Jupiter and the Io orbit, and we have therefore proposed to add ground-based observations of the Io tori in the visible to the U.V. auroral data expected from the HST. In order to prepare this programme, we have obtained two observing nights at ESO in September 1986 and then three more at the end of November 1986.

This type of observations is only possible within about two months of a Jovian opposition (most recently on September 10, 1986; the next will be in mid-October 1987) and during intervals of 3 to 6 successive nights, due to the 42.5-hour period of Io, which must be observed near the greatest elongation on either side of Jupiter. The length of the sequence as well as the amount of available observing hours per night decreases as one moves away from opposition, from about 9 to 10 hours on September 1, 1986, i.e. close to the centre of the best period, down to ~ 2 hours per night at the latter period in November.

The images were obtained with the 2.2-meter telescope at La Silla in the imaging mode, coupled with the RCA/CCD detector.

The strong emission from Io's continuum (illustrated in Figure 3) was significantly decreased by the use of an occulting mask in the telescope focal plane and centred on the image of Io. This coronographic mask, specially designed and built at the Space Telescope Science Institute in Baltimore to be mounted on the 2.2-m telescope, has been described in detail by Paresce and Burrows, 1987. It basically consists of a movable wedge, the angular width of which can be continuously varied from 2 arcseconds to 10 arcseconds and centred anywhere in the field of view. The positional angle can be changed, depending on the direction of the faint features to be observed. The associated optics introduce a magnification of 5, the resulting beam aperture is f/40, leading to negligible "beam aperture effects" in the very narrow band filters used. The pixel size on the sky is 7.23×10^{-2} arcsec and the field of view is about 23 by 37 arcsec, both well adapted for high-resolution imaging close to Io.

The use of the occulting mask centred on the bright source does not in itself eliminate the diffuse continuum close to the surface, as seen on Figures 4a and 4b. It is necessary to further decrease the transmitted continuum by means of very narrow band filters. Sophisticated interference filters or Fabry Perot interferometers can be used. During the runs of September and November 1986, we

investigated the neutrals and concluded that a spectral resolution of 5 Å or better was desirable. We have therefore used a 5 Å sodium interference filter, centred at 5890 Å and lent to us by the Service d'Aéronomie (C.N.R.S., France) in order to obtain the sodium cloud image shown in Figure 6.

Moreover, the efficiency of the occulting mask critically depends on the actual spatial resolution and the image stability during the exposure, which usually lasts from 20 minutes to a few hours. This includes the seeing and the telescope guiding accuracy.

We obtained a reasonable measurement of the image widening by the overall seeing parameters from the measurement of the FWHM of a nearby stellar image. During the September and November runs, we found values of the order of 0.5 to 0.9 arcsec. Compared to the ~ 1 arcsec diameter of the object, these were indeed excellent observing conditions. We were therefore able to use 3.5 arcsec for the mask width.

The second point has turned out to be much more critical. As previously noted, once we had acquired a narrow band image of Io's continuum plus the sodium cloud emission, we had to eliminate the continuum contribution. We then imaged the diffuse light from Io through a broadband ESO filter, with Io

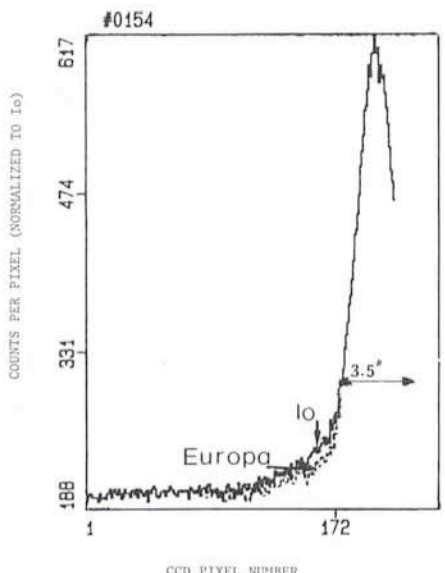


Figure 3: Cuts through simultaneous images (exposure 1 minute) of Io and Europa on November 24, 1986. The angular diameters are very similar and the signals have been normalized to Io. The image was acquired with the 5 Å bandpass NaI filter and without the occulting wedge. The small difference between the profiles ~ 100 pixels left of the maximum (~ 7.5 arcsec) is due to Io's sodium cloud and gives an idea of the small contrast with the reflected continuum. The 3.5 arcsec wide arrow corresponds to the size of the mask which was used to obtain Figures 4 and 6.

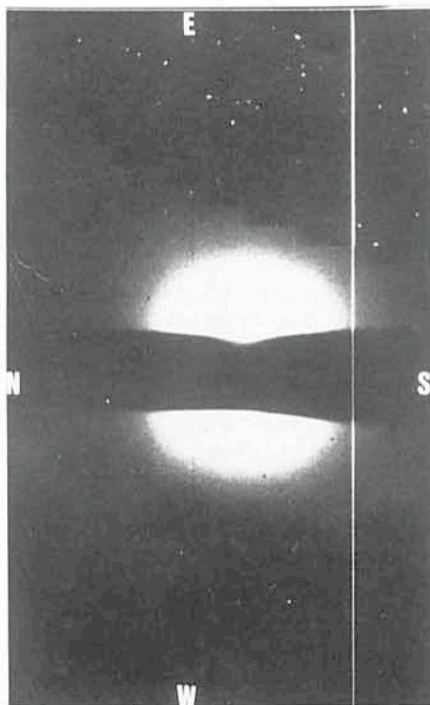


Figure 4: 1-minute exposures obtained on September 4, 1986, with the standard broadband V filter. Io is behind the occulting wedge, the width of which is 3.5 arcsec. One sees the wings of the distribution of the diffused continuum reflected by Io (Io's size = 1 arcsec), which must be subtracted by suitable image processing from the narrow band filter Na images of the neutral clouds. Figure b is shifted by about 0.3 arcsec from Figure a, perpendicular to the wedge. The observed difference in the diffused light distribution emphasizes the need of a very high pointing stability during long exposures.

being carefully located in the same place, and we must subtract this reference image from the first one, as described by Paresce and Burrows. Figures 4a and 4b illustrate the difference introduced in the reference broadband images when the centre of Io is shifted by only 0.3 arcsec perpendicularly to the wedge. This means that the location accuracy and the spatial stability of the images must be of the order of a few tenths of arcsec (< 0.5 arcsec) during the active experimental sequence

(narrow band + reference broadband image). This constraint on the guiding of the telescope is very severe for several reasons:

- First, the relative motion of Io in the sky, which must be introduced into the telescope computer for guiding, is fast and rapidly variable. For example, it can vary from 0 to ± 20 arcsec in α and ± 10 arcsec in δ during the same night. It is therefore necessary to adjust the guiding input parameters, approximately every 15 minutes.

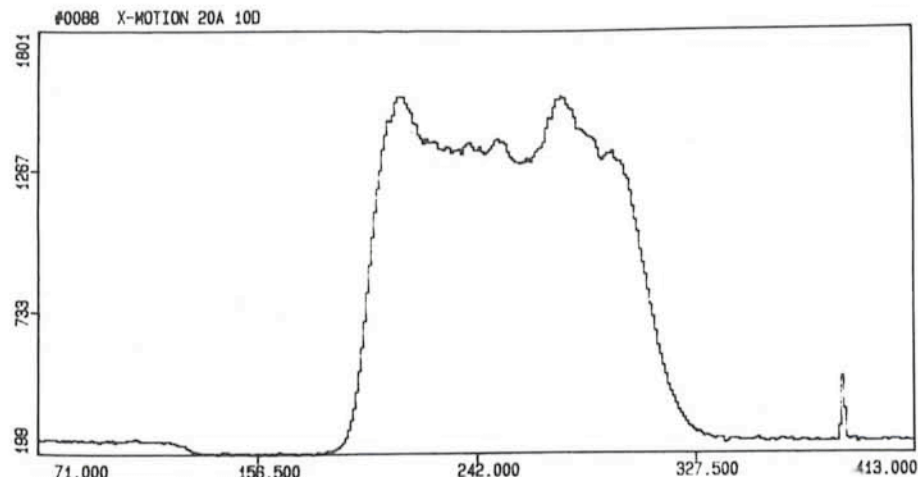


Figure 5: Calibration of the guiding motion of the telescope: A constant drift velocity $d\alpha/dt = 20$ arcsec per hour and $d\delta/dt = 10$ arcsec per hour is introduced and the signal from a star near Io is acquired during a 20-second exposure. The two-dimensional trail on the CCD detector provides the velocity scalings in α and δ . The intensity cut along the X-axis shows that the motion is not entirely uniform.



Figure 6: 20-minute exposure obtained on November 27, 1986, with a 5 Å bandpass filter centred on the 5890 Å NaI emission line. The circularly symmetric contribution of Io's continuum (cf. Figure 4) is easily distinguishable from the elongated sodium cloud. The orbit of Io is nearly in the NE-SW plane. Jupiter is outside the image in the SW direction.

- Second, the scaling factor between the input parameters and the real (actual) $d\alpha/dt$, $d\delta/dt$ of the line of sight on the sky must be perfectly known and regularly controlled. This was one by acquiring a star, introducing a standard motion drift in the computer and directly calibrating on the CCD the displacement of the star during the exposure time.

- Third, the motion of the telescope monitored by this calibrated "motion drift" must be uniform at the needed accuracy. Figure 5 which represents the photometric signal from the star during the above procedure shows that it is not perfectly regular, and probably introduces some "positional blur".

This delicate calibration study is obviously not a standard one, and it had to be done with the active support of the Operations Group at La Silla. It is good to report that the achieved results are already much better than those obtained by the procedures used by other groups, who report stabilities of 1 to 2 arcsec during an exposure, see Pilcher et al., 1985. The efforts at ESO should therefore be continued.

At the end of the November 1986 run, we obtained our first image of Io's sodium cloud, shown in Figure 6. The occulting mask was only 3.5 arcsec wide and the exposure lasted 20 minutes.

The data processing is now in progress with the use of reference broad-

Io's Tori and their role in the Jovian magnetosphere/atmosphere dynamics

Io is the innermost Galilean satellite of Jupiter. It travels along an orbit at the distance of $5.9 R_J$ from the centre of Jupiter (R_J is the Jovian radius) which corresponds approximately to an angular distance of 2 arcminutes as seen from the Earth. Its angular diameter is about 1 arcsecond ($\sim 3,600$ km) and its visual brightness $m_v = 5.1$.

Contrarily to most other "moons" which look like telluric planets or icy bodies, *Io* has a very special surface due to the fresh lava spread by its active volcanoes over the mineral crust. It is presently supposed to be mainly composed of a mix of silicate regoliths, basalts, with frozen SO_2 , S_2O , polysulfur oxydes and alkali sulfides (Gradie, 1985; Hapke, 1986; McEwen et al., 1986). A continuous, significant ejection of materials is observed, either by direct volcanic emissions or by sputtering of the surface compounds by energetic magnetospheric particle impact. It results in an atmosphere which mainly consists of oxygen, various sulphur molecules (S , S_2 , S_3), SO_2 and metallic species (Na, K) with a $\leq 1\%$ mixing ratio. Its size could be a few 10^6 km according to recent models and observations (Christey et al., 1986; Summers et al., 1985; Schneider et al., 1986; Ballester et al., 1986).

Additionally, *Io* is embedded in the Jovian magnetosphere and the neutral species which have been sputtered out are rapidly dissociated and ionized by the ambient hot plasma and give rise to ions which are immediately trapped by the magnetic field lines and are the major source of feeding of the inner Jovian magnetosphere.

This produces two classes of features:

1. Neutral clouds (Na, K, O, S) escaping from *Io*'s atmosphere at low velocity (~ 2 to 3 km s^{-1}), which roughly accompany it in its motion in the geographic (rotational) equatorial plane of Jupiter (Figure 1). The shape and size of these clouds depend on the ejection parameters related to the gravitational interaction of *Io* and of Jupiter, on the solar flux pressure (which is suspected to induce east-west asymmetries depending on the phase of *Io*) and on particle interactions, the more effective being ionizing collisions with electrons and ions of the magnetosphere and charge exchange with the ions trapped in the ionized tori when they intersect the geographic equatorial plane (see later). Depending on their lifetimes against such processes and diffusive rates, the neutral clouds can look like limited areas extending essentially forward *Io* along its orbit (for lifetimes of the order of a few tens of hours, i.e. the typical "banana shape" sodium cloud schematically drawn on Figure 1a), or like complete tori as in the model-predicted ones for OI, for lifetimes of hundreds of hours (Smyth and Schemansky, 1983) or SI (Durrance et al., 1983). Escaping accelerated jets are also occasionally observed with velocities greater than

50 km/s, giving evidence of charge-exchange with fast ionized species of the ionized tori.

2. Ionized tori, which are caused by the pick-up of the newly created ions by the magnetosphere. Since the magnetic field lines are rigidly rotating with the planet, their velocity at the *Io* jovicentric distance is about 4 times that of *Io* ($76 \pm 6 \text{ km s}^{-1}$ between $5.5 R_J$ and $6.5 R_J$, and $\sim 17 \text{ km s}^{-1}$ respectively), and the ions are immediately accelerated by the differential velocity. Due to this shorter rotation period and their longer lifetimes (from one hundred hours for SII to one thousand hours for SIII and OII; Pilcher et al., 1985) they give rise to closed tori of SII, SIII, SIV and OII, OIII in the magnetic equatorial plane of Jupiter, which differ by $\sim 10^\circ$ from the geographic one (Figure 1b). The low ionization level species OII and SII are mainly observed inwards of *Io*'s orbit, while the higher ionization level ones are almost exclusively observed outside of it, giving rise to the so-called "cold" and "hot" tori (Figures 1a and 2).

However, differences in the longitudinal dependence of the densities of the various ions seem to be present in the small data sets now available. For example, the shorter lifetime SII species exhibits a significant, two maxima longitudinal variation, while most of the time SIII does not. This is tentatively attributed to local plasma sources which are related to the Jovian magnetic anomaly, to the intersection with the orbits of the neutral clouds or to collisions with magnetospheric electrons of given energy (Pilcher et al., 1985). As in any plasma, the ratio of the intensity of selected emission lines can give information on the electronic temperature and density (T_e , n_e) as a function of the location.

Finally, these rotating ions interact with the Jovian magnetosphere, for which they constitute the major source of energy and mass loading, thus playing a key role in the dynamics of the magnetosphere and, beyond it, of the Jovian atmosphere. Here are some of the processes by which *Io* may control the Jovian environment (summarized in Figure 2):

- by diffusion in pitch-angle, the ions from the tori are a significant source of auroral emissions in the upper atmosphere of Jupiter, competing with the solar wind input;
- secondary electrons are created and are mirrored back towards the equator to populate the magnetosphere of a warm electron component;
- plasma instabilities are expected to appear along the magnetic flux tube of *Io*, again accelerating particles; and
- radial diffusion of the ions also takes place (rapidly outwards, slowly inwards), thereby feeding a large region in the magnetosphere.

band images such as those shown in Figure 4.

Acknowledgements

We are greatly indebted to Francesco Paresce and Christopher Burrows who designed, built and operated the excellent occulting mask without which these observations would not have been possible. They participated in the measurements as coinvestigators.

We are also grateful to Daniel Hofstadt and to the Operations Group at La Silla, and especially to Paul Le Saux, whose efficient support was crucial for the difficult problem of the image stability. We also want to thank Gérard Thuillier and Jacques Porteneuve who lent us the narrow band sodium filter used in this experiment.

References

- Bagenal, F., and Sullivan, J.D., 1981, *J. Geophys. Res.* **86**, 8447.
Ballester, G.E., Moos, H.W., Strobel, D.F., Summers, M.E., Feldman, P.D., Skinner, T.E., Bertaux, J.L., Festou, M.C., Lieske, J., 1986, *Am. Astr. Soc.* **18**, 774.
Brown, R.A., 1974, in *Exploration of the Planetary System*, Woszczyk and Iwaniszewska, Ed. p. 527.
Brown, R.A., Pilcher, C.B., Strobel, D.F., 1983, in *Physics of the Jovian Magnetosphere*, A.J. Dessler, Ed. Cambridge University Press, p. 197.
Christey, D.B., Johnson, R.E., McGrawth, M.A., Phipps, J.A., and Boring, J.M., 1986, *Bull. Am. Astr. Soc.* **18**, 775.
Durrance, S.T., Feldman, P.D., and Weaver, H.A., 1983, *Astroph. J.* **267**, L 125–129.
Gradie, J., 1985, *Bull. Am. Astr. Soc.* **17**, 692.
Hapke, B., 1986, *Bull. Am. Astr. Soc.* **18**, 774.
Kupo, I., Mekler, Y., and Eviatar, A., 1976, *Astroph. J. Lett.*, **205**, L 51–53.
Matson, D.L., Goldberg, B.A., Johnson, T.V., Carlson, R.W., 1978, *Science* **199**, 531.
McEwen, A.S., Soderblom, L.A., Johnson, T.V., 1986, *Bull. Am. Astr. Soc.* **18**, 774.
Paresce, F., and Burrows, C., 1987, *The Messenger*, **47**, 43.
Pilcher, C.B., Fertel, J.H., and Morgan, J.S., 1985, *Astroph. J.* **291**, 377.
Schneider, N.M., Wells, W.K., Hunten, D.M., Trafton, L.M., 1986, *Bull. Am. Astr. Soc.* **18**, 775.
Smyth, W.H., and Shemansky, D.E., 1983, *Astroph. J.* **271**, 865.
Summers, M.E., Strobel, D.F., Yung, Y.L., 1985, *Bull. Am. Astr. Soc.* **17**, 692.
Thorne, R.M., 1981, *Geophys. Res. Lett.* **8**, 509.
Trafton, L., 1975, *Nature*, **258**, 690.
Trafton, L., 1980, *Icarus*, **44**, 318.
Vidal-Madjar et al., 1982, Magellan Report on the Phase A Study, ESA Report SCI (82) 4, November 1982.

MCCP: Photometry Through Clouds!?

H. BARWIG and R. SCHOEMBS, Universitäts-Sternwarte München

1. Rapidly Variable Objects – a Challenge to Photometry

The investigation of cataclysmic variables (CV) has almost become a tradition at the Universitäts-Sternwarte München. CVs form a large group of close binary systems as for example novae, dwarf novae, X-ray bursters and polars. These objects normally exhibit orbital periods of up to a few hours, and some of them, additionally, show very rapid light variations at time scales of even less than seconds. In particular eclipse light curves of such systems offer a large amount of information allowing to derive fluxes and other relevant parameters separately for the individual components.

For years such photometric observations with the required high time resolution have been performed using conventional single-channel photometers which for this purpose suffer from essential disadvantages:

– Multiband measurements are fairly ineffective due to the sequential exchange of filters. The non-simultaneous measurements may seriously affect the calculation of colours (e.g. U-B, B-V). Additionally, large errors arise due to the unavoidable deadtime.

– Continuous photometric monitoring of variables could be done only during photometric nights, when comparison star and sky brightness had not to be checked too often. Non photometric nights caused considerable loss of observing time or resulted in annoying discussions about the reliability of data taken under poor weather conditions.

This inefficiency and inability of single-channel photometers after many useless nights initiated plans to develop a more appropriate photometric instrumentation.

2. MCCP – The New Photometer Concept

The instrumental development began in 1982. It ended with the prototype of the Multi-Channel Multi-Colour Photometer (MCCP) schematically displayed in Figure 1. A detailed description is given by Barwig et al. (1987).

The instrument consists of 3 separate fiber optic input channels, each splitting the light into 5 colours by means of highly efficient prism spectrographs. 15 photomultiplier tubes are used as photon-counting detectors. Hence the MCCP allows to measure three sources

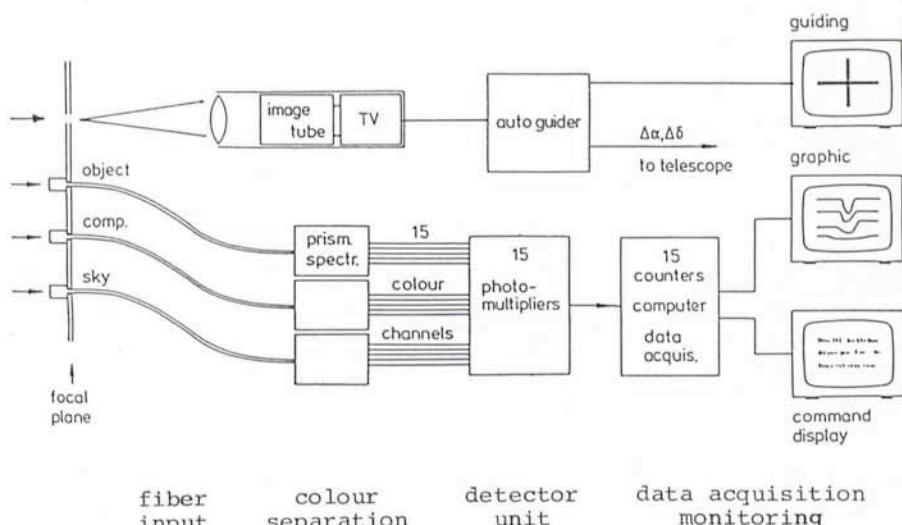


Figure 1: Block diagram of the three-channel five-colour photometer (MCCP).

(object, nearby comparison star and sky background) in 5 colours (UBVRI), all simultaneously and with high time resolution. Photometry relative to a calibrated comparison star can be performed with this instrument even during quite variable atmospheric conditions and spectral distributions can be measured even for erratic variable objects.

The instrument is equipped with a data-acquisition and monitoring system that is fully independent of other computer support. Furthermore, it contains power supplies, a cooling system and a meteorological station to measure the atmospheric conditions in the dome. The photometer has a built-in auto-guider system which can be interfaced via the handset connectors to practical-

ly any telescope that offers offset facilities. For operation, the MCCP only needs 220 V, 50–60 Hz, 4 Amps stabilized power and a telescope which can support 100 kp at its Cassegrain focus. The instrument has now been used many times at La Silla and other observatories as well. Guest groups have also used the MCCP with success. In its present state at least one well-trained and experienced user must accompany the instrument to guarantee proper installation, operation and packing.

3. Scene of Action: La Silla

Whenever the MCCP has arrived at La Silla after a long journey from Europe, it

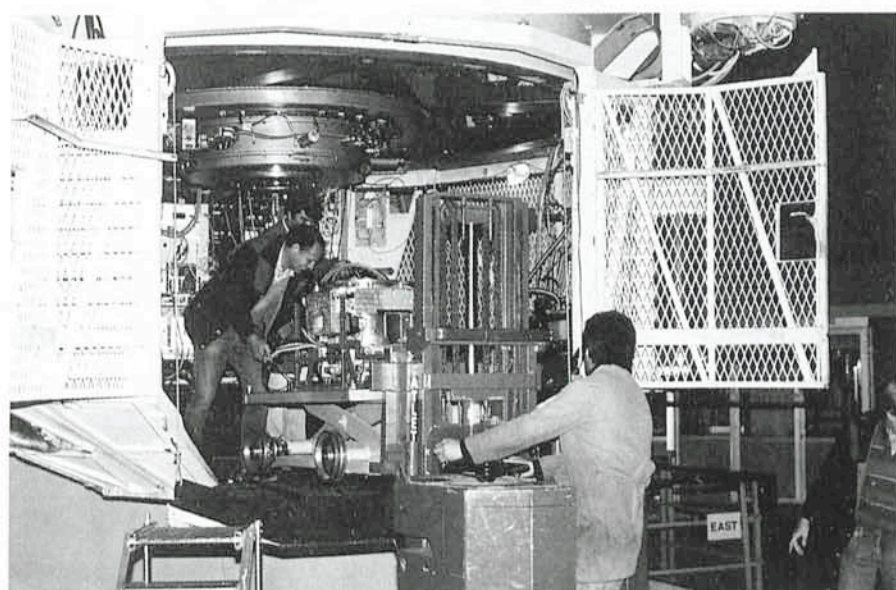


Figure 2: ESO experts mounting the MCCP at the 3.6-m telescope.

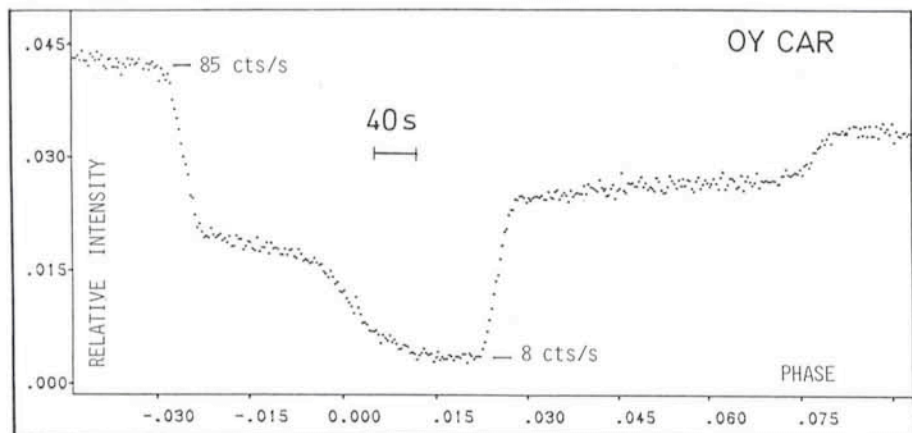


Figure 3: Averaged eclipse lightcurve in B of the short period ($P = 91$ min) cataclysmic binary OY Car, showing ingress and egress of white dwarf and hot spot. The data were obtained from 25 orbital cycles observed with the MCCP during 7 nights at the ESO 1-m telescope. Time resolution: 2 s. The indicated count rate of the very eclipse minimum corresponds to approximatively 18 mag.

is generally stored in the telescope building, waiting for the observers to drop in well in advance for operational tests and preparation. They start with the installation of a laboratory setup to check the complete system. First a calibration measurement is performed by means of artificial light sources simulating star and sky radiation. For

comparison the same tests had run before shipment. The consistency of the results, proper storage of the data, proper reading, plotting and reduction of them together with a 24-hour stability test of dark current and sensitivity guarantee the readiness for mounting at the telescope.

This procedure essentially depends

on the effective cooperation between astronomers and observatory staff: During the laboratory test the 15 detectors had to be cooled, and as known to all users of photomultiplier tubes, they don't like changes very much and easily get unstable when temperature or high voltage variations occur. Thus the aim is to restart cooling as fast as possible (within less than 5 minutes) after switching off in the lab and moving to the telescope floor. This problem has always been solved, thanks to the efforts of the experienced ESO staff (Fig. 2). After mounting and balancing, the whole equipment is rechecked. In the following, all electrical operations eventually necessary during observations at night must be tested for electric pickup (e.g. dome rotation, light switches in the dome building, shutters, elevator and platform operations, radio transmitters, etc.). When satisfying results are obtained, the time until start of observations is used to continuously monitor the dark currents of all 15 multipliers running an appropriate test programme.

First-night observing activities generally are quite stressing: For this special instrumentation usually the telescope

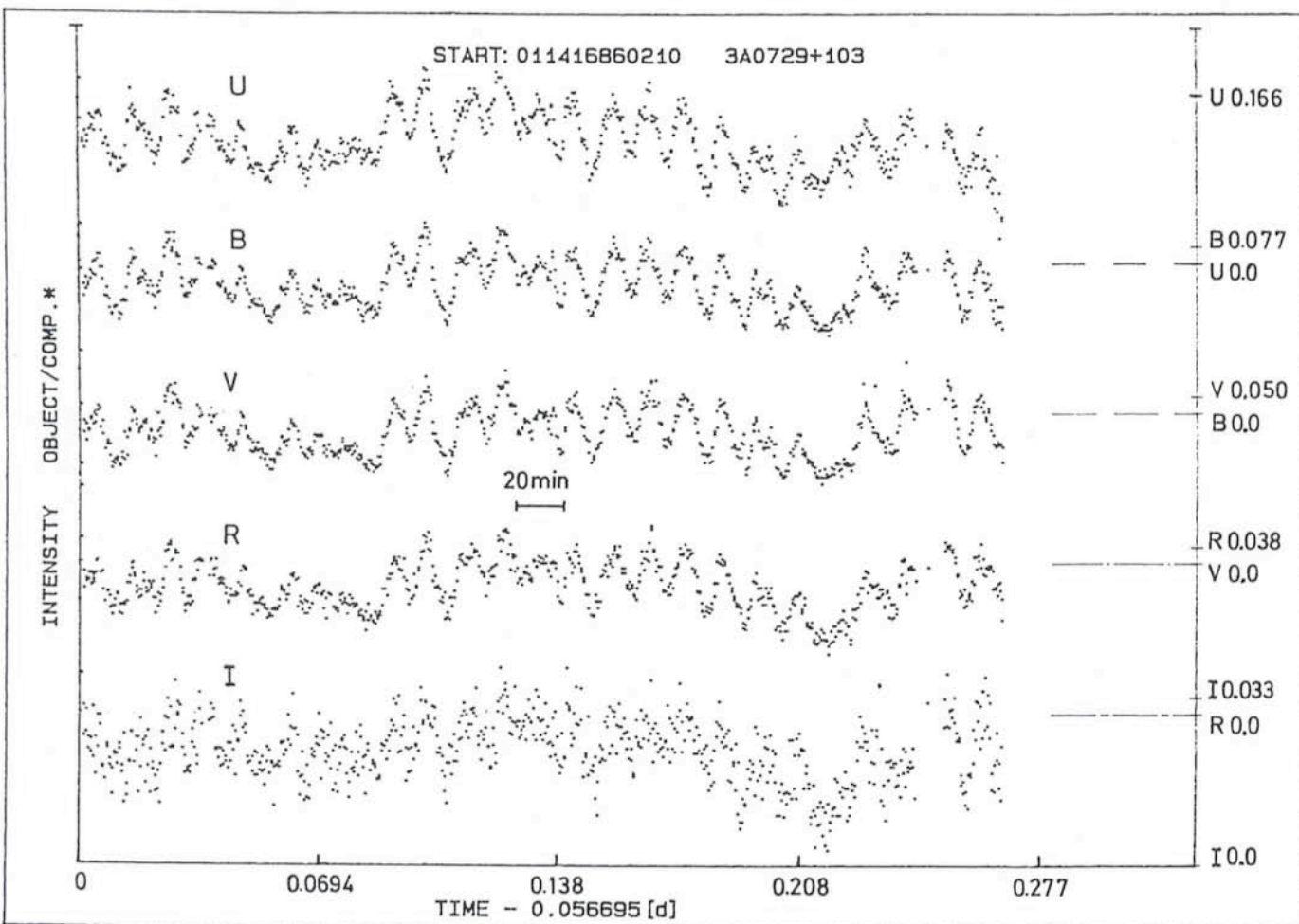


Figure 4: UBVRI lightcurves of the intermediate polar 3A 0729 +x 103 (BG CMi) showing short periodic variations (15 min) related to the rotating primary white dwarf. The amplitude is modulated with the orbital period of 3^h 14^m.

focus is completely off at the beginning, and the photometer coordinate system does not match to the local star acquisition system. Consequently, initialization takes more time. Then with dome lights off and photometer shutters open, the amount of straylight from indicator lamps, Cermet clock, TV displays, etc. be checked.

The orientation and scale of the telescope field in the photometer guiding system must be verified, the limiting magnitude of the autoguider must be checked as well as its proper adaption to the telescope control system to avoid guiding oscillations.

After all this, a mask plate has to be produced which holds the three fibers and a guiding diaphragm at their precise positions in the focal field. Of course, the preparation of the mask could also be done at home, but due to uncertainties of the correct scale and orientation of the focal field it has proven safer to use an option of the photometer which allows to drill a precise mask, live on the telescope.

Finally: Fibers are inserted – calibration – start measuring object – auto-guiding on. Now everything goes automatic, for hours, since this photometer is mainly used for variables which are monitored normally the whole night. When the results are looking good, the observer has time to go through a checklist to make sure that everything is really o.k.: Data are well presented on the graphic screen, there is regular storage on disk, autoguider regulation holds the star image within the errorbox indicated at the TV monitor, no oscillation, no drift, actual counts of object and comparison are consistent, programme parameter o.k.? . . . Yes! Observer can relax and watch the growing light curves on the monitor, check the transparency of the sky by following the comparison star on the graphic . . .

4. Performance – Present and Future

A large amount of photometric data could be gathered at La Silla until now, data that could have never been obtained with classical photometers. One example, presented by Schömb's et al. (1987a), concerns the monitoring of the short-period CV system OY Car during primary eclipse. The ingress and egress phases of the white dwarf last some 30 seconds only (Fig. 3). From colour variations within similar short time intervals the spatial temperature distribution of the eclipsed accretion disk can be derived. Another example is demonstrated in Figure 4, where the light variations of the intermediate polar 3 A 0729 + 103

are displayed. The MCCP has also been successfully applied to the investigation of optical pulses (timescale of milliseconds) from the X-ray burster MXB 1636 + 53. For this purpose the multichannel photometer had been attached to the 3.6-m telescope (See also Fig. 2). In order to investigate the extremely fast events produced by the neutron star of this object, a time resolution of 40 ms had to be used. Preliminary results are given by Schömb's et al. (1987b). Figure 5 finally displays the lightcurve of the eclipsing cataclysmic binary BD Pav, observed during a night so cloudy that even spectroscopists discontinued observation. BD Pav was measured as long as we could see our guiding star and as long as the observatory regulations permitted open domes. After reduction we found that for atmospheric absorptions of less than 80% the accuracy of the reduced data was only degraded according to the photon statistics.

In the near future the MCCP will be sent to La Silla for several additional observing programmes while at its home institute work has already started for a next generation instrument: Equip-

ped with computer-controlled positioning of the fiber optic channels it will offer 3 observing modes:

- 4-star multicolour photometry which allows to simulate different photometric systems (Strömgren uvby, Geneva system, etc.) by means of software;
- 8-channel spectral photometry with resolution of about 500;
- Multistar spectroscopy of up to 20 objects.

Each mode can be applied with a time resolution of 1 ms. A sophisticated software package shall optimize the observing routine in accordance with actual atmospheric conditions while complete reduction and preliminary analysis may be performed automatically during daytime, when the astronomer hopefully has already fallen asleep.

References

- Barwig, H., Schömb's, R., Buckenmayer, C.: 1987, *Astron. Astrophys.* **175**, 327.
 Schömb's, R., Dreier, H., Barwig, H.: 1987a, *Astron. Astrophys.*, in press.
 Schömb's, R., Pfeiffer, M., Häfner, R., Pedersen, H.: 1987b, *The Messenger*, **48**, 6.

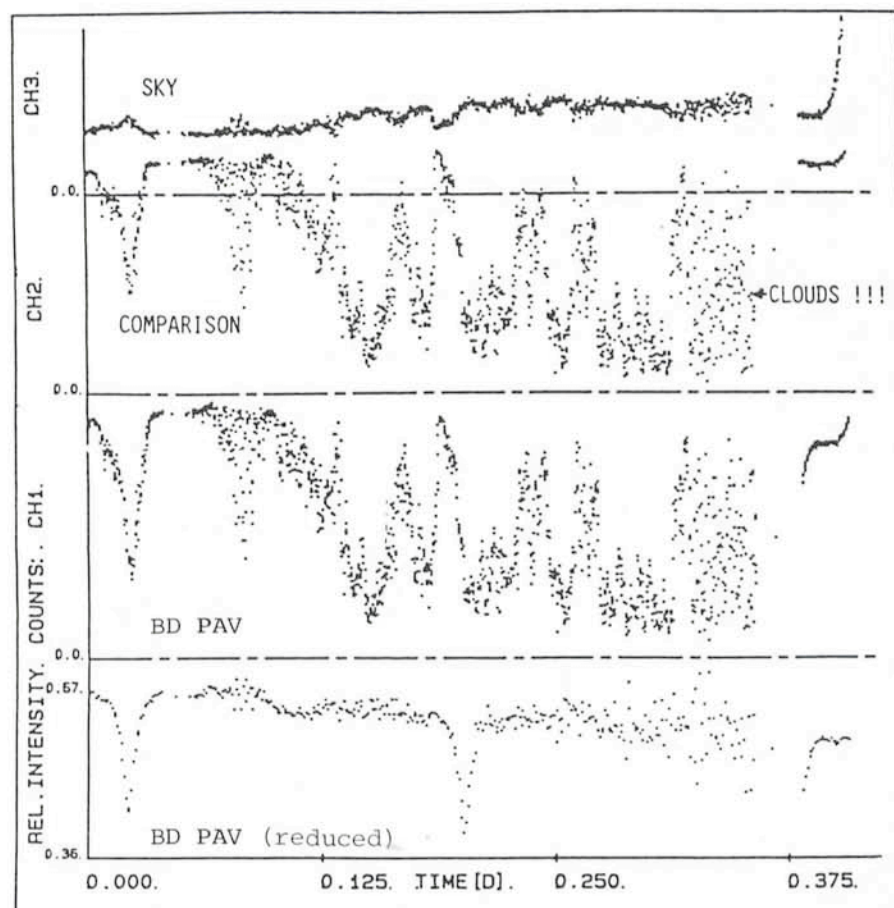
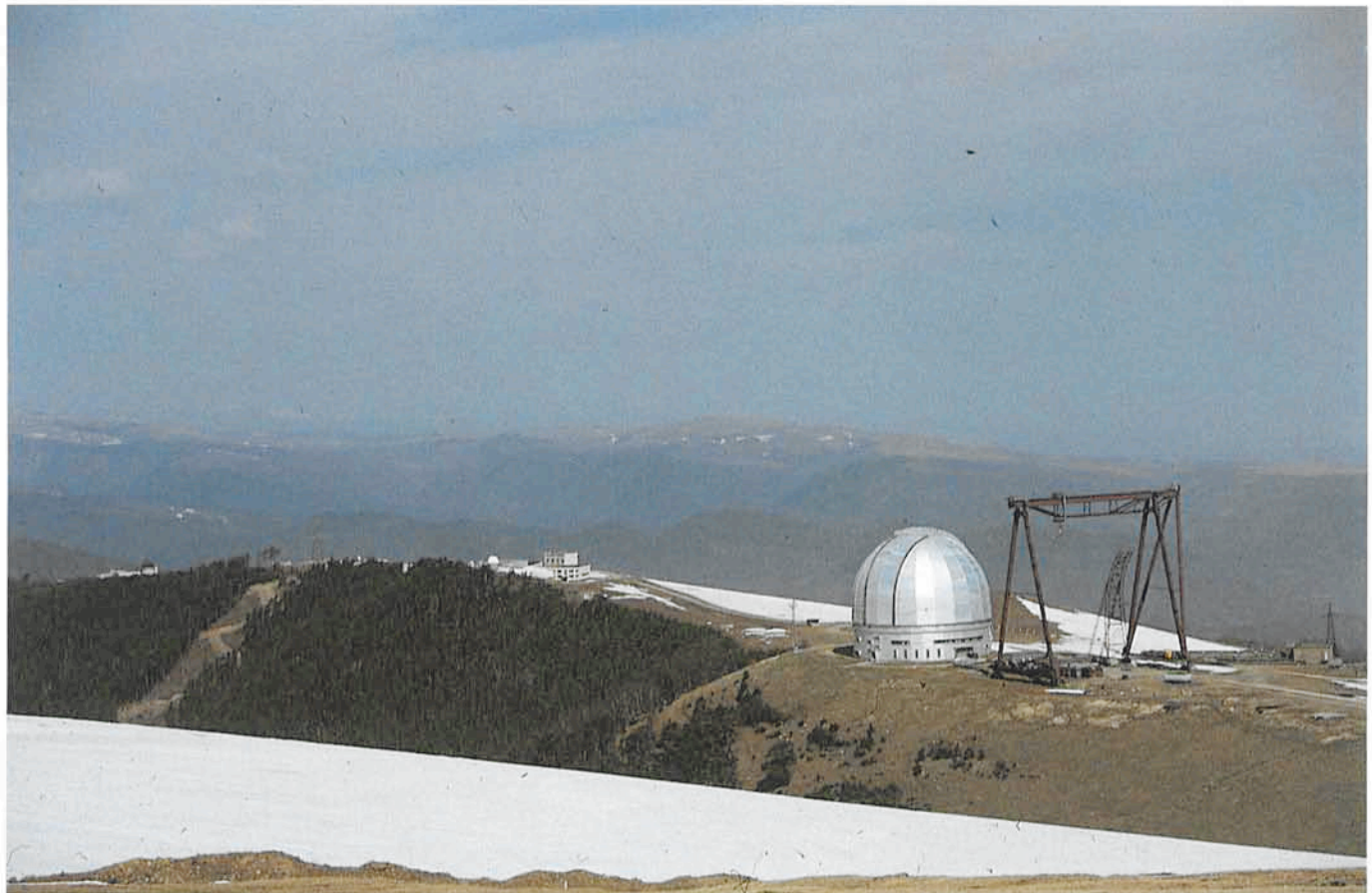


Figure 5: Simultaneous observations of BD Pav, nearby comparison star and sky during a non-photometric night. The reduced lightcurve (V-colour channels displayed only) demonstrates the ability to compensate highly variable atmospheric absorption.



View of the Special Astrophysical Observatory. To the right the 6-m dome (about 45 m diameter, 50 m high) and the service crane; the guesthouse is in the background to the left.

ESO VLT Delegation Visits 6-m Telescope

At the invitation of the Special Astrophysical Observatory (SAO) of the USSR Academy of Sciences, a small ESO delegation (Enard, Schneermann, West and Wilson) recently visited the 6-metre telescope which is installed near Zelenchukskaja, in northern Caucasus. It is at present the world's largest optical telescope and constitutes an interesting reference for those who are planning the construction of the VLT, the world's largest telescope of the future. The ESO delegation was warmly received by the Director of SAO, Dr. V.L. Afanasiev and the vice-Director, Dr. L.I. Snezhko, and was lodged in the guesthouse, near the 6-m building, about 2100 metres above sea level.

Detailed discussions were held about the construction and use of large telescopes. The ESO people gave comprehensive talks about the European Southern Observatory and its Very Large Telescope project and were in turn informed about various technical aspects and scientific programmes at the 6-m telescope. A detailed inspection of the alt-az telescope, including the

enormous bearings and the Nasmyth foci platforms, gave useful hints to the ESO engineers. Their SAO counterparts

were pleased to share their extensive experience, gained during more than 15 years, and to point out those particular



In front of the SAO main building at Nizhnyj Arkhiz, below the mountain and about 17 kilometres from the 6-m telescope by road. From left to right: V.F. Afanasiev, M. Schneermann, R. Wilson, L.I. Snezhko, R.M. West, D. Enard.

problem areas which must be considered, when ESO embarks on the construction of its VLT.

The weather was cooperative and there was ample opportunity to watch the astronomical observations which concentrated on IDS spectroscopy of the nuclei of active galaxies. SAO has recently adopted a flexible scheduling system, in which several programmes with different seeing requirements are on simultaneous standby. This system appears to have contributed to a more efficient exploitation of the available observing time.

The ESO delegation was interested to learn about the Soviet plans in connection with future large telescopes and the desire to continue the exchange of experience in such matters. There is little doubt that with the development of new astronomical sites in the USSR, in par-



The azimuth drive wheel.



At the foot of the 6-m service crane.

ticular in the high mountains of central Asia, astronomy in this country can look forward to a large observational potential.

After the stay at the 6-m telescope, the ESO people travelled to the other side of Caucasus and during a brief visit to Tbilisi, they had talks with colleagues from the Abastumani Astrophysical Observatory of the Georgian Academy of Sciences. Under the directorship of Academician E.K. Kharadze, plans are now under way for the installation of a large optical telescope at this observatory. Although the time was short, the ESO people were also given the opportunity to experience the legendary Georgian hospitality.

We owe sincere thanks to our hosts for making this visit so useful and pleasant.

R.M.W.

Major Film About Astronomy to be Produced

A major film about astronomy, telling the story of this science from Antiquity to our days and including a detailed overview of modern astrophysical research, is now being prepared by a French producer, with the support of the French Ministry of Education, La Villette, French television and other organizations. In view of the importance of this ambitious international project, which is carried out with the active collaboration of several well-known European astronomers, the European Southern Observatory has offered to provide advice and services during extensive shooting

sessions at the La Silla observatory and also at the Headquarters in Garching.

The project aims at a 6-hour series which will be shown on television in several countries. An associated, large (travel) exhibition and a comprehensive written documentation (book) will also be prepared. The work of astronomers, their celestial discoveries and the life at astronomical institutions, with buildings and instruments will be described.

In order to bring this project to a successful conclusion, the film people are now in the process of establishing contacts with observatories all over the

world and they would greatly appreciate any material (brochures, photos, etc.) at the following address: Mr. R. Pansard-Besson (Les Productions Berthemont), 47, rue de Rennes, F-75006 Paris, France.

The editors regret that the wrong institute was indicated after the name of D. Heynderickx (*The Messenger* No. 47, March 1987, p. 28). The correct affiliation is: Astronomisch Instituut, Katholieke Universiteit Leuven, Belgium.

Discovery of a Binary Quasar

G. MEYLAN, ESO

S. DJORGOVSKI, Harvard-Smithsonian Center for Astrophysics

R. PERLEY, National Radio Astronomy Observatory, and

P. McCARTHY, Berkeley Astronomy Department

1. Introduction

The discovery of quasars, about 25 years ago, was one of the most exciting events in the history of recent astronomy. Despite the slow growth in our understanding of their physical nature, these objects, which have the highest known redshifts, still provide the best available probe of the most remote observable regions of the universe. Notwithstanding the numerous observational and theoretical difficulties (few if any of the simplest and most basic questions about quasars can be answered with certainty), the enthusiasm of astronomers for the study of quasars has not declined.

Though long discussed and predicted by Eddington, Einstein, and Zwicky (e.g. see IAU Symposium # 119 and references therein), the still recent discovery of the gravitational lensing phenomenon is one of the most vigorous and growing subjects in modern extragalactic astronomy. A natural expectation, based on the observed degree of galaxy clustering at low redshifts and on reasonable extrapolations to large redshifts, indicates that some of the claimed "gravitational lens" systems are actually physical pairs of quasars with small separations (Bahcall et al. 1986). There are, in fact, several pairs of quasars known, with projected angular and redshift separations indicative of membership in large clusters or superclusters (e.g., 1146+111, 0952+698, and 1037-271). However, there are no *definite* close physical quasar pairs currently known at any redshift. Finding such a QSO pair would be very interesting, as it would provide diagnostics of processes and insight into phenomena which are not probed by the gravitational lensing: e.g. the nature of clustering at large redshifts, the role of gravitational interactions in triggering and fueling of galaxian nuclear activity.

2. The Observations

We report here the discovery of a pair of quasars with a redshift of 1.345, separated by 4.2 arcsec in projection, apparently associated with the radio source PKS 1145-071. It could be the first binary quasar known (Djorgovski et al. 1987).

The radio source OM-076 was first identified with a blue, 17.5^m stellar object on the Palomar Sky Survey by Radovich and Kraus (1971), and then "rediscovered" as PKS 1145-071 by Bolton, Shimmins, and Wall (1975), who confirmed the optical identification. The spectroscopy of the object by Wilkes (1986) identified it as a QSO with $z = 1.345$. VLBI measurements of the radio source were published by Preston et al. (1985). There was no mention by any author of the source's binary structure.

2a. The Imaging CCD Observations

It is well known that one of the common ways of obtaining the flatfields for an observation night (or even run) consists of taking sky median frames. Then

a number of about 5 exposures free of bright and/or very extended objects are obtained during the night. It is of course ideal if the chosen fields have in addition a scientific content!

At La Silla, last December, we took frames for sky median in regions extremely poor in stars but carefully selected for containing quasars which could be possible lens candidates. During the first night, the pair of quasars associated with the radio source PKS 1145-071 was discovered. The QSO was selected on account of a marginal elongation visible on the finding chart!

We obtained initial images of the field on the night of UT 1986 December 29, using the RCA 320 × 512 CCD # 5 mounted at the Cassegrain focus ($f/8.01$) of the ESO 2.2-m telescope, at La Silla. The effective pixel size was 0.363

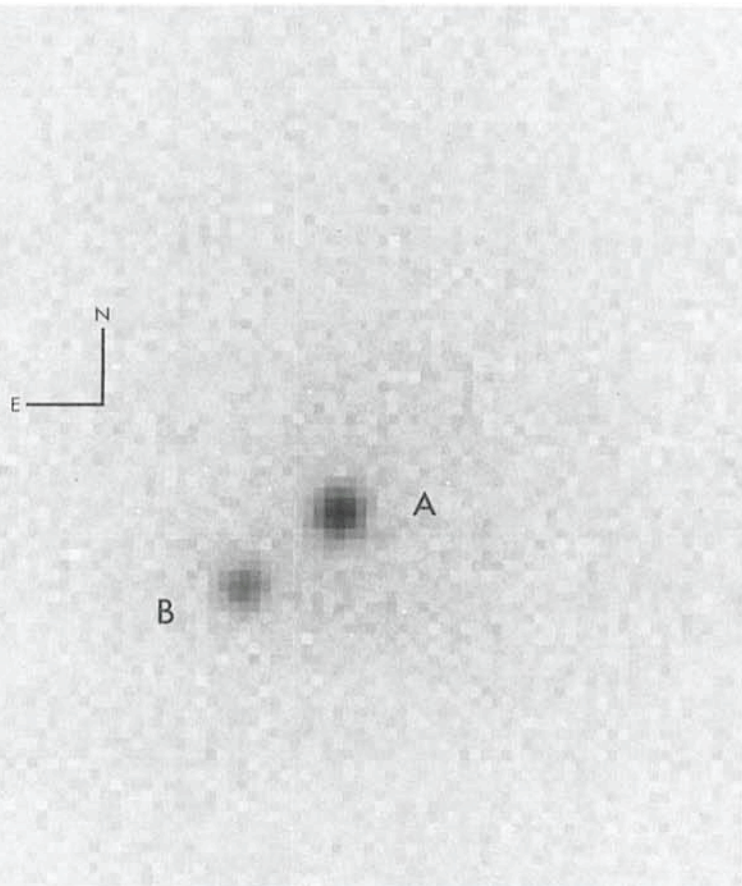


Figure 1: We report here the discovery of a pair of quasars with the redshift of 1.345, separated by 4.2 arcsec in projection, apparently associated with the radio source PKS 1145-071. Being the first image showing the binary character of this object, this figure displays the B-band CCD frame of the PKS 1145-071 field, obtained at ESO. The two QSO's are labeled as "A" and "B".

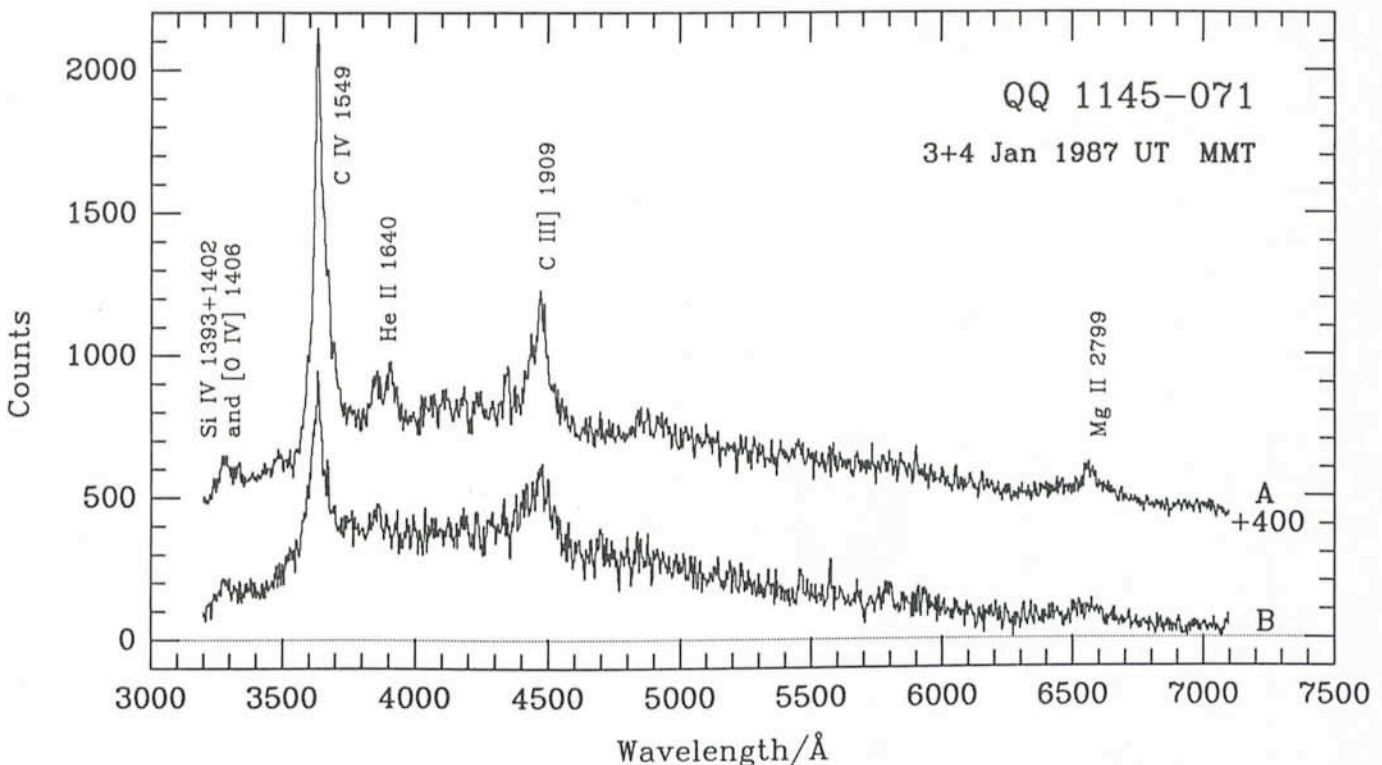


Figure 2: The spectra of the two quasars, obtained at the MMT: QSO A on the top, B on the bottom. The spectrum of the QSO A was shifted up by 400 units for clarity. Both spectra were rebinned to 3 Å bins (~ the instrumental resolution). The relative flux scale is arbitrary.

arcsec. The meteorological conditions were not of great quality: marginally non-photometric and with a seeing $\text{FWHM} = 1.5$ arcsec (the next night quite a few frames had $\text{FWHM} = 0.6$ arcsec!). One B and one V exposure of 300 s each were obtained. The B frame is shown in Figure 1.

The separation of the two components is:

$$\Delta\alpha_{A-B} = -3.3 \pm 0.1 \text{ arcsec}$$

$$\Delta\delta_{A-B} = +2.6 \pm 0.1 \text{ arcsec}$$

which corresponds to a total separation of 4.2 ± 0.1 arcsec in the direction $\text{PA} = 128^\circ$. Our magnitude zero points are uncertain (approximate magnitude of the QSO A is ~ 18), but we can derive accurate intensity ratios for the two images, $I_A/I_B = 2.15 \pm 0.15$ in the B band, and 2.7 ± 0.1 in the V band.

Because of the equatorial position of this object, it can also be observed from the northern hemisphere: this was the beginning of a cascade of observations!

2b. The Spectroscopic Observations

Spectra of the two components were obtained on the nights of UT 1987 January 3 and 4, by using the Reticon spectrograph on the Multiple Mirror Telescope at Mt. Hopkins. We used the low resolution ($300 \text{ lines mm}^{-1}$) grating, and 2×3 arcsec entrance apertures. The seeing was fairly good, but transparency variable, which prevented adequate

flux calibration of the data. The spectra confirmed immediately that both objects A and B are quasars, at apparently the same redshift. The total integrations for the QSO's A and B were 600 s and 2000 s respectively on 3 January, and 960 s and 2160 s on 4 January.

The total spectra are shown in Figure 2. They appear similar at a first glance. But they exhibit significant differences. The CIV 1549 line clearly has a larger equivalent width in the QSO A. In the A component, the HeII 1640 appears stronger than in B, and with an absorption feature. The MgII 2799 is only marginally existant in B. The line widths also seem different.

The redshift of this quasar, based on the CIV line alone is $z_A = 1.345 \pm 0.001$. The measurements of the CIV 1549 and HeII 1640 lines for the QSO B are difficult because of blending.

Considerable care was given to the measurement of velocity difference between the two QSO's. We did wavelength calibration in two different ways. We measured redshift difference from the strong CIV line, and from the cross-correlation of spectra, for the two nights separately, using different portions of the spectra, and employed two different centring methods for the emission lines and cross-correlation peaks. Different methods and variation of parameters enabled us to estimate our internal errors.

From the centring of the CIV line only,

we obtain $\Delta z_{A-B} = 0.001 \pm 0.003$, independently for both nights, corresponding to the rest-frame velocity difference $\Delta v_{A-B}^{\text{rf}} = 300 \pm 800 \text{ km s}^{-1}$. A more accurate method, cross-correlation using complete spectra in wavelength range 3200–7000 Å, gives $\Delta z_{A-B} = (9.3 \pm 2.7) \times 10^{-4}$, or $\Delta v_{A-B}^{\text{rf}} = 280 \pm 80 \text{ km s}^{-1}$ for the 3 January data, and $\Delta z_{A-B} = (6.5 \pm 3.8) \times 10^{-4}$, or $\Delta v_{A-B}^{\text{rf}} = 200 \pm 110 \text{ km s}^{-1}$ for the 4 January data, which have somewhat more reliable wavelength calibration and a better signal-to-noise ratio. Similar numbers are obtained if one uses the wavelength range 3200–4800 Å. However, if we exclude the portion dominated by the CIV line, and use the data in the range 3800–7000 Å, the difference drops to $\Delta z_{A-B} = (4.1 \pm 3.1) \times 10^{-4}$, or $\Delta v_{A-B}^{\text{rf}} = 120 \pm 90 \text{ km s}^{-1}$ for the 4 January data (the 3 January data do not have enough signal to do this test).

2c. Radio Observations

Short observations of PKS 1145-071 were obtained with the Very Large Array (VLA) on the night of UT 1987 January 9. In view of the configuration available ("C"), only the data taken at 2 and 1.3 cm had sufficient resolution to clearly determine whether the object contained two points of emission, or one. All the data were calibrated by short observations of nearby point sources. Subsequently, the standard self-calibration

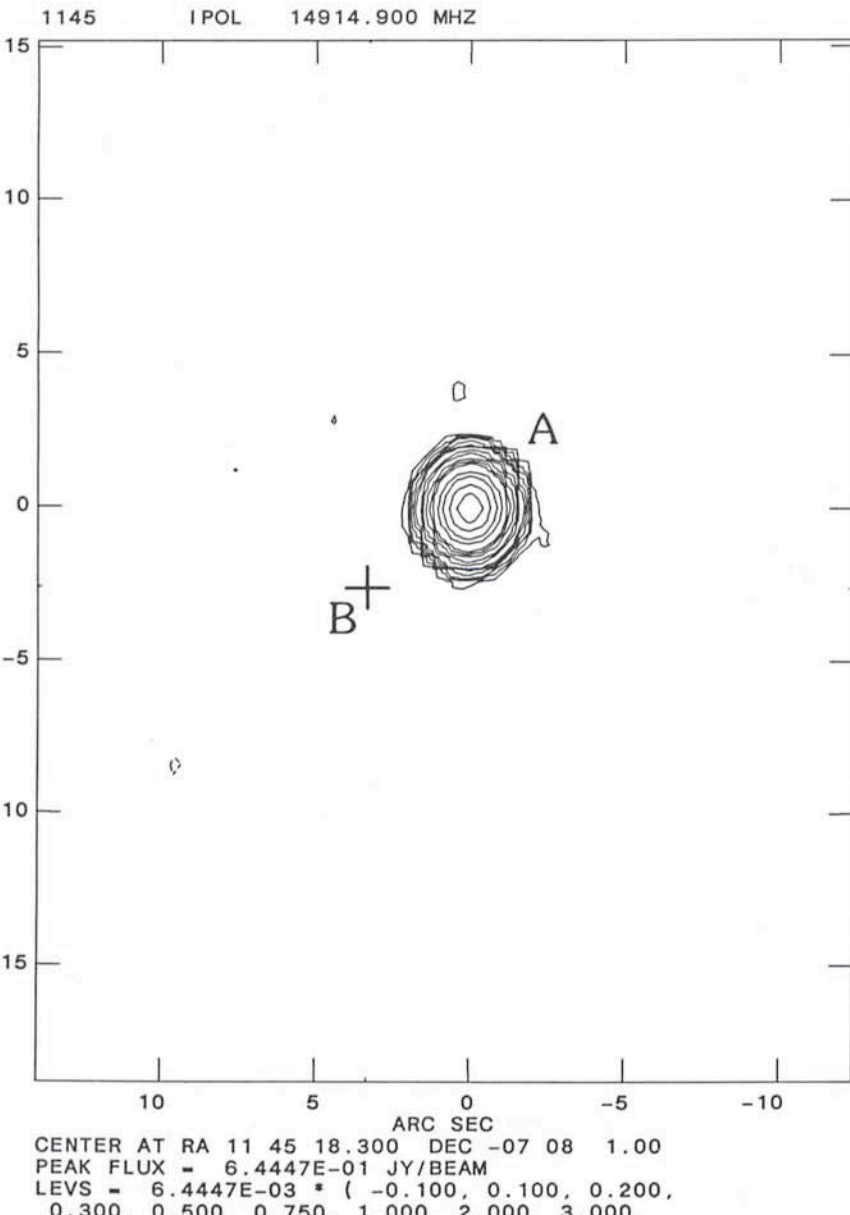


Figure 3: Radio map of PKS 1145-071, obtained at VLA at 2 cm, in the C configuration. The position of the QSO B is marked with the cross. The residual noise in this map is 0.23 mJy.

routines were applied, and the resulting maps have excellent dynamic range, $\sim 2700 : 1$ at 2 cm and 6 cm, and $\sim 200 : 1$ at 1.3 cm. The 2 cm map is shown in Figure 3. The source is unresolved at all frequencies, and there is no trace of a secondary image.

The best-fit radio position of the source (epoch 1950.0) is:

$$\begin{aligned} \alpha &= 11^{\text{h}} 45^{\text{m}} 18.29^{\text{s}} \\ \delta &= -07^{\circ} 08' 00.56'' \end{aligned}$$

with errors of 0.05 arcsec in each coordinate. We obtained the optical position of the brighter of the two QSO's from the independent measurements of both red (E) and blue (O) prints of the Palomar Sky Survey, by using the Center for Astrophysics dual axis measuring machine. Some 20 SAO stars were used

to establish the coordinate system. The final mean position (epoch 1950.0) is:

$$\begin{aligned} \alpha &= 11^{\text{h}} 45^{\text{m}} 18.30^{\text{s}} \\ \delta &= -07^{\circ} 08' 01.05'' \end{aligned}$$

with errors of 0.6 arcsec in each coordinate. There is thus no doubt that the radio source is associated with the QSO A.

3. Discussion and Conclusions

There are only a few systems for which the gravitational lensing interpretation is now reasonably well established, viz., 0957+561, 1115+080, 2016+112, and probably 2237+030. To this date there is no detection of lens objects in two other possible cases, 1635+267, and 2345+007. The non de-

tection of any lens object is of course not equivalent to the non existence of such object! Nevertheless these two last cases could be regarded also as tentative true pairs of physically distinct quasars.

In the case of PKS 1145-071, the imaging and spectroscopic data are marginally consistent with the interpretation of the pair as a gravitational lens. The crucial evidence comes from our radio maps: the intensity ratio on cm wavelengths is *at least several hundred*, which should be compared to the optical intensity ratio of ~ 2.5 . In order to salvage the gravitational lens hypothesis, we would require dramatic $L_{\text{Opt}}/L_{\text{Radio}}$ variability on the time scales corresponding to the path delay (~ 1 year), a variability never before observed for an extragalactic source. We thus conclude that the QSO pair 1145-071 is most likely a genuine binary quasar. The above pair has the smallest angular separation known for this kind of objects.

It is tempting to compare this system with the two other QSO pairs, 1635+267 and 2345+007, both of which are radio-quiet, and for both of which the spectroscopic and imaging evidence for gravitational lensing are about equally good as in the case of 1145-071 here. For these two systems there is no obvious lensing cluster and/or galaxy to very faint magnitude levels. Pending further studies, we should leave these two cases open, as they may be interpreted either way.

A physical binary quasar should be an interesting object to study, as it may provide us with some clues about the origin and the fuel of QSO activity. Evidence for tidal interactions is often indicated in the low-redshift QSO-galaxy associations, and even proposed as a possible trigger of the QSO activity (cf. Stockton 1986, and references therein). Tidal shocks may facilitate a runaway gravitational collapse of the central cluster in participating galaxies, and thus actually form the central "engine", or feed more stars and gas into it if it already exists. Galaxy collisions also provide plausible means of transporting the ISM fuel to the central engines. In the 1145-071 A+B system we may be seeing such fateful interaction occurring at an early epoch when the comoving density of quasars was considerably larger than it is today. In any case, the projected separation and the velocity difference between the two QSO's are consistent with a tidal encounter.

To interpret our data in terms of physical scales, we note that in a Friedman cosmology (with $H_0 = 100 \text{ km s}^{-1} \text{ Mpc}^{-1}$, $\Lambda_0 = 0$, and $q_0 = 0$), the distance modulus to the system is $(m-M) = 44.1$, and the projected separation of 4.2 arcsec

corresponds to 25.0 kpc. If we substitute $q_0 = 1/2$, these numbers become 43.44, and 18.1 kpc respectively.

From the knowledge of the projected separation a of the two components and from the (significant) difference in velocity between A and B, it is possible to determine a direct estimation of the total mass of the system, under the hypothesis of orbital motions of the two components around their centre of gravity of the system. Using Kepler's third law, we have:

$$(M_A + M_B) \sin^3 i = 2.89 \cdot 10^5 \frac{a}{\text{kpc}} \frac{V^2}{\text{km}^2 \text{s}^{-2}} M_\odot \quad (1)$$

If we take $a = 25.0$ kpc and $V = 250$ km/s (mean of the determinations using the complete spectra, i.e. 3200–7000 Å, for $\sin i = 1$, the total mass of the system equals $M_A + M_B = 4.5 \cdot 10^{11} M_\odot$ (lower bound).

Concerning absorption lines, it is worth mentioning that, with an angular separation of 17.9 arcmin, the projected distance between the lines of sight to the two quasars Tololo 1037-27 and Tololo

1038-27 is of the order of 4 Mpc. Thus the absorption line systems in these two quasars could give the largest distance over which correlated absorption quasar spectra has been reported to date (Ulrich 1986). In the case of PKS 1145-071 A+B, the absorption feature in the H α 1640 of the A component only could give the smallest distance (less than 25 kpc) known so far over which differential absorption is observed, the intervening material being only at a very small distance from the concerned object.

Another exciting possibility is that this pair is situated towards a high-redshift galaxy cluster: if quasars are rare events, then two quasars could be suggestive of a high galaxy density. Mere existence of rich clusters at such large redshifts provides an interesting timing constraint for the theories of large-scale structure formation. No such rich environment is visible on our short exposure frames. Studies of "normal" galaxies in this hypothetical cluster (i.e., those not selected by their large radio power, or strong line emission) should be extremely valuable for the investigations of

galaxy evolution at large look-back times. Deep imaging and spectroscopy are needed to pursue this potentially highly rewarding possibility, an ideal proposal for the VLT!

It is a pleasure to thank T. Courvoisier for extremely stimulating discussions and advice.

References

- Bahcall, J., Bahcall, N., and Schneider, D. 1986, *Nature* **323**, 515.
- Bolton, J., Shimmins, A., and Wall, J. 1975, *Austr. J. Phys. Suppl.* **34**, 1.
- Djorgovski, S., Perley, R., Meylan, G., and McCarthy, P. 1987, *Astrophys. J. Lett.* submitted.
- Preston, R., Morabito, D., Williams, J., Faulkner, J., Jauncey, D., and Nicolson, G. 1985, *Astron. J.* **90**, 1599.
- Radovich, M., and Kraus, J. 1972, *Astron. J.* **76**, 683.
- Stockton, A. 1986, *Astrophys. Space Sci.* **118**, 487.
- Ulrich, M.-H. 1986, in proc. of *Second ESO/CERN Symposium*, G. Setti and L. van Hove, eds., p. 87.
- Wilkes, B. 1986, *Monthly Notices Royal Astron. Soc.* **218**, 331.

Preliminary Abundances in Three Cool Supergiants of the SMC

M. SPITE and F. SPITE, Observatoire de Paris, Section de Meudon

Introduction

It is quite well known that the objects of the Magellanic Clouds (even the younger objects) have lower abundances of heavy elements than similar objects of our Galaxy (see for example Lequeux, 1983). The whole history of the chemical evolution of the Magellanic Clouds is not yet fully understood. Stellar spectroscopy can contribute to a better knowledge of the abundances in the MC. The pioneering work of Przybylski was begun a long time ago (LMC, 1968, SMC, 1972) using photographic plates at the coudé spectrograph of the 1.88-m (74-inch) telescope at Mount Stromlo. Subsequent work was made by other astronomers, especially by B. Wolf (1972, 1973) using similar techniques at the ESO 1.5-m spectrographic telescope. The use of photographic plates (the only detector available for such a problem at that time) pushed the astronomers towards the observation of blue (hot) stars, since the sensitivity of photographic emulsions is at maximum in the blue part of the spectrum. Foy (1981) and Thevenin and Foy (1986)

used the ESO ECHELEC spectrograph and the electronic camera (Baranne, 1976) for the analysis of cooler supergiants.

New Observations and Analysis

As soon as the CASPEC spectrograph with its CCD detector became available (D'Odorico et al., 1983) it appeared that it was perfectly suited for the determination of stellar abundances (D'Odorico et al., 1985; Spite et al., 1985; Spite, 1986). M. Dennefeld called our attention to the subject of the abundances in the Magellanic Clouds, and we decided to try to improve the previous knowledge about the abundances in the Clouds by careful observations and analysis of a few supergiants. Some difficulties in this task are obvious. The determination of the temperature of such stars is affected by uncertainties (the calibration of the colours of the supergiants is not completely reliable, the reddening of the stars is not accurately known and the profiles of the hydrogen lines are not always reli-

able). Moreover, these stars, even when not known as variable, may still be slightly variable. Finally, the spectral lines could be affected by non-LTE effects.

The best way to tackle this problem was to select rather cool supergiants for observation. The spectra of cool stars display numerous absorption lines: faint and strong lines, lines originating from low and high excitation levels, lines of various elements. From the accurate measurements of these lines, a number of constraints are found for the model atmosphere, so that, by iteration, a model can be adjusted, from which reliable abundances can be derived. The best accuracy of the measurements of the equivalent widths of lines is achieved when using the red part of the spectrum, where the continuum is more easily determined, and this is made possible by the good sensitivity of the CCD detector in the red.

Observations of supergiants were begun at the ESO 3.6-m telescope with the CASPEC spectrograph, but the programme was severely disturbed by

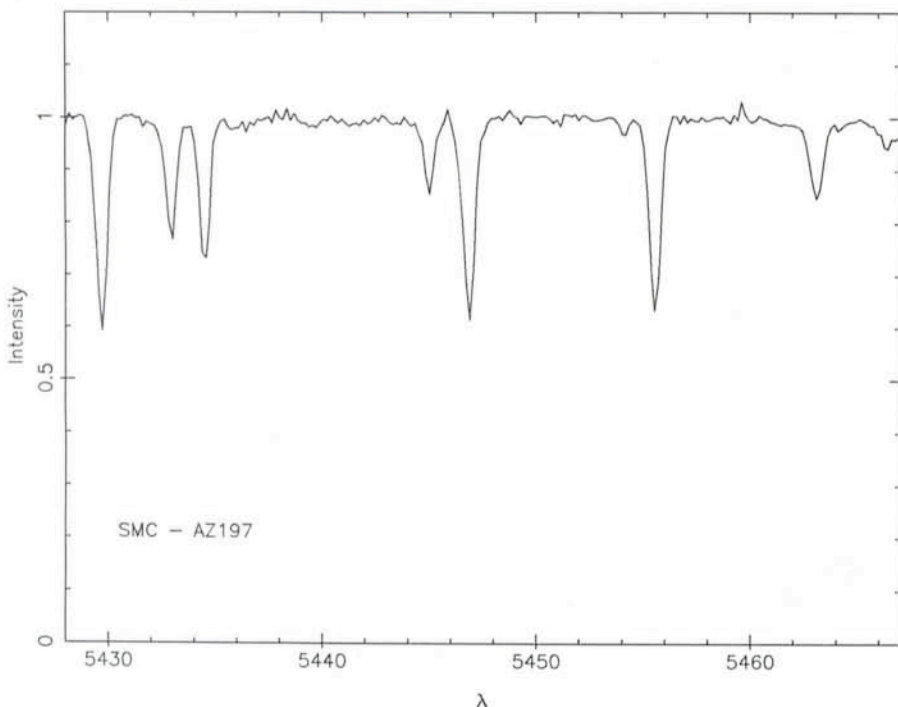


Figure 1: A (small) part of the spectrum of a supergiant field star of the Small Magellanic Cloud, obtained at the ESO 3.6-m telescope, using the CASPEC spectrograph.

cloudy weather. A few good spectra of stars in the LMC and SMC were obtained, as well as one spectrum of a star in a young globular cluster of the SMC (Spite et al., 1986). An example of one of the spectra obtained in the SMC is shown (Fig. 1). Preliminary results are now available for the three field stars observed in the SMC. The curve of growth of iron of the star AZVI 197 is shown in Figure 2. The curve and the abscissae were computed by using the models of Gustafsson et al. (1975). The scatter of the measured lines is rather small and, more importantly, there is no apparent stratification of the lines originating from low or high excitation levels: this is an evidence that the choice of the model temperature was correct.

Global Metallicity

Let us recall that the iron abundance may be considered as a determination of the global metallicity of the star (we will come back later to refinements such as the variations in the relative abundances of the elements), as well as the oxygen abundance may be considered as a determination of the global "metallicity" (heavy element content) of the gaseous objects such as HII regions and planetary nebulae. Let us also recall that the metallicity of the Sun is representative of the metallicity of the (young) Population I of the Galaxy and is universally adopted as the standard for intercomparisons of metallicities.

Dufour (1983) and by Peimbert (1983) for the SMC and LMC. Taking into account the error bars, the mean metallicity of the SMC supergiants and the "metallicity" of the SMC gaseous objects may be considered as being in fair agreement.

Relative Abundances of the Metals

If we concentrate now on the pattern of the relative abundances of the elements, it appears that the light metals are less deficient than iron: this is what is normally found in the metal-deficient stars of the Galaxy. However, some exceptions are to be noted: (1) magnesium (essentially ^{24}Mg), which is less deficient than iron in the Galaxy, seems to be as deficient as iron in the three supergiants. (2) Sodium (essentially ^{23}Na), which has the same deficiency as iron in the Galaxy, has a smaller deficiency than iron in the three supergiants. In other words, magnesium and sodium have, in the three SMC stars, a behaviour which is the opposite of their behaviour in the Galaxy. (3) Yttrium and barium (^{89}Y and ^{138}Ba) seem to be less deficient than iron. These peculiarities have, of course, to be checked, in order to find if they are real abundance effects or artefacts introduced by the imperfections of the model and/or imperfections in the adjustment of the model.

Table 1 provides: (1) the iron abundances relative to the Sun (i.e. iron deficiencies) found for the three supergiants (they are remarkably similar), (2) the mean of these deficiencies, (3) the mean oxygen deficiencies proposed by

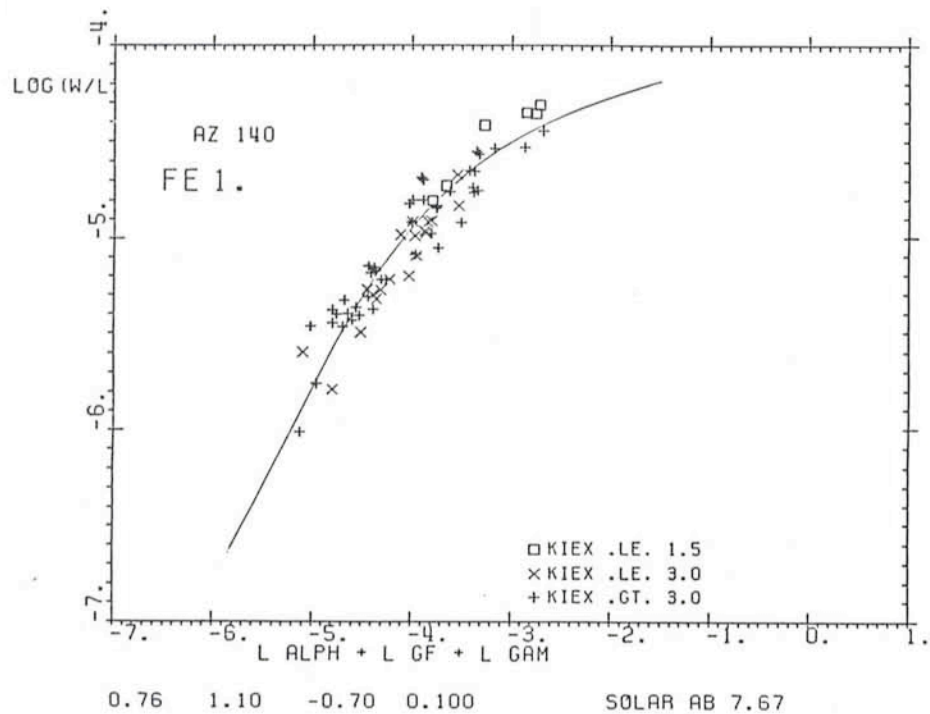


Figure 2: Curve of growth of neutral iron lines in the star AZ140 (a supergiant of the SMC). The abscissa is an auxiliary quantity, computed from the model and from atomic data. The ordinate is the logarithm of the measured quantity W/λ : the experimental values are represented by symbols related to the lower level of the corresponding atomic transition. No stratification of the symbols is observed, at variance with the stratifications clearly observed when the effective temperature of the model is not correctly adjusted.

Conclusion

It is hard to derive a firm conclusion from preliminary results. However, let us note that the cool supergiants analysed here are not very different from the luminous giants of globular clusters, which we have analysed previously, and for which we found abundances similar to the ones found by other authors. Przybylski and Foy have already argued that the abundances found in the supergiants of the Magellanic Clouds should be reliable.

Therefore, if it is accepted to have

OBJECT	Fraction of solar metallicity	[Fe/H]	[O/H]
star AZVI 140	0.19	-0.72	
star AZVI 197	0.22	-0.66	
star AZVI 369	0.18	-0.74	
Mean (SMC stars)	0.2	-0.7	
SMC HII (Dufour)	0.16		-0.8
SMC HII (Peimbert)	0.10		-1.0
SMC PN (Peimbert)	0.16		-0.8
LMC HII (Dufour)	0.40		-0.4
LMC HII (Peimbert)	0.32		-0.5
LMC PN (Peimbert)	0.25		-0.6

Let us recall the classical notation: $[X] = \log X_* - \log X_0$

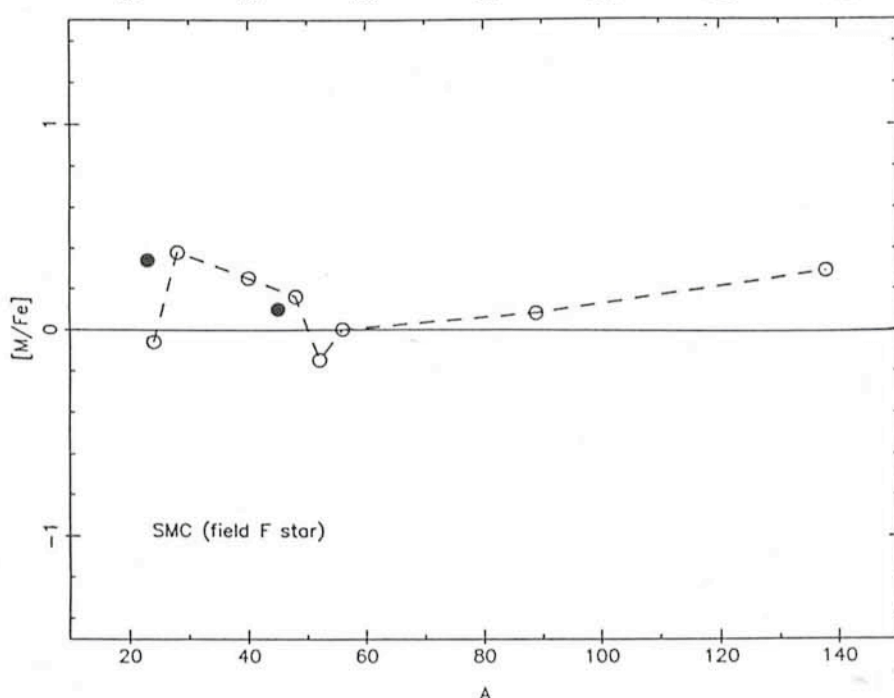
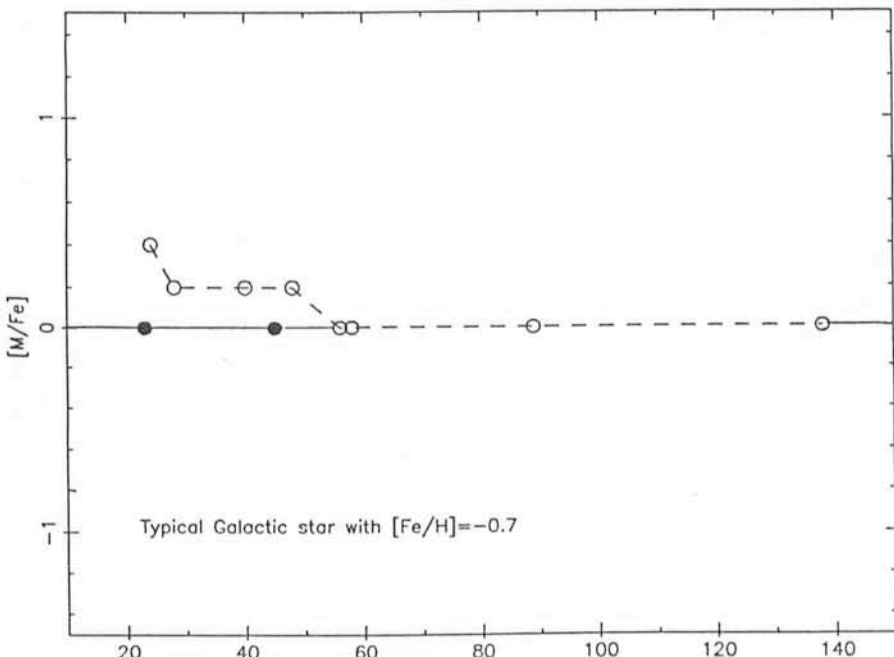


Figure 3: Patterns of elemental abundances in Galactic dwarfs (upper part) and in SMC supergiants (lower part). The abscissa is the atomic number, the ordinate is the (logarithmic) ratio of the abundance of the element relative to iron. In both cases, a smaller deficiency of the light metals is apparent, but the two metals Sodium ^{23}Na (filled circles) and Magnesium ^{24}Mg (open circles) have opposite behaviours.

(provisionally) a very optimistic and naive view of the results here presented, it could be admitted that the metallicity of all the young supergiants in the SMC agree, within determination errors, with the „metallicity” (i.e. oxygen abundance) of young gaseous objects such as HII regions and planetary nebulae. With some further optimism, it could be guessed that the agreement found for the SMC holds also for the LMC, and that therefore the global metallicity of young stars in the LMC will be the one found for oxygen in the gaseous objects. As a consequence, the best choice for the progenitor of the supernova 1987A would be the metallicity found for oxygen in the gaseous objects in the LMC, i.e. about $\frac{1}{3}$ of the solar metallicity (see Table 1).

Acknowledgements

We are indebted to P. François for taking part in this work and to M. Dennefeld for calling our attention to the problem of abundances in the Magellanic Clouds. We are also indebted to T. Richtler who measured V , R , I colours for the stars observed spectroscopically. We thank R. Cayrel for useful comments. We are grateful to S. D'Odorico for helpful advice about the use of the CASPEC + CCD system.

References

- AZV = AZVI = AzV = Azv = AZ see Azzopardi and Vigneau, 1982.
- Azzopardi, M., Vigneau, J.: 1982, *A & A Suppl.* **50**, 291.
- Baranne, A.: 1976, *Advances in Electronics and Electron Physics* **40 B**, Proceedings of the 6th Symposium on Photoelectronic Image Devices, eds. B.L. Morgan, R.W. Airey, D. McMullan, p. 641.
- Dennefeld, M.: 1985, private communication.
- D'Odorico, S., Enard, D., Lizon, J.L., Ljung, B., Nees, W., Ponz, D., Ruffi, G., Tanne, J.F.: 1983, *The Messenger* **37**, 24.
- D'Odorico, S., Gratton, R.G., Ponz, D.: 1985, *A & A* **142**, 232.
- Dufour, R.J.: 1984, see Van den Bergh, S.

- and De Boer, 1983, p. 353.
 Foy, R.: 1981, *A & A* **103**, 135.
 Gustafsson, B., Bell, R. 2A., Eriksson, K., Nordlund, A.: 1975, *A & A* **42**, 407.
 Lequeux, J.: 1983, see Van den Bergh, S. and De Boer, 1983, p. 67.
 Peimbert, M.: 1983, see Van den Bergh, S. and De Boer, 1983, p. 363.
 Przybylski, A.: 1968, *M.N.R.A.S.* **139**, 313.
 Przybylski, A.: 1972, *M.N.R.A.S.* **159**, 155.
 Spite, F.: 1986, ESO-OHP Workshop, J.P. Baluteau and S. D'Odorico eds. Garching, p. 251.
 Spite, F., François, P., Spite, M.: 1985, *The Messenger* No. 42, 14.
 Spite, M., Cayrel, R., François, P., Richtler, T., Spite, F.: 1986, *A & A* **168**, 197.
 Thevenin, F., Foy, R.: 1986, *A & A* **155**, 145.
 Van den Bergh, S., De Boer, K.: 1983, eds. of the IAU Sympos. 108: *Structure and Evolution of the Magellanic Clouds*, Reidel, Dordrecht.
 Wolf, B.: 1972, *A & A* **20**, 275 (LMC).
 Wolf, B.: 1973, *A & A* **28**, 335 (SMC).

Distant Clusters of Galaxies

A. CAPPI¹, G. CHINCARINI^{2,3}, P. CONCONI³, I. MANOUSSOYANAKI⁴, and G. VETTOLANI⁵

¹Bologna; ²Università degli Studi di Milano; ³Osservatorio Astronomico di Brera, Milano; ⁴Istituto di Fisica Cosmica e Technologie Relative, CNR, Milano; ⁵Istituto di Radioastronomia del CNR, Bologna

The information we receive from astronomical objects is, thanks to the finite speed of the electromagnetic radiation, related to their past status. Such differentiation between past and present becomes meaningful only on a large scale or, equivalently, over long times. The clock and time unit are set by the stellar evolution and by the dynamical time.

A glance at Figure 1 shows indeed that at $z = 0.5$ the look back time for $\Omega_0 = 1.0$ and $H_0 = 50 \text{ km sec}^{-1} \text{ Mpc}^{-1}$ is about $6 \cdot 10^9$ years, a time which is long enough to allow the evolution off the main sequence of some stars and comparable to the free-fall time of large and massive clouds of gas. The collapse time of a cluster of galaxies (Gunn and Gott, *Ap.J.* **176**, 1, 1972) is of the same order of magnitude, however, it is inde-

pendent of the particular cosmological model. It is striking, indeed, to consider what Figures 1 and 2 tell us. At $z \geq 0.5$ and depending on the values of q_0 and H_0 we may look at the Universe before cluster formation, or we may look only at extremely rich clusters of galaxies (since these have a much shorter collapse time). To us seem fundamental not only the fact that the observations of distant clusters of galaxies give information on the evolution of galaxies but also the awareness that searches and statistics on distant clusters may give constraints on the geometry of the Universe in a simple and straightforward way. This observational work must be allowed and must be done since it is within the state of the art of modern observations.

The geometry of space, indeed, remains one of the fundamental tasks of observational cosmology. The classical tests: magnitude-redshift and angular diameter-redshift, need to be investigated up to $z = 0.9/1.0$ and the evolution effects must be understood before any conclusion can be drawn.

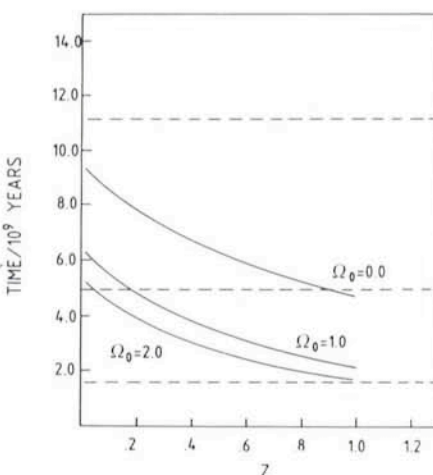


Figure 2: Same as Figure 1 for $H_0 = 100 \text{ km sec}^{-1} \text{ Mpc}^{-1}$. For $\Omega_0 = 0.0$ a cluster like Coma would form at about $z = 0.9$.

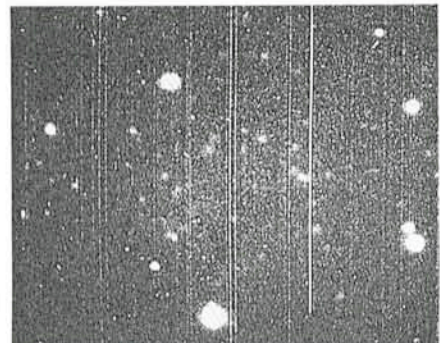


Figure 3: CCD image (3.6 m telescope + EFOSC) of a cluster at $z = 0.69$.

The standard candle for these tests is generally taken to be the first ranked cluster galaxy. This is, however, the one galaxy that is most affected by statistical fluctuations and luminosity and/or dynamical evolution. Often it is a radio source and it is unclear yet to what extent we are dealing with a well defined and low intrinsic dispersion standard candle. As stressed also by Tammann, the use of the 5th brightest galaxy is a better choice, and we must try to measure more, and fainter, magnitudes.

The deep knowledge we have today on stellar evolution and the present and planned instrumentation allows a realistic approach to the fundamental and fascinating field of cosmic evolution. Signs of detection can be found in the early work by Butcher and Oemler (*Ap.J.* **219**, 18, 1978) and by Dressler and Gunn (*Ap.J.* **270**, 7, 1983). Such signs are however inconclusive and only mark the beginning of a set of new observations which can now be done in a systematic way.

To detect evolution means to evaluate the differences between the same object at two different epochs. The astronomical equivalent is to observe what we believe to be the realization of the same object (or even better the realiza-

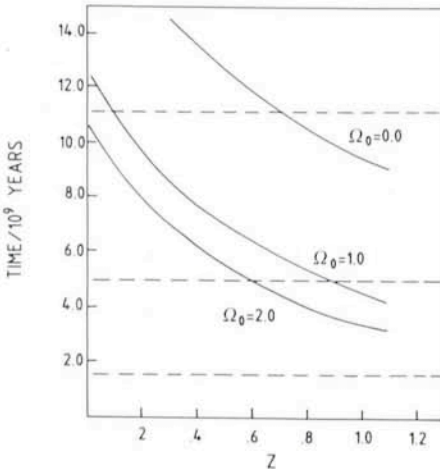


Figure 1: Cosmic time as a function of redshift for $H_0 = 50 \text{ km sec}^{-1} \text{ Mpc}^{-1}$ and values of Ω_0 as marked (continuous line). The dashed lines mark the cluster collapse time for a cluster which is 5 times less dense than Coma ($t_c = 11.2 \cdot 10^9$ years, top line), as dense as Coma ($t_c = 5 \cdot 10^9$ years, central line) and 10 times denser than Coma ($t_c = 1.6 \cdot 10^9$ years, bottom dashed lines).

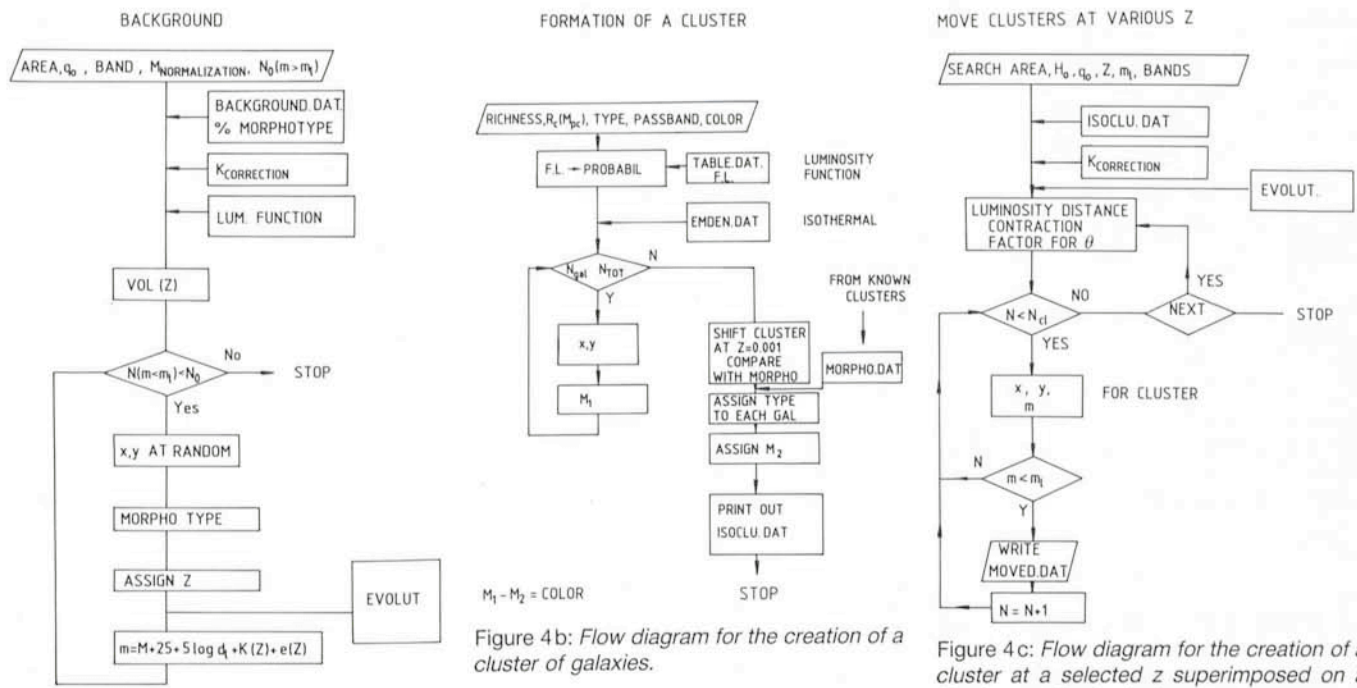


Figure 4a: Flow diagram for the creation of non-cluster galaxies ("background").

tion of the same class of objects) at two different epochs. Such an approach, therefore, requires a good morphological knowledge, in the context we are dealing with, of nearby and distant clusters of galaxies. The first step is the availability of fair samples; that is catalogues.

Catalogues of Clusters of Galaxies and the Detection of Distant Clusters

The northern sky has been searched systematically for clusters of galaxies by George Abell and the result is his perused catalogue (*Ap. J. Suppl. Series 3*, 211, 1956). The catalogue is very incom-

plete for clusters at $z > 0.3$ but forms, however, a fundamental listing for detailed and statistical studies of the nearby present epoch universe. George Abell was not able to complete the survey of the southern sky he initiated in collaboration with Harold Corwin (Abell, G., and Corwin, H., 1983, in *Early Evolution of the Universe and its Present Structure*, p. 179, edited by G. Abell and G. Chincarini, Reidel). The catalogue of the southern Sky is now being completed (Abell, Corwin and Olowin, in preparation). This catalogue will be similar in various aspects to its northern counterpart and therefore practically useless for studies of very distant clusters, $z > 0.4$. The need for deeper surveys – as we have said we must study the $\log N_c - cz$ relation and the effects of evolu-

tion – motivated the search conducted by Gunn, Hoessel and Oke (*Ap. J.* 306, 30, 1986), who observed a limited region of the northern sky detecting 418 galaxy clusters in the redshift range $0.15 \leq z \leq 0.92$. We observed one of these clusters, at $z = 0.69$, with the EFOSC attached to the Cassegrain focus of the 3.6-m ESO telescope at La Silla. The analysis of the data has just begun; a preliminary and not yet fully corrected CCD image is reproduced in Figure 3. We do not know yet which kind of a cluster we are dealing with, indeed before we know it we must have a sizeable sample so that we can study the characteristics of clusters at high redshifts. A first hint, however, of the kind of objects we can observe at high z is given (a) by the considerations related to cluster formation (see Figures 1a, 1b) and (b) by the probability of detecting a cluster at a given z .

The eye, or any devised algorithm, recognizes a cluster of objects as a den-

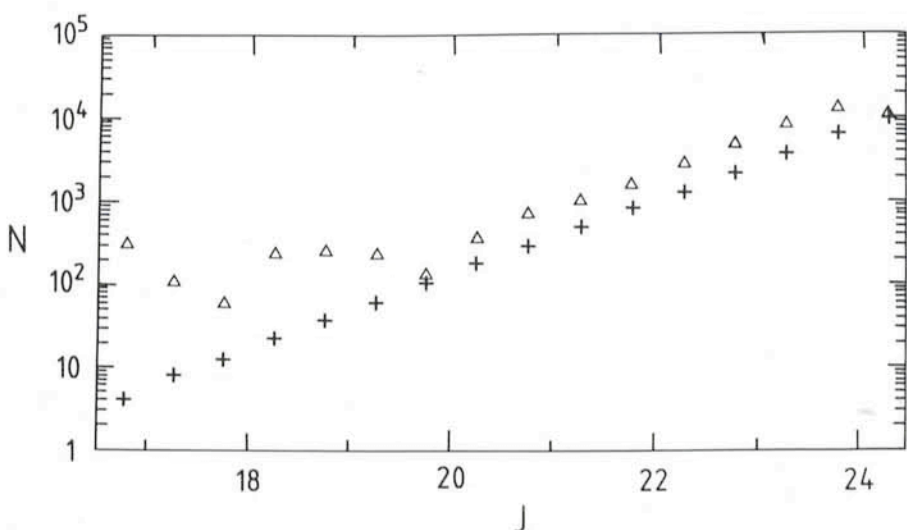


Figure 5: Counts of galaxies by Jarvis and Tyson (crosses) and by Koo (triangles).

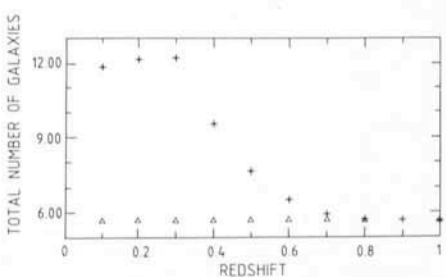


Figure 6: "Background" galaxies (triangles) and total number of cluster galaxies (crosses) expected in a $10' \times 10'$ field. The magnitude limit is $J = 25$ and the cluster is of richness class $R = 2$ (R2) and population type E dominant (T1).

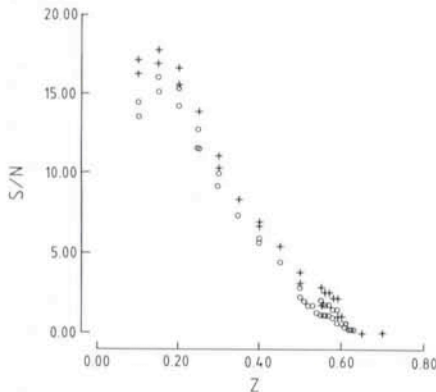


Figure 7: Signal to noise ratio (searching area with diameter 0.250 Mpc) as a function of redshift (z) for an R2, T1 cluster (without evolution) for 2 simulations.

sity enhancement over a background of objects. The probability of detection is therefore a strong function of the signal to noise ratio, s/n . The problem has been studied by simulating the universe using our present knowledge. The ingredients are illustrated in Figure 4a for the creation of the background, in Figure 4b for the creation of a cluster and in Figure 4c for what should simulate an area of the sky observed (1) in a selected passband (for now we have used J and F colours), (2) to a given limiting magnitude (we have used m_f^J (J, K) = 23 and 25, and (3) without taking into consideration the detector noise (which will be the next ingredient). Naturally we are faced with various uncertainties and approximations, some of which are:

1. At very faint magnitudes the galaxy counts are uncertain by about a factor 2 (Koo, Ph.D. thesis, Univ. of California, 1981; Jarvis and Tyson, *A.J.* **86**, 476, 1981), Figure 5.
2. At large redshifts the K correction plays a dominant role and may indeed completely bias the observed population in the clusters and in the background. We urgently need, in

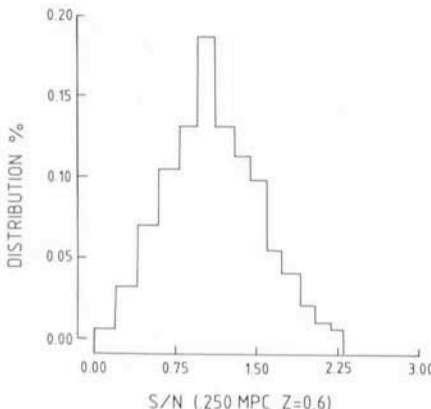


Figure 8: Distribution of the s/n ratio derived for a cluster R2, T2 (spiral-poor). The histogram is based on 800 simulations.

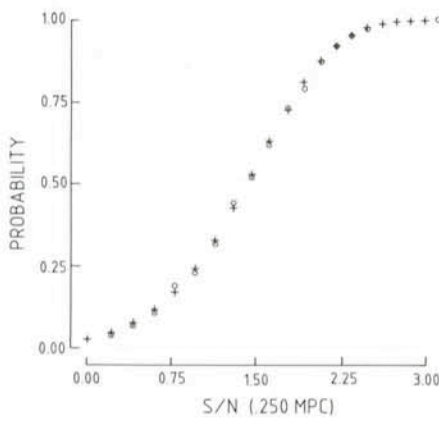


Figure 9: Probability of detection as a function of s/n . Open circles as derived numerically using 3000 simulations, crosses as computed analytically.

deed, to know the far ultraviolet energy distribution of a statistically valid sample of spiral and elliptical galaxies.

3. For the non-cluster galaxies we placed the galaxies at random. We believe this is a reasonable approximation for the galaxy distribution

over a small area of the sky. Non-cluster galaxies were added, with the constraint given by the observed counts, up to $z = 2.0$.

4. The cluster galaxies were assumed to satisfy an isothermal distribution. The population (galaxy type) was assigned according to a mean derived from observations of nearby clusters.

It is clear that at large z we may face a different distribution (clusters may be forming) and population (galaxy may show signs of cosmic evolution). But this is, indeed, the scope of the simulations. The difference between what we expect and what we observed should be due (assuming we have full control of the observational effects) to the phenomena we want to understand: (1) geometry, (2) formation epoch and (3) cosmic evolution.

On a $10' \times 10'$ area the number of background and cluster galaxies ($R2 \rightarrow$ richness class 2, $T1 \rightarrow$ rich in elliptical/lenticular galaxies, $J25 \rightarrow m_f^J = 25.0$) as a function of redshift is illustrated in Figure 6. The definition of a search area (0.250 Mpc diameter for instance) allows then a measure of the ratio s/n as a function of the redshift z , Figure 7. Note that due to various realizations of

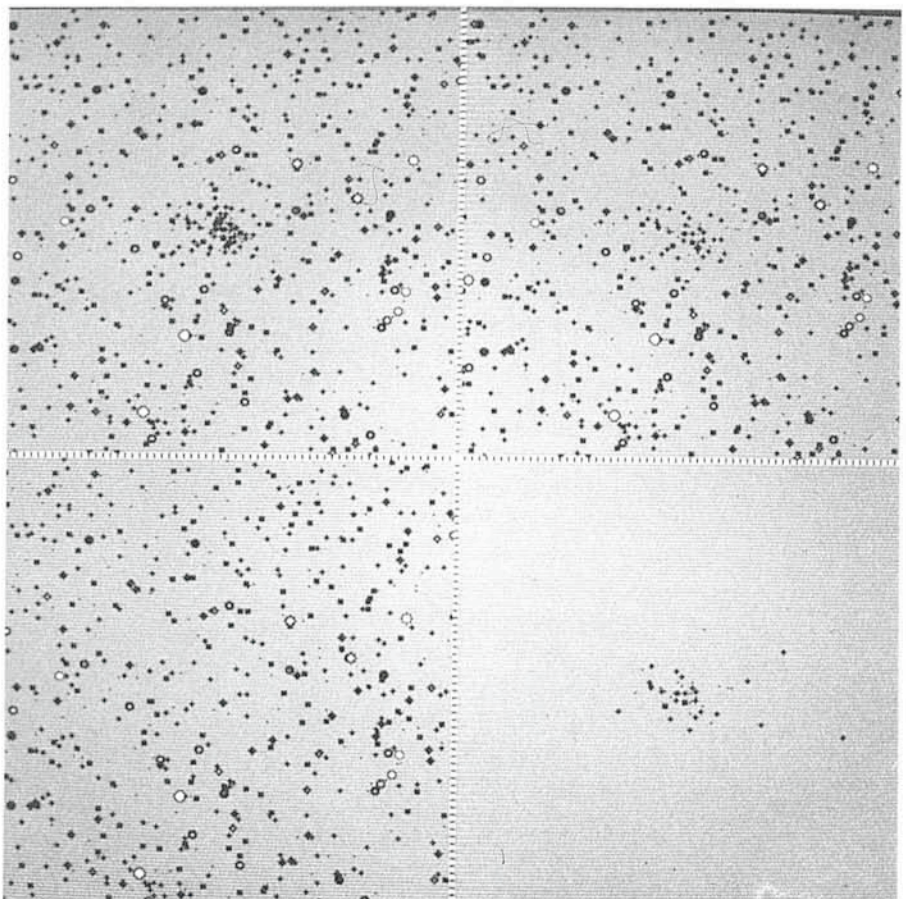


Figure 10: Background simulation at $J = 25$ (bottom left), cluster simulation (bottom right) at $z = 0.7$, cluster + background without evolution (top right) and cluster + background with evolution according to model C of Bruzual (top left). Cluster of richness class R2.

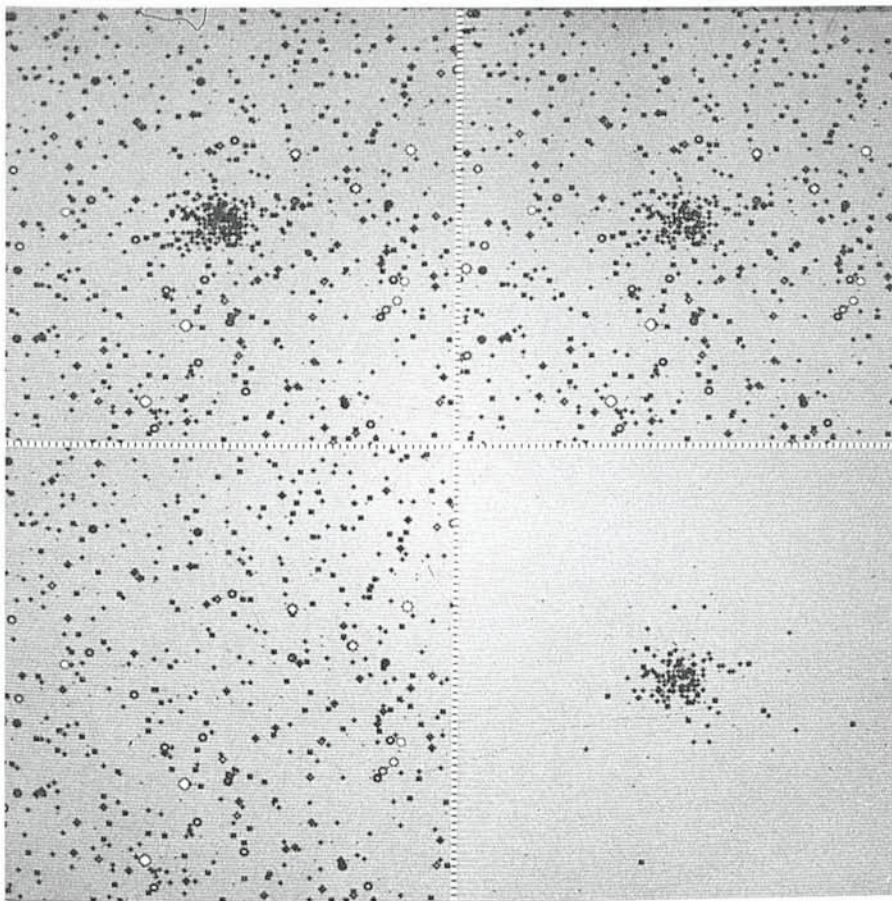


Figure 11: Same as for Figure 10 for a cluster of richness class R4.

the same model we have a dispersion of s/n at a given z , an effect which is illustrated in Figure 8 for a cluster at $z = 0.6$ (the histogram has been derived from the analysis of 800 simulations). Such dispersion must be accounted for when we determine the probability of detecting a cluster at a certain z , and indeed it may reflect the statistics playing in the real universe in the process of cluster formation. A first important result is that, without taking into account any form of evolution, a cluster (in this case of richness class $R = 2$) is already lost in the background at $z = 0.6$.

The probability of cluster detection has been computed as a function of the signal to noise s/n (and therefore as a function of z) both analytically and using 3,000 simulations for clusters of various richness and population. The result is illustrated in Figure 9 where the agreement between theory and numerical experiments is excellent. As we have said earlier, however, such probability of detection is a curve of mean values which should be convolved, at each s/n , with the dispersion histogram of Figure 8.

The result of what we have described so far (note that the addition of the de-

tector noise will make detection even more difficult) is that even unevolved clusters of richness class 4 are hardly detectable for $z \geq 0.6/0.7$ (there is some difference between elliptical dominated clusters [T1] and spiral rich clusters [T3]). Since clusters have been detected at $z > 0.8$, then either we are detecting only extremely rich clusters or evolution plays an important role in making a cluster more visible at large z . We may be dealing with a combination of the two effects. (Note that some detection could be due to a projection effect, that is an enhancement of density when two clusters are seen along the same line of sight).

An idea of how the evolution may increase the probability of detection is depicted in Figures 10 and 11. In each figure is reproduced the simulated background (bottom left), the simulated cluster (bottom right), the cluster superimposed on the background (top right) and the evolved cluster superimposed on the background (top left). In each case the evolution has been illustrated by using model C of Bruzual (*Ap. J.* **273**, 105, 1983); that is a burst of star formation lasting about 10^9 years. The limiting magnitude of the simulated sample is $J = 25$ and the area $10' \times 10'$. Each galaxy point is coded, even if not marked in the figure to avoid confusion, in magnitude, colour, galaxy type, position and redshift. Figure 10 refers to a spiral-poor cluster (T2) of richness class 2 (R2) at a redshift $z = 0.7$ while Figure 11 refers to a spiral-poor cluster of richness class 4 (R4) at a redshift $z = 0.7$.

The evolution of galaxies enhances the cluster visibility!

The new evolutionary models which are being completed by Buzzoni (Brera Astronomical Observatory, Milano) and the observations and analysis of a fair sample of clusters of galaxies will certainly allow important cosmological conclusions to be drawn.

The Giant Luminous Arc in the Centre of the A 370 Cluster of Galaxies

G. SOUCAIL, *Observatoire de Toulouse, France*

Recently, people have been very excited by the announcement of the discovery of two giant luminous arcs in the centre of distant clusters of galaxies, namely A 370 and Cl 2242-02 (1). These structures lie in the proximity of giant E

galaxies and extend over about 100 kpc. Their origin is still unknown and controversial, and their nature can be understood in terms of strong star formation in the cluster core (by galaxy/galaxy interactions or by cooling flows

from the dense Intra-Cluster Medium) or eventually a gravitational lensing configuration.

Indeed, the arc in A 370 was first discovered by a team from the Toulouse Observatory (B. Fort, G. Mathez, Y.

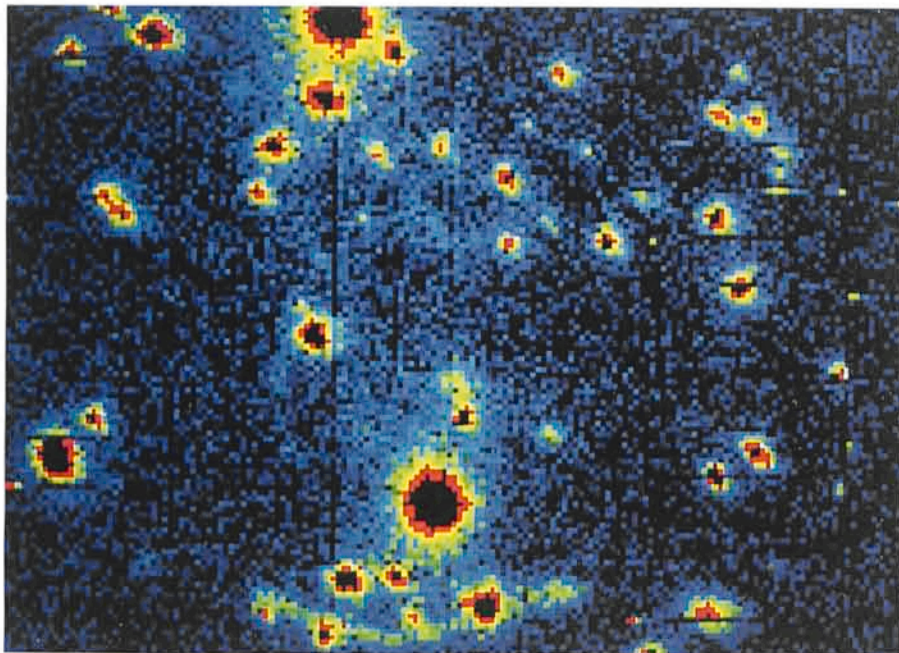


Figure 1: Image of the core of the cluster of galaxies A 370 ($z = 0.374$), dominated by two giant galaxies (# 20 and # 35). The arc is located southward galaxy # 35 and has a linear size of ~ 8 kpc wide and 160 kpc long. In the lensing hypothesis it is an image of a galaxy at redshift $z = 0.59$. Note the galaxies superimposed on the arc, especially the brightest one (# 37) whose influence has been taken into account in the lensing model.

Mellier and G. Soucail), during an observing run in September 1985 at CFHT. With multi-colour photometry, we have shown that the structure is very thin and blue (2), without being able to determine its physical origin. It was then reobserved in November 1986 at CFHT and at ESO with EFOSC, where the spectrum of the Eastern end of the arc was obtained. After the data reduction, we found that the light probably comes from a galaxy at a redshift of 0.59. So our best interpretation of the phenomenon is that we are observing an exceptional configuration of gravitational lensing, with the whole cluster as the deflector and a galaxy at $z = 0.59$ as the source, both objects nearly perfectly aligned on the same line of sight.

In collaboration with F. Hammer from Meudon, we have modelled this configuration using a simple multi-point mass model, and compared the predictions with the observed geometry of the arc. If the system source/deflector is perfectly aligned, the theory predicts the formation of a circular ring as it has been described by Zwicky in 1937 (3). But if the source lies at 1" from the cluster-centre, one can predict the formation of two symmetric arcs. Only one is observed in A 370, but the second one should be located near a very bright galaxy, # 20 (cD type, see Figure 1), and the model must take into account the influence of that massive galaxy as a secondary deflector. If its mass is high enough it is possible to predict the quasi-total fading of the second arc,

leading to the geometry observed in A 370. Moreover, we have studied the influence of the brightest galaxy superimposed on the arc, and it is then possible to explain the enlargement of the arc eastwards this galaxy, where the spectrum was obtained (see Figure 2).

All the details of this model have been presented in a paper submitted to *Nature* in April (4), with a discussion of several other possible mechanisms able to create such a structure. In order to confirm or disprove the lensing hypothesis, we need to obtain the spectrum of the entire structure and to test whether the redshift of the light is $z = 0.59$ or not. We are waiting for this summer when the cluster will be observable again ...

In the case of the other arc discovered in Cl 2242-02, actually both the redshifts of the cluster and of the arc are unknown so that it is not possible to model a lensing configuration. However, this cluster will be observable this summer too, and we can hope that these data will soon be available.

It should be noted that such a discov-

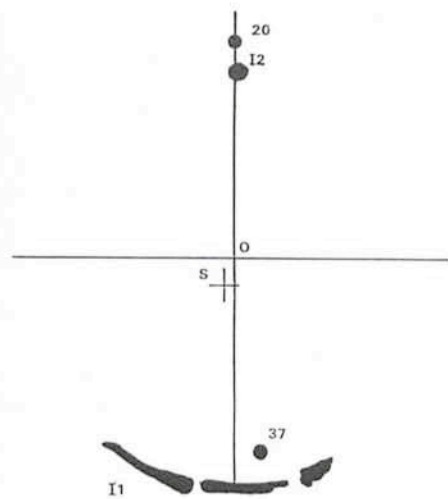


Figure 2: Schematic diagram of the lensing configuration in a three point mass model: $2.25 \cdot 10^{14} M_{\odot}$ for the cluster core (point 0) $3 \cdot 10^{12} M_{\odot}$ for galaxy # 20 and $0.7 \cdot 10^{12} M_{\odot}$ for galaxy # 37. I1 and I2 are the two images of a circular source which would appear in S without lensing. Note the large break to the right of I1. The details of such a configuration will be given in a paper submitted to *Nature*.

ery is very important because if the lensing model is confirmed, it leads to the determination of masses in a very original way. For example, in the case of A 370, we are able to "measure" the mass crossed by the light along the line of sight, containing mainly the mass of the cluster core, with a good accuracy:

$$M \sim 1 \text{ or } 2 \cdot 10^{14} M_{\odot}$$

Moreover, the model can lead to the determination of the Mass-to-Light ratio in the cluster core ($M/L_R \sim 200$ in A 370) and inside the individual galaxies ($M/L_R \sim 20$). The existence of the dark matter can be confirmed without any physical assumptions such as the virial theorem, and it is possible to study the repartition of the dark matter in the universe.

References

- (1) Paczynski, B.: 1987, *Nature* **325**, 572.
- (2) Soucail, G., Fort, B., Mellier, Y., Picat, J.P.: 1987, *Astron. Astrophys.* **172**, L 14.
- (3) Zwicky, F.: 1937, *Phys. Rev.* **51**, 290.
- (4) Soucail, G., Mellier, Y., Fort, B., Hammer, F., Mathez, G.: 1987, submitted to *Nature*.

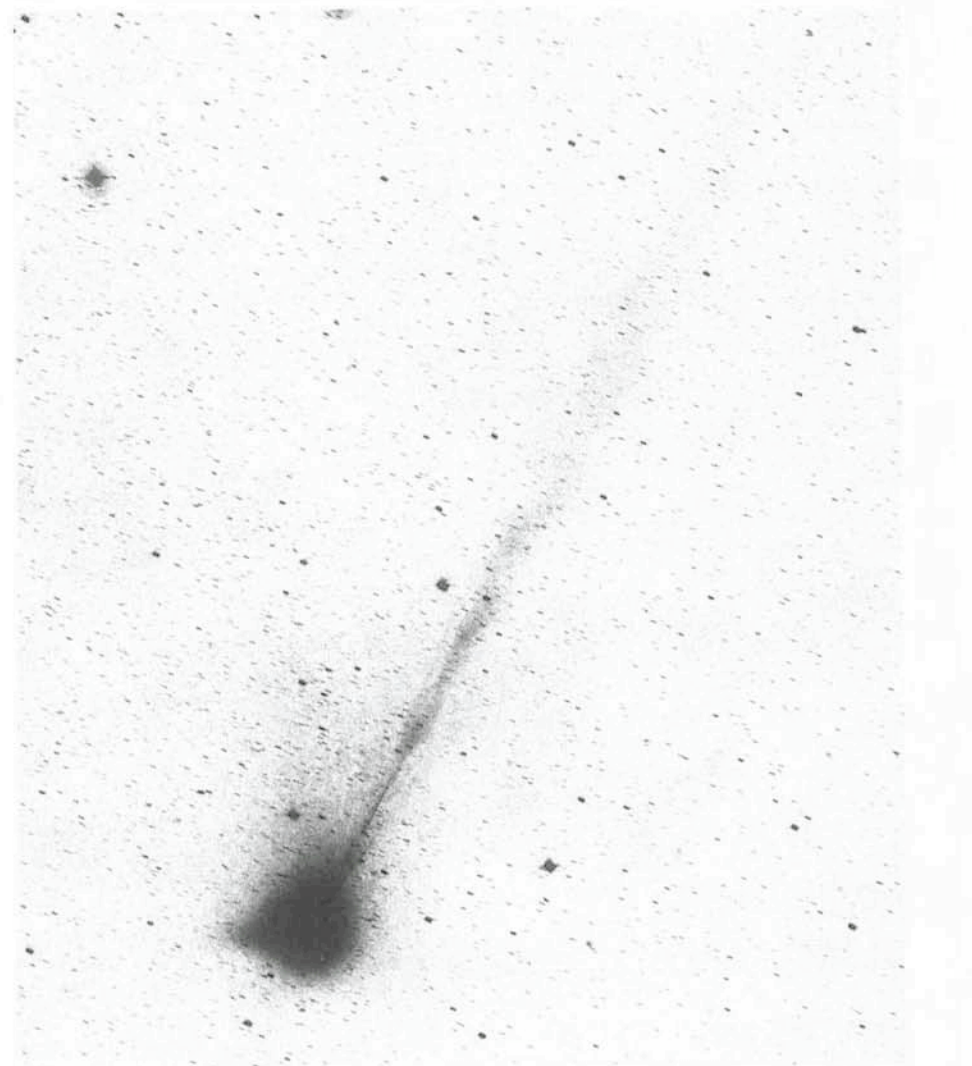
Latest News about SN 1987A

After a relatively rapid decline in brightness during the first half of June, the rate levelled off at about 0.01 mag/day in V after June 24. Radio emission at 22 GHz was detected on June 20–22 with the 13.7-m millimetre-wave antenna at Itapetinga, Brazil. The signal strength was 500 ± 70 mJy. From IUE observations it is seen that emission lines are developing in the ultraviolet spectral region. This would indicate that it is now possible to look inside the expanding shell. Infrared speckle observations at ESO appear to show a light echo; the size seems to be smaller than expected (June 29, 1987).

Comet Wilson Photographed from La Silla

This contrast-enhanced photo of Comet Wilson was obtained with the ESO 1-m Schmidt telescope on March 28, 1987 (30-minute exposure on IIa-O emulsion with a GG 385 filter; observers: H.-E. Schuster and G. Pizarro). This was three weeks before perihelion and the development of a long, straight ion tail can be seen. It measures about 3 degrees, corresponding to approximately 11 million km (projected) and points towards southwest. Note also the streamers near the coma. A short, stubby dust tail is seen towards north (to the left in this picture).

On this day, the distance to the Earth was 210 million kilometres. The comet was situated in the constellation Sagittarius and moving rapidly south while approaching the Earth. The magnitude was estimated at about 6.5. In early May, when the comet came within 90 million kilometres from the Earth, the magnitude was about 5. At that time, observations were made with several telescopes on La Silla; it is expected that some of the results will be reported in the next issue of the *Messenger*. Thereafter, it became fainter as it rapidly receded, and by early June 1987 the magnitude had dropped to about 7.



The Strange Supernova 1987 A Passes Maximum

The bright Supernova 1987 A in the Large Magellanic Cloud, about which initial reports were included in the *Messenger* No. 47, appears to be different from all others observed so far.

That is the unanimous conclusion of astronomers who have observed this rare object with ESO telescopes since the explosion in late February. After much hard work to meet a late March deadline, the collective, preliminary results from the ESO La Silla observatory of no less than 38 astronomers appeared in six "Letters to the Editor" in the May (I) 1987 issue of the European journal *Astronomy & Astrophysics*. They covered astrometry, optical and infrared photometry, polarimetry, optical and infrared spectroscopy and high-resolution spectroscopy. These articles have been bound together in a special Reprint which can be obtained by request to the ESO Information and Photographic Service (address on last page).

Due to its southern position, SN 1987 A cannot be observed from the northern hemisphere. A rather weak radio emission was detected in Australia during the first days after the explosion, but otherwise all astronomical observations until now have been made in UV, visual and IR light. Despite repeated efforts by satellite- and balloon-based instruments, no X-ray or gamma-ray radiation has been detected. Therefore the interpretation of this exceptional event rests heavily on measurements at a few optical southern observatories, among them the European Southern Observatory.

Light Maximum by Mid-May

More than three months of observations have now been made of SN 1987 A. Measurements of its brightness showed an initial increase to a maximum near visual magnitude 4.5 on

February 28. During the next few days, the brightness dropped slightly, but after March 5, it increased again, reaching visual magnitude 4.0 in late March. The ultraviolet light was nearly constant after March 10, while the intensity increased in all other spectral regions. In the infrared, the rate of brightening was about 5 % per day in late March. The visual brightness also continued to rise and by May 10 it attained magnitude 2.8, that is about half the intensity of the Polar Star. A plateau was then reached which lasted until about May 20, whereafter the supernova began to fade slowly. By early June, it is still too early to make predictions about the future rate of decline.

The time from the initial rise to the maximum, almost 3 months, is unexpectedly long and has never been observed for any other supernova. At the distance of the Large Magellanic Cloud, and taking into account the measured

foreground absorption of about 0.6 magnitudes, the maximal absolute magnitude of the supernova was about -16. This is somewhat fainter than a normal Type II supernova. From the light curve alone, SN 1987 A would therefore appear to belong to a hitherto unknown class.

A B Supergiant Exploded

Accurate astrometry at ESO in late February which was confirmed by measurements in other places, indicated that SN 1987 A's position in the sky was less than 0.1 arcsecond from where a 12th-magnitude star, Sanduleak -69 202, was seen before the explosion. It was found that this star had two nearby companions, at distances of about 3.0 and 1.4 arcseconds, respectively. None of these could therefore have been the progenitor of the supernova. A new reduction of the IUE (International Ultraviolet Explorer) satellite data in early April indicated that these two companions were still there, but also that the central star of Sanduleak -69 202 had disappeared. Thus there is now general agreement that it must have been this star that exploded.

However, its spectral type was measured at ESO in the mid-1970s as B3 Ia, that is a hot supergiant, and according to current evolutionary theories it should not yet have reached the critical phase. Most theories predict that the supernova precursor should have been a more evolved, cool supergiant of spectral type M. For some time it was thought that an M supergiant might also have been present in the Sanduleak system, but photometry of old plates in different spectral regions soon ruled this possibility out. Theoretical astrophysicists are therefore now confronted with the problems of why and how the hot B star blew up at this stage of its evolution.

Neutron Star or Black Hole?

Continued monitoring by fast photometry at La Silla has not yet shown the existence of a pulsar in SN 1987 A, that is a rapidly spinning neutron star, supposed to be created in a supernova explosion of Type II. If there is such an object at the centre of SN 1987 A, its light must still be obscured by the surrounding, rapidly expanding envelope of material. However, some astronomers think that the neutron star which was created at the supernova explosion may have been transformed into a black hole within a few hours.

This might explain why two bursts of neutrinos were observed by particle detectors, early in the morning of February

23, 1987. The first event was detected at 02 : 52 UT in the Mount Blanc tunnel between France and Italy and a second event was seen at 07 : 35, simultaneously in Japan and in the USA and possibly also by an experiment in the USSR. Could it be that the first neutrino shower was emitted at the time of the initial collapse of the core, when a heavy neutron star was formed, which was too heavy to be stable, and that it collapsed into a black hole, some 4 1/2 hours later? To solve this question, observations of the left-over central object and its surroundings are needed. In any case, the spread in arrival times of the observed neutrinos have already led to refined estimates of the neutrino mass. This measurement in turn has direct compact on cosmology, because of the (predicted) enormous numbers of neutrinos in the Universe.

In this connection, the very early sightings of SN 1987 A have become extremely important, in order to establish the accurate lightcurve (and thereby the temperature and expansion rate) during the first 24 hours. More photographs by Australian amateurs have recently been found and are being studied. The non-sighting of the supernova in the morning of February 23 by Mr. A. Jones, an experienced amateur astronomer in New Zealand, has taken on new significance and the corresponding upper limit to the brightness may be crucial for the correct interpretation of the neutrino events. It is interesting to note how amateur observations with simple and inexpensive means contribute to the highly sophisticated and expensive particle physics experiments!

The Envelope Expands

Infrared observations showed that the temperature of the expanding envelope was 5,800 K on March 1; on this day, the diameter was 5,600 times the diameter of the Sun, that is almost equal to the size of the orbit of planet Neptune. Ten days later, the temperature had dropped to 5,200 K and the diameter of the envelope had grown to 9,100 times that of the Sun. The expansion velocity fell from initially 18,000 km/sec to about 10,000 km/sec in late March and to 5,000 km/sec by mid-May.

In late March there were signs of some extra light in the far infrared (12 μm), possibly because the strong light from the supernova was being re-radiated by surrounding interstellar dust ("infrared echo"). However, infrared speckle interferometry with the ESO 3.6-m telescope on May 8 and 9 did not show any extended emission (≥ 0.3 arc-

sec), but the weather conditions were not optimal for this kind of work. However, speckle observations in visible light with the AAT and Cerro Tololo 4-m telescopes in late April and early May indicated the presence of an (emission line?) object, only ~ 0.06 arcsec almost due south of the supernova, and ~ 3 magnitudes fainter. The nature of this object is still unknown and a detailed investigation must await the time when the supernova has become significantly fainter.

In the beginning, the spectrum of the supernova changed rapidly, in fact much faster than any other supernova observed so far. Only 20 days past maximum, the optical spectrum already resembled that of a Type II supernova, when it is 100 days after maximum light. Also for this reason, most astronomers expressed doubt whether SN 1987 A can be classified as Type II. From early May onwards, the spectra showed more and more features, suggesting that the surrounding envelope was breaking up into smaller pieces and filaments.

Intervening Clouds

No less than 24 narrow absorption line systems were detected in very-high resolution spectra of SN 1987 A, obtained with the Coudé Echelle Spectrometer at the 1.4-m CAT at La Silla. They originate when the light from the supernova passes through interstellar clouds in the LMC and in our Galaxy, and also through clouds in intergalactic space between them. The presence of Calcium, Sodium and Potassium was observed and also Lithium-7. This is the first time ever that neutral Lithium, Calcium and Potassium have been detected in interstellar space outside the Galaxy.

ESO Workshop on July 6-8, 1987

The observations at La Silla will continue as long as possible. It is of course not possible to predict how rapidly the brightness is going to decline, but nobody doubts that SN 1987 A will be followed as long as possible. In this connection, however, observations will become difficult when the brightness drops below magnitude 13, because of interfering light from the close companions, mentioned above.

Meanwhile ESO is now preparing for the first full-scale international meeting about "SN 1987 A in the LMC", which will take place at the ESO Headquarters in Garching bei München, on July 6-8, 1987. More than 100 supernova specialists from all continents intend to participate. The topics will include all aspects

of supernova research, from the precursor star to the evolution of the envelope

and interaction with the surrounding interstellar medium. The outcome of this

important meeting will be reported in the next issue of the *Messenger*. *The editor*



This colour photo is a composite of three black-and-white photos taken with the ESO 1-m Schmidt telescope on February 27, 1987, four days after the explosion of SN 1987 A. The supernova is the bright star to the right; the cross is an optical effect in the telescope, caused by the plateholder support. Most of the fainter stars in this picture belong to the Large Magellanic Cloud. The bright nebula left of the supernova is 30 Doradus, also known as the Tarantula Nebula, due to its shape.



Figure 1.

Recent NTT Pictures

Substantial progress has been made in the preassembly of the NTT telescope at INNSE at Brescia.

Figure 1 shows the status of the fork at the end of May. The azimuth axial hydrostatic bearing has been tested at full load. The tube has been preassembled and will shortly be integrated into the fork.

Figure 2 shows in the background other components of the telescope (wooden boxes containing prime mirror cover and the two toothed altitude wheels on top of the dummy simulating the mirror plus the mirror cell) ready for the preassembly. It is expected to terminate the mechanics assembly with full integration by July 1987.

M. Tarenghi (ESO)



Figure 2.

Infrared Spectroscopy of Supernova Remnants

A.F.M. MOORWOOD and I.J. DANZIGER, ESO

E. OLIVA, Arcetri Observatory

Infrared emission lines of [FeII] and molecular hydrogen (H_2) falling in the atmospheric windows between $1\text{ }\mu\text{m}$ and $5\text{ }\mu\text{m}$ offer great potential for the study of moderate to low velocity ($< 100\text{ km s}^{-1}$) shocks, particularly those propagating in relatively dense regions where optical lines may be either not excited or obscured by dust. Such regions include the surroundings of forming stars, galaxy nuclei and supernova remnants. The new infrared grating/array spectrometer IRSPEC (Moorwood et al., 1986) at the ESO 3.6-m telescope is well suited to such observations and we report here some preliminary results for SNR's obtained with this instrument.

For diagnostic purposes, Fe^+ is of particular interest because of the possibility of determining N_e , T_e and A_v , in addition to its relative abundance, from lines of a single ion. The first detection of [FeII] lines in the infrared in a SNR was reported by Seward et al. (1983) who observed the $1.644\text{ }\mu\text{m}$ and $1.600\text{ }\mu\text{m}$ transitions in the high density remnant MSH 15-52 with a low resolution filter spectrometer.

Figure 1 shows IRSPEC spectra of the [FeII] $1.644\text{ }\mu\text{m}$ and $1.256\text{ }\mu\text{m}$ lines on the Large Magellanic Cloud remnant N 49. These lines originate from the same upper level and the observed $1.256/1.644$ ratio of 1.3 in this relatively

unobscured remnant agrees with that expected from the latest ratio of transition probabilities (Nussbaumer and Storey, private communication). Because remnants in the LMC subtend smaller angular sizes than those in the Galaxy they can be mapped more easily and, for N 49 and N 63 A, we have determined the total [FeII] ($1.644\text{ }\mu\text{m}$) luminosities to be in excess of $200\text{ }L_\odot$, a result of particular relevance to separate observations and interpretation of this line in galaxy nuclei which are beyond the scope of this article.

Exploratory spectra have confirmed that the $1.644\text{ }\mu\text{m}$ and $1.256\text{ }\mu\text{m}$ lines are the brightest [FeII] lines observable from the ground between $1\text{ }\mu\text{m}$ and $5\text{ }\mu\text{m}$. IRSPEC is more sensitive at $1.644\text{ }\mu\text{m}$ and this line has been detected in all the galactic SNR's observed so far (Puppis A, Kepler and RCW 103)

as well as N 49, N 63 A and N 103 B in the LMC. The highest surface brightness is exhibited by RCW 103 in which the $1.644\text{ }\mu\text{m}$ line could be "peaked-up" and a region of $\sim 30 \times 70''$ mapped with $5''$ resolution by stepping the telescope to produce the false colour [FeII] image reproduced in Figure 2. An H band ($1.5\text{ }\mu\text{m}-1.8\text{ }\mu\text{m}$) spectrum on the peak is shown in Figure 3. In addition to the prominent $1.644\text{ }\mu\text{m}$ line this also reveals several other lines attributable to [FeII] including the $1.60\text{ }\mu\text{m}$ line which is shown at higher s/n ratio in the insert spectrum, made with a longer integration time in order to determine the density sensitive $1.60/1.64$ line ratio. From this and the $1.26/1.64$ ratio we obtain values of $N_e = 4.10^3\text{ cm}^{-3}$ and $A_v = 6$ mag. respectively which are somewhat higher but still consistent within the uncertainties with earlier estimates by

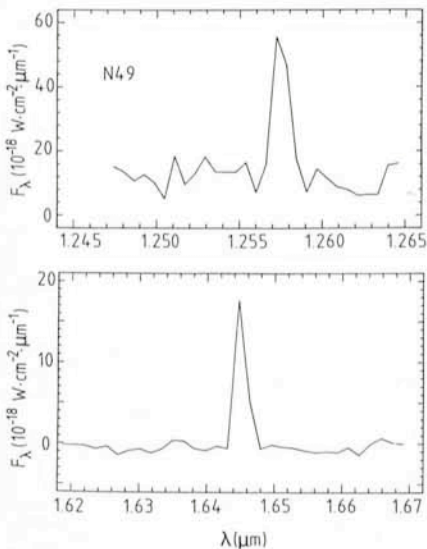


Figure 1: Lines of [FeII] at $1.256\text{ }\mu\text{m}$ and $1.644\text{ }\mu\text{m}$ in the Large Magellanic Cloud supernova remnant N 49. These lines originate from the same upper level and their ratio is thus a measure of the extinction.

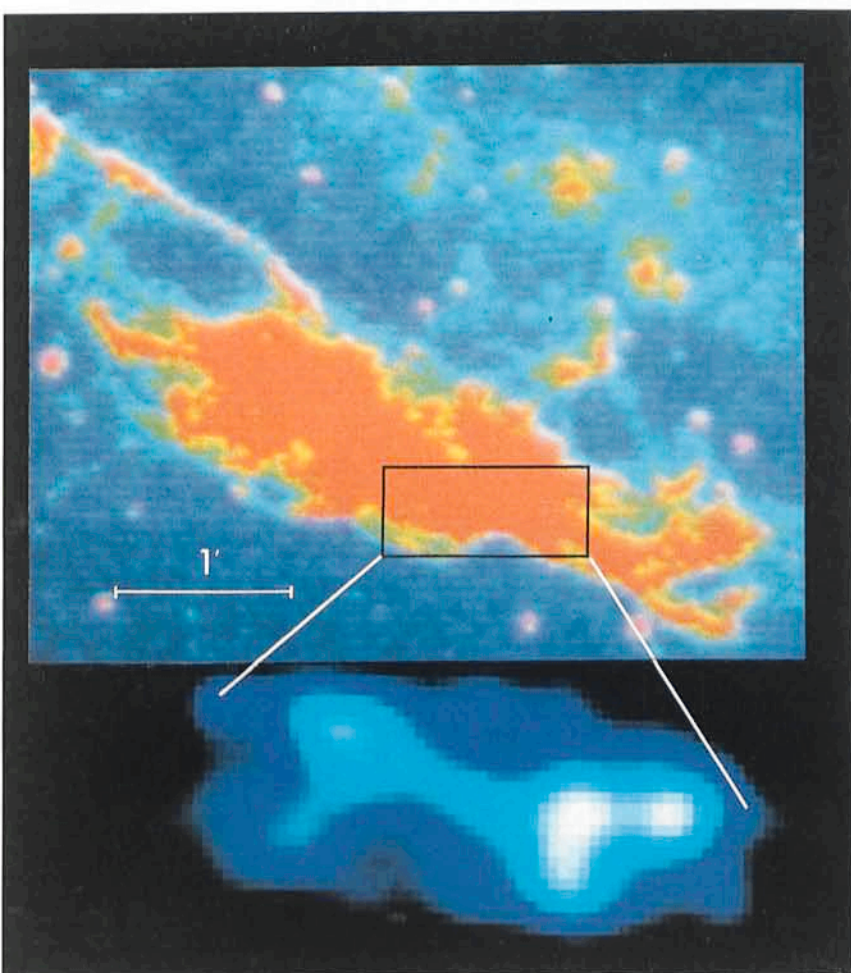


Figure 2: An [OIII] ($0.5007\text{ }\mu\text{m}$) "TAURUS" image of the most prominent optically emitting region of the galactic supernova remnant RCW 103 and, below, an [FeII] ($1.644\text{ }\mu\text{m}$) image of the portion indicated, obtained by mapping with IRSPEC.

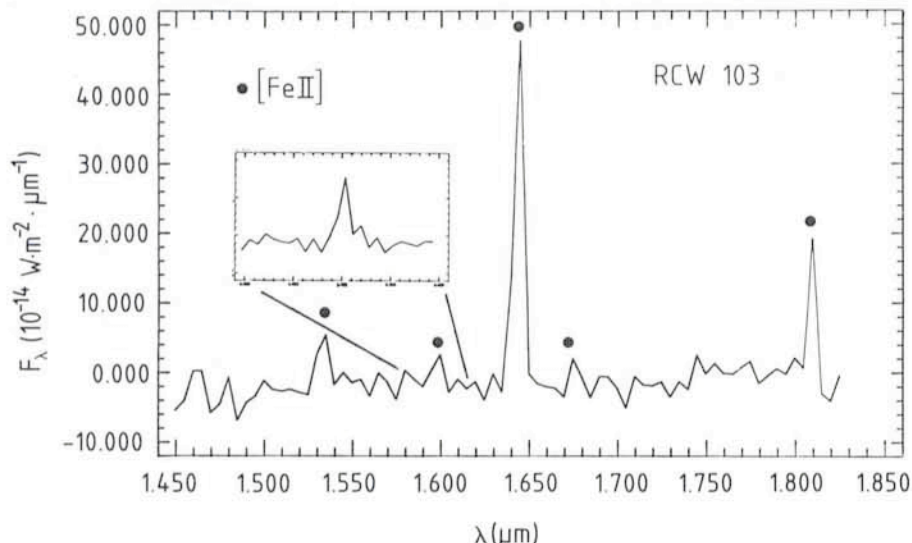


Figure 3: An H band spectrum on the position of peak [FeII] ($1.644 \mu\text{m}$) emission in RCW 103 (white in Fig. 2). Several other [FeII] lines are present including one at $1.60 \mu\text{m}$ whose intensity relative to the $1.644 \mu\text{m}$ line is density sensitive. The insert spectrum shows a better measurement of this line made with a longer integration time.

Leibowitz and Danziger (1983) based on optical [SII] lines and the Balmer decrement.

In addition to [FeII], lines of HI ($\text{Br}\gamma$ at $2.165 \mu\text{m}$) and H_2 (1–0 S(1) at $2.12 \mu\text{m}$) have also been detected in RCW 103

at 2 % and 6 % respectively of the $1.644 \mu\text{m}$ line intensity. To our knowledge, H_2 has only been detected previously in IC 443 which is known to be associated with a molecular cloud (Treffers, 1979). From the $1.644/\text{Br}\gamma$

ratio we derive $\text{Fe}^+/\text{H}^+ = 5 \cdot 10^{-5}$ assuming a Case B recombination hydrogen spectrum. Further interpretation of this quantity is model dependent due to the unknown ionization structure. Simple models however give $\text{Fe}^+ = \text{Fe}$ and $\text{H}^+ \leq 0.1\text{H}$ implying $\text{Fe}/\text{H} \leq 5 \cdot 10^{-6}$ or a depletion factor of > 0.8 for Fe and hence relatively little grain destruction. Of great interest in the future therefore is to see how this ratio varies from remnant to remnant.

We consider these first results to be encouraging both from the point of view of demonstrating the detectability of useful infrared lines and as an observational test of the available Fe^+ atomic data. Further attempts to exploit their astrophysical potential are clearly warranted as is their inclusion in future theoretical shock models.

References

- Leibowitz, E.M., and Danziger, I.J.: 1983, *Mon. Not. R. astr. Soc.*, **204**, 273.
- Moorwood, A.F.M., Biereichel, P., Finger, G., Lizon, J.-L., Meyer, M., Nees, W., and Paureau, J.: 1986, *The Messenger*, **44**, 19.
- Seward, F.D., Harnden, Jr., F.R., Murdin, P., and Clark, D.H.: 1983 *Astrophys. J.*, **267**, 698.
- Treffers, R.R.: 1979, *Astrophys. J.*, **233**, L17.

NEWS ON ESO INSTRUMENTATION

F/35 Infrared Photometer at the 2.2-m Telescope

An infrared system consisting of an infrared photometer/adaptor, detector units and an F/35 chopping secondary mirror was installed and tested on the 2.2-m telescope in March 1987 in a collaboration with Heidelberg's Max-Planck-Institut für Astronomie.

MPIA developed and built the chopping mirror and its associated functions for focus and rotation. As can be seen in Figure 1, this infrared secondary is mounted in the original Coudé ring and, therefore, a change from visible (F/8) to infrared (F/35) observing requires a change of top rings.

The infrared photometer is a duplicate of that at the 3.6-m telescope, as described in the *Messenger* No. 39 by A. Moorwood and A. van Dijsseldorp. It is equipped at present with bolometer and InSb detector units which are basically identical to those offered at the 1-m and 3.6-m telescopes.

This new instrument has been offered

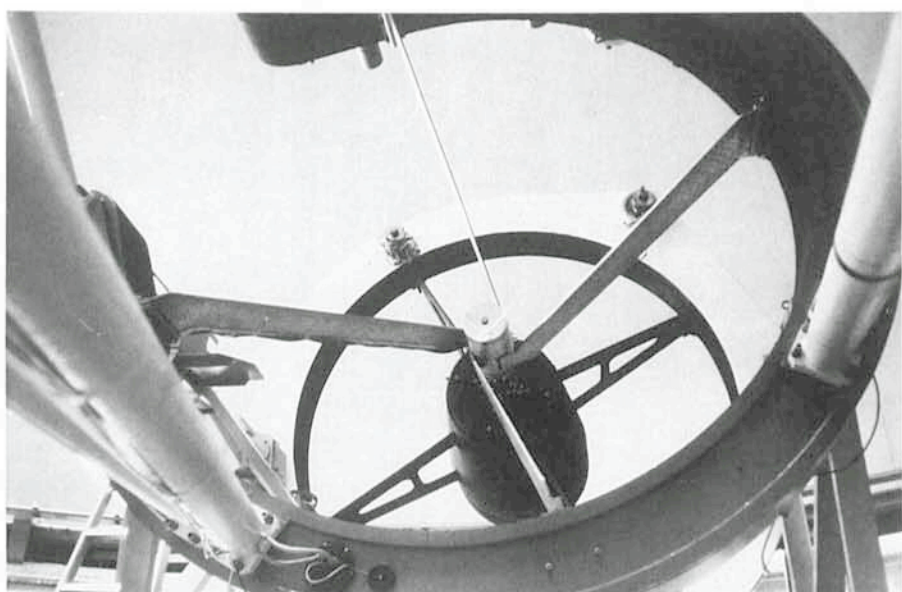


Figure 1: F/35 infrared chopping secondary mirror mounted on the 2.2-m telescope. The mirror is only 21 cm in diameter. Behind is the "normal" F/8 front ring which has just been exchanged with the coudé ring used to support the infrared secondary.

to visiting astronomers as of October this year. Preliminary limiting magnitudes (1σ in 30 minutes integration time through a 7.5 diameter diaphragm) are given in the table.

These limits are consistent with those achieved at the 3.6-m telescope, after scaling for the difference in telescope diameters, except at $\lambda \geq 10 \mu\text{m}$ where

Band	J	H	K	L	M	N	Q
Centre wavelength (μm)	1.25	1.65	2.2	3.8	4.8	10.3	18.6
Limiting magnitude	19.6	19.3	18.4	13.8	11.0	6.8	3.3

the only measurements possible at the 2.2-m were affected by thin cloud.

A. van Dijsseldonk, A. Moorwood, ESO
D. Lemke, MPIA, Heidelberg

Progress Report on DISCO: A Project for Image Stabilization at the 2.2-m Telescope

F. MAASWINKEL, S. D'ODORICO and G. HUSTER, ESO

F. BORTOLETTO, Istituto di Astronomia, Università di Padova, Italy

1. Introduction

It is well known that the resolution of earth-bound large telescopes is normally limited by the atmosphere, and not by diffraction. The astronomical image formed by a large telescope consists of a number of speckles, caused by the atmospheric refractive index variations. Every speckle is defined by a coherence zone over the pupil of size r_0 , also known as the seeing parameter. These coherence zones cause a blurring of the image and also a motion of the centre of gravity of all the speckles. In addition, image motion can have local origins (dome seeing, tracking and guiding errors). As a result, short-time exposures, where the motion is frozen, may have a higher resolution than long exposures.

Until recently, little was known experimentally about the temporal behaviour of image motion. A theoretical model, originally proposed by Kolmogorov, describes the decrease of the power spectrum of image motion with temporal frequency¹. Recently, experimental data on power spectra of image motion have been published in the context of site testing² and speckle interferometry³. In cases of good seeing, which we define somewhat arbitrarily as $r_0 \geq 15\text{cm} \Rightarrow \text{FWHM} = 0.7''$, the frequency dependence of the power spectra was indeed observed² (if the seeing is bad, the number of speckles is too large and image motion is averaged out). A typical time constant of the image motion is estimated from these data as 200 msec. Under such conditions, an imaging facility which corrects the image motion may improve the resolution of long integrations. Such a device is presently under construction at ESO for the 2.2-m tele-

scope, and it is called DISCO, acronym for Direct Image Stabilized Camera Option. A similar stabilizer has been operating at the 2.2-m telescope of the University of Hawaii for some time⁴. The main task of DISCO will be to enable the observer in case of good seeing to switch within few minutes from "normal"

exposures at the Cassegrain focus of the telescope f/8, (image scale of $0.35''/\text{pixel}$ for a RCA CCD) to stabilized exposures with $0.14''/\text{pixel}$. The possibility of a quick changeover in the observation mode is considered an advantage, since periods of good seeing might be limited to a fraction of the night and in any case

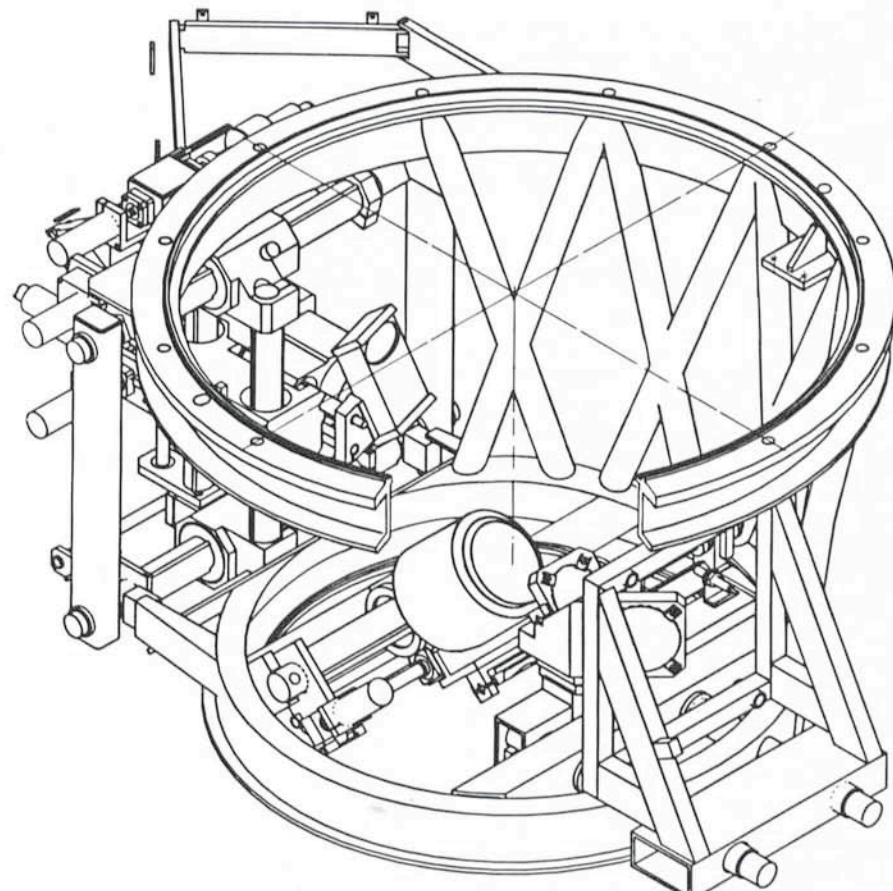


Figure 1: Three-dimensional CAD view of the new 2.2-m telescope adapter. The stabilizer mirror is visible in the centre on its linear translation stage.

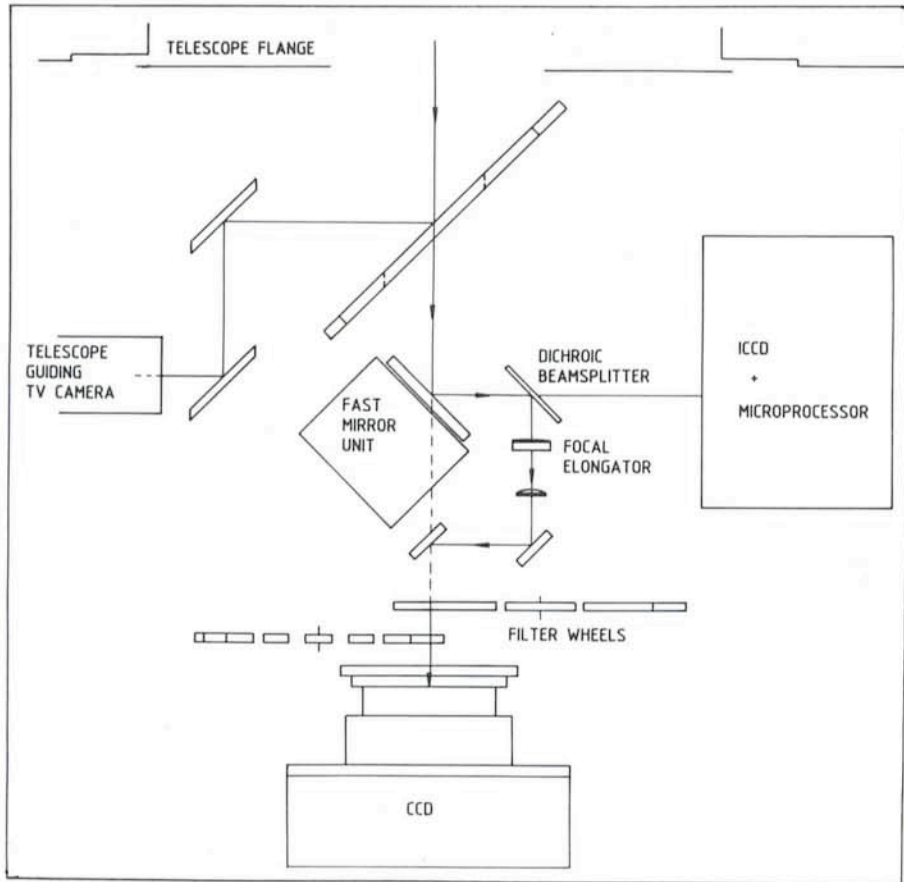


Figure 2: Optical diagram of the adapter.

the high resolution mode might be required for a part of the observing programme only. Finally, image stabilization is a first natural step towards a fully adaptive optics system and one may expect to gather valuable experience and useful data on the image quality on La Silla from DISCO observations.

2. The Design and Operating Concept of DISCO

To realize DISCO, a new lightweighted adapter for the 2.2-m telescope was designed and is now under construction (Fig. 1). The adapter will be used with the direct image CCD camera and with spectrographs. It includes an offset autoguider based on a SIT camera. The offset guider XYZ motion units are using the ESO standard DC motors; this makes it possible to position the guide probe accurately ($\leq 0.3'$) within the acquisition field which may be a help for automatical acquisition or remote control. The field for guiding is $30' \times 30'$, comparable to the present camera. The new adapter has been prepared to include in a later stage spectrographic calibration units, and Risley prisms (in the focal elongator). The optical diagram is drawn schematically in Figure 2. The conventional imaging mode is the f/8 focus. In this case the stabilizer mirror is

not in the beam path. If the seeing is good ($r_0 \geq 10-15$ cm), the observer

may expect an additional advantage in the angular resolution by switching to the stabilized mode. To this aim the fast mirror unit (see Fig. 3) is remotely inserted into the main beam (under 45°). It consists of a high-quality (surface flat $\leq \lambda/10$) mirror which can be re-positioned within 1 msec around 2 axes; its dynamic range is 8×10^{-4} rad; this covers a field of $4.5''$ on the sky. From the mirror the beam is reflected onto a dichroic beamsplitter (also under 45°). The blue beam (light ≤ 560 nm) is imaged onto an ICCD camera, and is used for the acquisition of the centre of gravity. The red part (light ≥ 580 nm) is reflected from the beamsplitter, passes through a focal elongator and forms (via 2 additional 45° mirrors) an image onto the CCD camera: this is available as stabilized image.

The signals to drive the mirror are calculated every 20 msec by a fast microprocessor. This is done as follows: at the beginning of a stabilized run the observer selects a suitable guide star on the ICCD camera by placing a subframe of 16×16 pixels around it (the camera covers a field of $1.5' \times 1'$, corresponding well with the isoplanatic patch). Then this subfield is digitized after integration every 20 msec; in the present configuration the system is limited to TV rates by the camera electronics. For astronomical applications this means a limiting magnitude for the guide star $m_B = 13$ within $1' \times 1'$ from the object. Initially

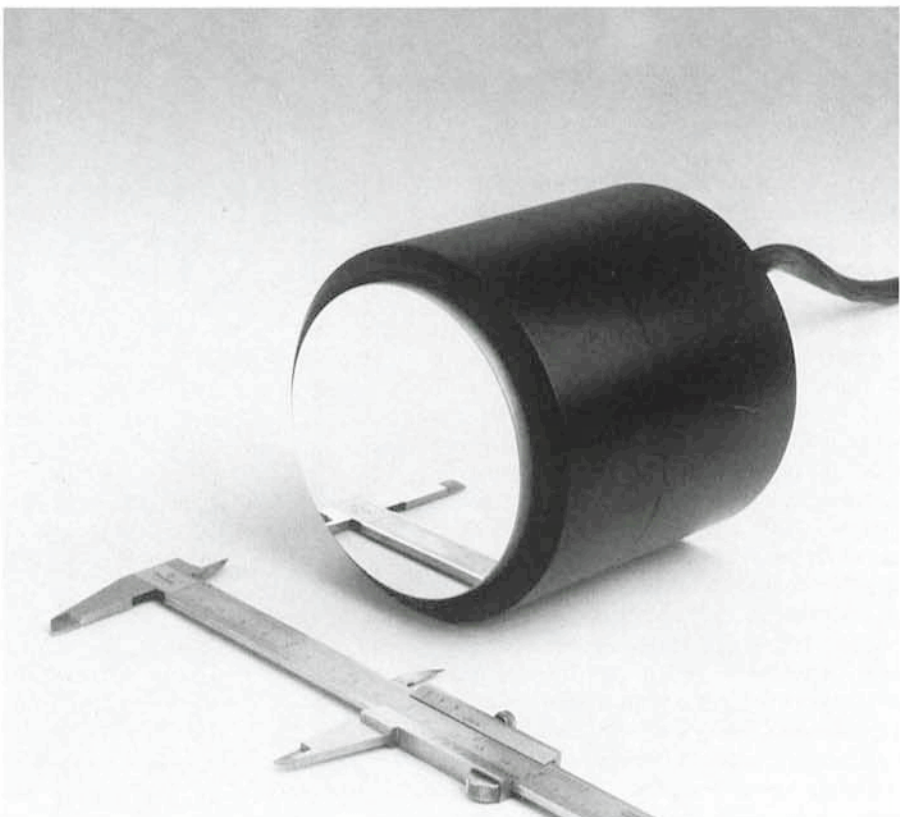


Figure 3: The stabilizer mirror unit.

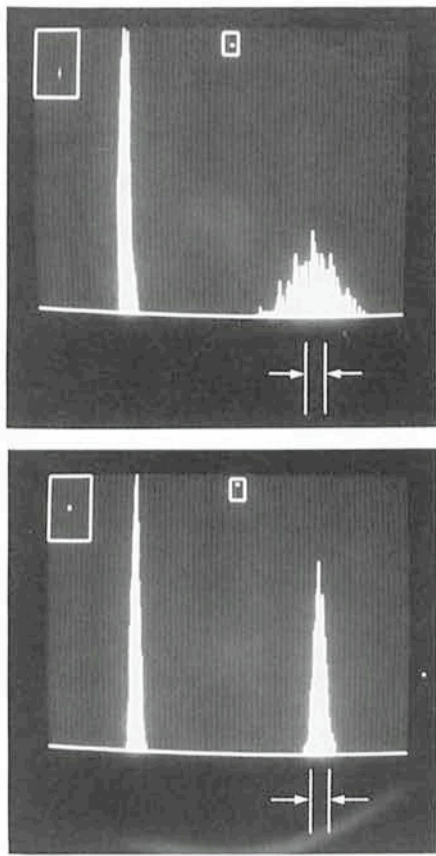


Figure 4: non-stabilized (upper) and stabilized (lower) runs with the fast loop. The arrows below the y-histograms indicate a width of 1/2 pixel.

the imaging in stabilized mode will be possible only at wavelengths ≥ 580 nm. A second dichroic reflecting the blue light will be ordered soon; then also wavelengths ≤ 580 nm can be stabilized, although one has to be aware that the seeing parameter scales as $r_0 \propto \lambda^{1/2}$, therefore the stabilization is more effective for longer wavelengths.

The digitalization and the display of image information is performed by a fast video digitizing VME card. The centre of gravity within the subframe and the new mirror coordinates are calculated with a 68010 microprocessor (also VME based). The entire operation: reading out of the subframe, digitalization, calculation of new coordinates and repositioning of the mirror takes 4 msec for a 16×16 subframe or 2 msec for an 8×8 subframe. The total cycle time is then 24 msec; two samples (i.e. 50 msec) are needed to acquire a frame (Shannon sampling theorem). Therefore the stabilization starts to be effective if the atmospheric coherence time is longer than 50 msec. It was mentioned earlier that good seeing has a typical time scale for image motion of 200 msec; therefore under such conditions DISCO is expected to improve the resolution.

3. Present Status of the Project, Results from the First Laboratory Tests

The fast moving mirror was delivered to ESO in September 1986; in dynamic tests in the optical lab it was verified that the surface remains flat during the fast motion. The microprocessor was acquired; all the software was written in assembler language to obtain maximum speed in calculations. In the mean time the structure and the mechanical functions of the adapter are being manufactured by external European firms, and these will be delivered in the summer of 1987.

In the laboratory, first tests of the DISCO fast loop have been made. Atmospheric image motion was simulated using a galvanometer scanner mirror, which was excited with electrical noise having a power spectrum similar as in 2,3. A pinhole source was imaged with this mirror and the stabilizing mirror onto a CCD camera. In this way, apparent image motion along one axis was simulated. The results of the stabilization are shown in Figure 4: it contains photographs of the video display of the VME control system. The upper photograph is the non-stabilized case: in the upper right box is the momentary ("real-time") image of the reference star in the selected subframe (in this case 16×16). The upper left box shows a zoomed display of the centres of gravity, as calculated by the microprocessor. The lower curves are histograms of the centres

of gravity in x and y direction. Comparing the upper and the lower picture, a significant improvement in the y-histogram is noticed. The microprocessor also gives the number of centres of gravity, which would be contained in a circle with a preset radius ("energy concentration"). Taking a radius of 1/4 pixel the stabilized image has 570 out of 1,023 samples in the circle, the non-stabilized has 190 out of 1,023 samples. We notice that these simulations were made with high S/N ratio, and on one axis. Under such conditions the centre of gravity can be calculated with an accuracy of 1/10 of a pixel. Further tests to simulate different observing conditions at the telescope will be carried out in the next months.

It is planned to have a first test of the instrument at the telescope towards the end of 1987. Provided that the seeing conditions will be appropriate, we hope to demonstrate that DISCO can be a valuable tool for those aiming at high-resolution imaging. The full implementation of the facility is expected to take place during 1988.

References

- (1) Roddier, F., Progress in Optics, **XIX**, ed. E. Wolf (North-Holland, Amsterdam), 281–376.
- (2) Merill, K.M., Favot, G., Forbes, F. and Morse, D., *S.P.I.E.*, **628**, 125, 1986.
- (3) Aime, C., Petrov, R.G., Martin, F., Ricort, G. and Borgnino, J., *S.P.I.E.*, **556**, 297, 1985.
- (4) Thompson, L.A. and Ryerson, H.R. *S.P.I.E.*, **445**, 560, 1984.

MIDAS Memo

ESO Image Processing Group

1. Application Developments

The Inventory package for detection and classification of objects has been significantly improved by Dr. A. Kruszewski. He will in the coming month integrate these modifications in MIDAS.

In order to provide a high-quality crowded field photometry system, the ROMAFOT, package (Buonanno, R., Buscema, G., Corsi, C.E., Ferraro, I., Iannicola, G.: 1983, *Astron. Astrophys.* **126**, 278) has been adopted by MIDAS as the standard system for this purpose. The implementation of this package is done in close collaboration with Dr. R. Buonanno and is expected to be terminated during the summer. General MIDAS tables for exchange of informa-

tion between the different packages are being designed to make combined use easy.

The Time Series Analysis package for unequally spaced data developed by the ST/ECF was fully implemented and will be released in the 87 JUL 15 release of MIDAS. It includes different methods for calculation of Power spectra and periodicity determination of data in MIDAS tables.

As a result of the collaboration with the Image Processing Group in Trieste, two new commands for interactive analysis of spectra developed by F. Pasián and G. Sedmak, are under testing. The commands, being the nucleus for future interactive developments, will be available in the 87 JUL 15 release.

2. MIDAS Hot-Line Service

As announced in the last issue of the Messenger, a MIDAS *Hot-Line* service has been started. Questions and problem reports concerning MIDAS can be sent to the Image Processing Group by Telex (52828222 eso d, attn.: MIDAS HOT-LINE) or electronic mail (SPAN: ESO MC1:: MIDAS or EARN/BITNET: MIDAS @ DGAESO 51).

A MIDAS Support telephone extension was created with the number + 49-89-32006-456 (note: the number was misprinted in the last MIDAS Memo). This extension can be used in urgent cases to obtain help with MIDAS-related problems.

3. New MIDAS Directory Structure

In anticipation of the portable MIDAS, a new directory structure will be introduced for the MIDAS system. The general structure has been based on the AIPS model but adapted to the special needs of MIDAS. It will allow a clear separation of the released version of MIDAS and of the local code which has been developed for the MIDAS environment. Special directories will be created for calibration data, tutorials and test procedures. The structure will also be used for the portable version and thus support different operating systems (e.g. VAX/VMS and UNIX). This will make it possible to maintain support of old releases of VAX/VMS.

4. Status of the Portable MIDAS

The development of the portable version of MIDAS is now well under way and still on schedule for release in the spring of 1988. The new version of the ST routines which interface application programmes to the system has been written in C and based on a set of operating system dependent OS routines. The ST and OS levels have been tested successfully on the beta-test sites. These tests included a number of different UNIX implementations on computers such as Bull SPS 9, Apollo DN 570, DN 3000, DSP 9000 (Alliant FX), Sun 3/160 and HP 9000.

The new set of TB routines for table access will be tested in May-June. It is expected that a VAX/VMS version of the OS routines will be made during the summer after which performance of the implementations can be compared. Also during the summer, a conversion of the application code from VAX-Fortran to standard Fortran-77 with five well-defined extensions will be started.

STAFF MOVEMENTS

Arrivals

Europe:

BROCATO, Enzo (I), Student
HEYER, Hans (D), Laboratory Technician (Photography)
JOHANSSON, Lennart (S), Fellow
NEUVILLE, Hélène (F), Adm. Clerk Purchasing
POSTEMA, Willem (NL), Mechanical Design Engineer

Departures

Europe:

AURIÈRE, Michel (F), Fellow
AZZOPARDI, Marc (F), Associate
BORTOLETTO, Favio (I), Fellow (Astronomical Detector)
CAVAZZINI, Egido (I), Associate
MALASSAGNE, Serge (F), Designer/Draughtsman
STAHL, Otmar (D), Fellow

New ESO Posters and New Edition of ESO Publications and Picture Catalogue Available

Eight beautiful colour posters (60 x 80 cm) have just become available. They show the most recent aerial view of the ESO observatory La Silla, a model of the ESO 16-m Very Large Telescope, the Supernova 1987 A in the Large Magellanic Cloud, Messier 104 – the Sombrero Galaxy, the barred spiral galaxy NGC 1365, Comet Halley and the Milky Way, the Large Magellanic Cloud, and the Eta Carinae Nebula.

If you want to know more about prices and how to obtain the posters or any other material – like slide sets, colour prints, postcards, video tapes, brochures, books, etc. – please apply for the new edition of the ESO Publications and Picture Catalogue. It is free of charge and will be sent to you on written request to the ESO Information and Photographic Service, Karl-Schwarzschild-Str. 2, D-8046 Garching b. München.

The Chilean Consul General Visits ESO

The Chilean Consul General in Munich, Mr. Hans Zippelius, visited the ESO Headquarters on May 12, 1987. After an introductory stroll through the building, the discussion focussed on the

various ESO projects, including the Very Large Telescope. From left to right at the VLT model: the Consul General, Dr. R. West (ESO) and the Chilean Consul in Munich, Mr. Rodolfo Berlinger.



El Cónsul General Chileno visita ESO

El Cónsul General de Chile en Munich, Sr. Hans Zippelius, visitó la sede de la ESO el día 12 de mayo de 1987. Después de una visita de introducción por el edificio, la discusión se concentró en los varios proyectos de la ESO, incluyendo el Gran Telescopio (VLT).

De izquierda a derecha con el modelo del VLT: El Cónsul General, Dr. R. West (ESO) y el Cónsul Chileno en Munich, Sr. Rodolfo Berlinger.

Tiempo para un cambio

En la reunión celebrada en diciembre del año pasado informé al Consejo de mi deseo de terminar mi contrato como Director General de la ESO una vez que fuera aprobado el proyecto del VLT, que se espera sucederá hacia fines de este año. Cuando fue renovada mi designación hace tres años, el Consejo conocía mi intención de no completar los cinco años del contrato debido a mi deseo de disponer de más tiempo para otras actividades. Ahora, una vez terminada la fase preparatoria para el VLT, y habiéndose presentado el proyecto formalmente al Consejo el día 31 de marzo, y esperando su muy probable aprobación antes del término de este año, me parece que el 1º de enero de 1988 presenta una excelente fecha para que se produzca un cambio en la administración de la ESO.*

En la próxima década el proyecto del VLT afectará todas las actividades de la ESO y tendrá un efecto reciproco en la comunidad científica de los países miembros. El VLT no tan sólo es un gran proyecto en términos financieros, sino también la mayoría del personal de la ESO tendrá que dedicarle una gran parte de su tiempo. Lo mismo vale para muchos científicos e ingenieros en los países miembros, ya que está previsto que gran parte de los instrumentos científicos sean desarrollados en laboratorios europeos.

Mientras la ESO tendrá que dedicar gran parte de sus recursos al VLT, se presentarán al mismo tiempo otras necesidades esenciales: el SEST está comenzando a funcionar, el NTT está casi terminado y necesita ser equipado completamente con instrumentación, y esperamos que el ST-ECF tenga el Telescopio Espacial por el cual preocuparse. Todo ésto abre una era de grandes oportunidades a los astrónomos europeos, pero mientras continúa la construcción del VLT, se requerirá de un gran esfuerzo para utilizar los nuevos instrumentos de una manera efectiva.

Un aspecto particularmente importante se refiere al funcionamiento de La Silla, el cual, naturalmente, sigue teniendo la mayor prioridad. Es aquí, más que en cualquier otro lugar, donde la comunidad astronómica europea encuentra los frutos de las grandes inversiones que se han hecho.

Hace algunos años decidimos averiguar si se podrían encontrar lugares para el VLT con aun mejores cualidades que las que presenta La Silla, a pesar de que La Silla ya cuenta entre los mejores lugares en el mundo. Investigaciones demostraron que Paranal presenta una frecuencia de nubes bastante menor y hay menos humedad. Se están efectuando mediciones de visibilidad y los primeros resultados, aun inconclusos, son promete-

dores. Por eso se decidió que Paranal sería presentado como la opción más probable para ubicar el VLT, a pesar de que no habrá que decidirse definitivamente antes de tres años.

Paranal es un alejado lugar en uno de los desiertos más secos del mundo. Mientras un buen camino de ripio pasa cerca, no existe ninguna población en muchos kilómetros a la redonda. Por lo tanto la completa infraestructura deberá ser construida por la ESO. Sería caro y tomaría mucho tiempo construir Paranal al estilo de La Silla, pero afortunadamente ésto no es necesario.

Actualmente se está usando control remoto en La Silla en una forma experimental. Para el VLT será el principal modo de uso. Sin duda le seguirán diagnóstico y mantenimiento a control remoto. Con estas tecnologías tendría que ser posible hacer funcionar el Paranal con un reducido número de personal calificado. Otro factor que acentúa esta conclusión es que el VLT – como también el NTT – operarán con muy pocos cambios de instrumentación.

Supongamos que el VLT fuera ubicado en el Paranal, que pasará con los otros telescopios de la ESO? Con un diámetro equivalente a 16 m, el VLT representaría un 85 % del total del área colectora de fotones de los telescopios de la ESO. Sería difícil imaginar que la ESO continuaría operando otro lugar a un alto costo por los restantes 15 %. A la larga parece existir sólo una solución: Si el VLT se ubica en el Paranal, todos los telescopios de la ESO tendrán que funcionar allá. Esto implicaría cambiar algunos telescopios de La Silla. El 2.2 m, el CAT, el 1.5 m danés y el SEST no presentarían mayores problemas; sería difícil cambiar el 3.6 m, excepto si se

usara como «telescopio de zenith» para estudios cosmológicos. Lo que realmente valdrá la pena cambiar de ahora en diez años más, deberá verse entonces.

El NTT presenta un problema particular. Dentro de un año estará listo para ser instalado en Chile. Si realmente se elige el Paranal como el lugar para el VLT, no sería entonces más razonable ubicarlo allá? Mientras las ventajas de aprender a manejar un telescopio moderno en Paranal antes de la llegada del VLT serían importantes, existen serios problemas con respecto al plazo; todo ésto se está analizando actualmente. En caso que la ubicación en el Paranal presentara atrasos imprevistos, el NTT será ubicado en La Silla.

Los astrónomos están acostumbrados a ver los telescopios como instrumentos de uso casi eterno. Quizás ésto fue razonable en un tiempo cuando se necesitaba poca mantenimiento y la instrumentación era relativamente simple. Hoy en día, sin embargo, los costos de operación e instrumentación de un telescopio moderno en un lugar alejado y el procesamiento de los datos excede en mucho el capital invertido, calculado a través de una o dos décadas. Ello implica que la adquisición de nuevos telescopios significa automáticamente el cierre de los telescopios existentes.

El VLT representa el futuro a largo plazo de la ESO. Sin él la Organización no podría sobrevivir mucho tiempo más. Sin embargo, La Silla continuará proporcionando datos esenciales para el trabajo científico de una vasta comunidad por más de una década. Por eso está claro que, incluso si el Paranal llega a desarrollarse, tendrá que hacerse todo para garantizar la continuación del funcionamiento de La Silla en su presente estado de alta calidad.

L. WOLTJER, Director General

Dos nuevas series de diapositivas de la ESO

ESO anuncia la aparición de dos nuevas series de diapositivas, que se podrán obtener a partir del 1º de julio de 1987:

– Objetos en el cielo austral

– Supernova 1987A en la Gran Nube Magallánica

Ambas series incluyen 20 diapositivas de 5 x 5 cm de alta calidad, acompañadas por un detallado texto explicativo y presentadas en un cuaderno con una linda cubierta. La primera serie contiene espectaculares vistas en color de seleccionados objetos del cielo austral, fotografiadas con los telescopios de la ESO en los últimos años. La segunda serie, que contiene algunas diapositivas en color y otras en blanco y negro, resume las más importantes observaciones de la supernova más brillante desde hace 383 años. Además de imágenes tomadas del campo de la Nube Magallánica antes y después de la explosión, incluye escogidos espectros y otros resultados de observación de La Silla.

Para obtener las series, que también son útiles para fines educacionales, envíe DM 35,- (precio de costo incluyendo gastos de franqueo) a:

ESO Information and Photographic Service
Karl-Schwarzschild-Strasse 2
D-8046 Garching bei München
Federal Republic of Germany

No olvide indicar su nombre y dirección detallada. Rogamos considerar que el envío podrá tomar algunas semanas.

* El día 4 de junio el Consejo designó unánimemente al Prof. H. van der Laan como nuevo Director General por un período de cinco años a partir del 1º de enero de 1988.

ESO, the European Southern Observatory, was created in 1962 to... establish and operate an astronomical observatory in the southern hemisphere, equipped with powerful instruments, with the aim of furthering and organizing collaboration in astronomy... It is supported by eight countries: Belgium, Denmark, France, the Federal Republic of Germany, Italy, the Netherlands, Sweden and Switzerland. It operates the La Silla observatory in the Atacama desert, 600 km north of Santiago de Chile, at 2,400 m altitude, where thirteen optical telescopes with diameters up to 3.6 m and a 15-m submillimetre radio telescope (SEST) are now in operation. A 3.5-m New Technology Telescope (NTT) is being constructed and a giant telescope (VLT=Very Large Telescope), consisting of four 8-m telescopes (equivalent aperture = 16 m) is being planned for the 1990's. Six hundred scientists make proposals each year for the use of the telescopes at La Silla. The ESO Headquarters are located in Garching, near Munich, FRG. It is the scientific-technical and administrative centre of ESO, where technical development programmes are carried out to provide the La Silla observatory with the newest instruments. There are also extensive facilities which enable the scientists to analyze their data. In Europe ESO employs about 150 international Staff members, Fellows and Associates; at La Silla about 40 and, in addition, 150 local Staff members.

The ESO MESSENGER is published four times a year: normally in March, June, September and December. ESO also publishes Conference Proceedings, Preprints, Technical Notes and other material connected to its activities. Press Releases inform the media about particular events. For further information, contact the ESO Information and Photographic Service at the following address:

**EUROPEAN
SOUTHERN OBSERVATORY**
Karl-Schwarzschild-Str. 2
D-8046 Garching bei München
Fed. Rep. of Germany
Tel. (089) 32006-0
Telex 5-28282-0 eo d
Telefax: (089) 3202362

The ESO Messenger:
Editor: Richard M. West
Technical editor: Kurt Kjær

Printed by Universitätsdruckerei
Dr. C. Wolf & Sohn
Heidemannstraße 166
8000 München 45
Fed. Rep. of Germany

ISSN 0722-6691

El Telescopio Sueco-ESO Submilimétrico

Durante los últimos dos años se han producido importantes cambios en la parte sur de la hilera de telescopios en La Silla, y donde antes se encontraba una estación meteorológica, se encuentra ahora un telescopio submilimétrico de 15 metros (ver fotografía en pág. 3). El telescopio, diseñado por ingenieros de IRAM, fue construido por cuenta del Consejo Sueco de Investigación de Ciencias Naturales (NFR) y la ESO. Será operado en conjunto por ESO y el NFR (a través del Observatorio Espacial de Onsala).

El Telescopio Sueco-ESO Submilimétrico, SEST, representa un importante avance en el dominio milimétrico-submilimétrico. Es el único telescopio de esta especie en el hemisferio austral y entre los primeros de su género en el mundo entero.

SEST extenderá la parte observational del espectro de radio hacia el infrarrojo y dará la posibilidad a los astrónomos europeos de

investigar las nubes moleculares de la Vía Láctea austral y otras galaxias cercanas, proporcionando información sobre la evolución estelar y la dinámica galáctica. Les dará la posibilidad de investigar las propiedades del continuo de radio de las estrellas, las regiones HII y el polvo interestelar en esta nueva región de longitud de onda, y proporcionará nuevos valiosos datos sobre los quásares y radio galaxias en el régimen de longitud de onda submilimétrico.

Finalmente, con el SEST no se descuidarán los objetos del sistema solar. En efecto, quizás ya el próximo mes será posible observar el cometa Wilson. Serán de gran interés las observaciones de atmósferas planetarias y de la emisión continua desde planetas y asteroides en ondas submilimétricas.

Estamos a la espera de estos interesantes descubrimientos que han sido posibles gracias al esfuerzo de las muchas personas involucradas.

Contents

L. Woltjer: A Time for Change	1
R.S. Booth, M.J. de Jonge, P.A. Shaver: The Swedish-ESO Submillimetre Telescope	2
List of ESO Preprints	5
R. Schoembs, M. Pfeiffer, R. Haefner, H. Pedersen: High Speed Multicolour Photometry of the X-ray Burster MXB 1636-53	6
Two New Slide Sets From La Silla	9
S. di Serego Alighieri: Line and Continuum Imaging	10
D. Bettoni, G. Galletta: Velocity and Velocity Dispersion Fields of NGC 6684: An SB0 Galaxy with a Ring	13
A. Acker, B. Stenholm: IDS Spectroscopy of Planetary Nebulae	16
ESO Exhibition in Brussels Visited by King Baudouin	19
S. Cristiani: OPTOPUS Observations of Quasar Candidates	20
A. Heck, D. Egret: SIMBAD, the CDS Database	22
ESO Press Releases	24
R. Prange, A. Vidal-Madjar, J.C. Gérard: A Study of the Neutral and Ionized Iota Tori	25
H. Barwig, R. Schoembs: MCCP: Photometry Through Clouds!?	29
R.M.W.: ESO Delegation Visits 6-m Telescope	32
Major Film About Astronomy to be Produced	33
G. Meylan, S. Djorgovski, R. Perley, P. McCarthy: Discovery of a Binary Quasar	34
M. Spite, F. Spite: Preliminary Abundances in Three Cool Supergiants of the SMC	37
A. Cappi, G. Chincarini, P. Conconi, I. Manoussoyanaki, G. Vettolani: Distant Clusters of Galaxies	40
G. Soucail: The Giant Luminous Arc in the Centre of the A 370 Cluster of Galaxies	43
Latest News about SN 1987 A	44
Comet Wilson Photographed from La Silla	45
The editor: The Strange Supernova 1987 A Passes Maximum	45
Recent NTT Pictures	48
A.F.M. Moorwood, I.J. Danziger, E. Oliva: Infrared Spectroscopy of Supernova Remnants	49
NEWS ON ESO INSTRUMENTATION	
A. van Dijsseldonk, A. Moorwood, D. Lemke: F/35 Infrared Photometer at the 2.2-m Telescope	50
F. Maaswinkel, S. D'Odorico, G. Huster, F. Bortolotto: Progress Report on DISCO: A Project for Image Stabilization at the 2.2-m Telescope	51
ESO Image Processing Group: MIDAS Memo	53
Staff Movements	54
New ESO Posters and New Edition of ESO Publications and Picture Catalogue Available	54
The Chilean Consul General Visits ESO	54
Algunos Resúmenes	54